Sonification of Motion of Robotic Systems with Many Degrees-of-Freedom

By

Amal Kacem

A dissertation proposal submitted for the degree of
Doctor of Philosophy
Electrical and Computer Engineering
the University of Michigan – Dearborn
2025

Doctoral Committee:
Associate Professor Alireza Mohammadi, Chair
Professor Hafiz Malik
Assistant Professor Khouloud Gaaloul
Professor Selim Awad

Amal Kacem

Akacem@umich.edu

ORCID iD: 0000-0002-6247-7248

https://orcid.org/0000-0002-6247-7248

ACKNOWLEDGEMENTS

The completion of this PhD dissertation would not have been possible without the support, guidance, and encouragement of many individuals and institutions, to whom I owe a great debt of gratitude.

First and foremost, I would like to express my deepest gratitude to my supervisor, Dr. Alireza Mohammadi, for your invaluable mentorship and guidance throughout this journey. Your wisdom, patience, and unwavering support provided me with the foundation to navigate the challenges of research and academia. I am profoundly thankful for your constructive feedback, which has shaped both this dissertation and my growth as a researcher.

I also extend my heartfelt thanks to my thesis committee members, Professor Hafiz Malik, Professor Khouloud Gaaloul, and Professor Selim Awad, for their insightful suggestions, critical evaluations, and constant encouragement. Your input has significantly improved the quality of this work, and I am grateful for the time and effort you invested in my research.

I would also like to thank the University of Michigan for the funding and resources that made this research possible. The support I received from the National Science Foundation (NSF) as well as the robotic equipment donation by Omron Foundation, Inc were essential for the successful completion of the experimental work in this dissertation.

Above all, I would like to express my deepest love and gratitude to my husband, Khalil Zbiss, with whom I had the pleasure of working and collaborating. This journey

has been especially meaningful because we have shared every step of it together—not just as partners in life but as lab mates and collaborators in every project. Your continuous support, intellectual insight, and the joy of working with you made this experience even more fulfilling. From the long nights in the lab to celebrating milestones, every moment was enriched because of you. I am so fortunate to have had you by my side through this incredible journey, both academically and personally.

Lastly, I would like to thank my family and friends for their unwavering support, patience, and encouragement. I am immensely grateful to my parents Farid and Saoussan and my brother Amine "Ninou", for their heartfelt support—emotionally and financially—throughout my academic journey. Your generosity and belief in my potential made it possible for me to pursue my undergraduate and graduate studies without the added burden of financial worries. I am deeply thankful for the sacrifices you made to ensure that I had every opportunity to succeed and for your constant encouragement throughout this process. I sincerely dedicate my success to you, Mom and Dad.

And to my friends, who reminded me to take breaks and offered moral support, I am grateful for your presence in my life.

This dissertation is the product of many contributions, and I am forever thankful to all who have been part of this journey.

PREFACE

This thesis focuses on the field of human-robot interaction (HRI) and specifically on the sonification of robotic motion. It aims to foster more natural and effective communication between robots and human users. The choice of the study is motivated by the increasing complexity of robotic systems, where real-time, non-visual communication is essential. Traditionally, robots convey their movements and intentions through visual displays or speech. However, these methods often fail in situations with an overwhelming amount of information or when rapid, unconscious interpretation is required. This gap forms the basis of the current study, prompting the search for an alternative communication method.

The main idea of this research is that non-speech sounds, particularly sonification, can effectively communicate complicated robotic movements and intentions to human users, even in highly complex robotic systems with numerous degrees of freedom. While existing sonification techniques have shown promise, they are limited to robots with simple configurations and with a low number of degrees of freedom. To bridge this gap, This study proposes a new approach based on the Wave Space Sonification (WSS) framework. The main objective of this research is to systematically sonify robot motion so that auditory information effectively and intuitively communicates the robot's state to human users, especially in situations where visual communication is inadequate or unavailable.

The significance of this study lies in its potential to enhance collaboration between humans and robots, particularly in industrial settings where human operators closely

interact with autonomous systems. By making robotic motion more comprehensible through sound, this research paves the way for safer and more efficient interactions, reducing the risk of errors and enhancing overall system performance. The findings show that the WSS-based approach can effectively represent complex robotic behaviors in real-time. The conclusions derived from the experimental results suggest that sonification is not only achievable but also advantageous in promoting smoother and more intuitive human-robot collaboration.

This dissertation contributes to the broader field of HRI by introducing a new method that extends the use of sonification in robotic systems. This study recommends further investigation of sound design for different robotic configurations and testing the sonification method in various real-world situations. This work establishes a foundation for future research on using auditory representations to improve the safety and efficiency of human-robot systems, especially in critical environments where quick and accurate interpretation of robotic actions is essential.

The following section presents a comprehensive list of my publications during the course of my PhD. The first four papers are closely tied to the central theme of this dissertation, which focuses on the sonification of the motion of redundant robots. These publications delve into the challenges of monitoring the kinematic behavior of robots with many degrees of freedom and propose innovative sonification techniques as an alternative to traditional visual methods. Specifically, they explore how auditory feedback can be effectively applied to hyper-redundant robotic mechanisms, providing intuitive ways to interpret complex motion patterns and improve system monitoring. Additionally, these works extend the sonification approach to teams of mobile robots, addressing the need for scalable and efficient methods to track and analyze the motion of multiple robotic systems simultaneously.

The final two publications included in this list represent research I contributed to outside the scope of the specific focus on sonification. Although not directly related to

the core subject of this dissertation, these papers highlight my broader work within the field of robotics, covering topics such as automation and robot design. While these projects fall outside the main narrative of this dissertation, they demonstrate the range of my research interests and contributions during my PhD journey.

List of Publications

1. A Kacem, K Zbiss, A Mohammadi, 2023, *A Numerical Integrator for Forward Dynamics Simulations of Folding Process for Protein Molecules Modeled as Hyper-Redundant Robots*, 2023 IEEE/RSJ International Conference on Intelligent Robots and Systems (IROS 2023) - **Discussed in Chapter II in Section 2.5.1** [1]

2. A Kacem, K Zbiss, A Mohammadi, 2024, *A Numerical Integrator for Kinetostatic Folding of Protein Molecules Modeled as Robots with Hyper Degrees of Freedom*, Robotics 13 (10), 150 - **Discussed in Chapter II in Section 2.5.1** [2]

3. A Kacem, K Zbiss, A Mohammadi, 2024, *Wave space sonification of the folding pathways of protein molecules modeled as hyper-redundant robotic mechanisms*, Multimedia Tools and Applications 83 (2), 4929-4949 - **Discussed in Chapter IV** [3]

4. A Kacem, K Zbiss, A Mohammadi, 2024, *Transforming Motion Into Sound: A Novel Sonification Approach for Teams of Mobile Robots*, International Symposium on Flexible Automation 87882, V001T07A005 - **Discussed in Chapter V** [4]

5. K Zbiss, A Kacem, M Santillo, A Mohammadi, 2022, *Automatic collision-free trajectory generation for collaborative robotic car-painting*, IEEE Access

10, 9950-9959 [5].

6. K Zbiss, A Kacem, M Santillo, A Mohammadi, 2024, *Automatic Optimal Robotic Base Placement for Collaborative Industrial Robotic Car Painting*, Applied Sciences 14 (19), 8614 [6]

TABLE OF CONTENTS

LIST OF FIGURES

Figure

LIST OF APPENDICES

Appendix

LIST OF ABBREVIATIONS

DOF Degrees of Freedom

ETA Electronic Travel Aids

HRI Human-Robot Interaction

INS Indoor Navigation Systems

KCM Kinetostatic Compliance Method

VIPs Visually Impaired People

WSS Wave Space Sonification

ABSTRACT

by

Amal Kacem

Effective human-robot interaction is increasingly vital across various domains, including assistive robotics, emotional communication, entertainment, and industrial automation. Visual feedback, a common feature of current interfaces, may not be suitable for all environments. In settings where visibility is low or where robotic operations generate extensive data, audio feedback serves as a critical supplementary communication layer. Sonification, which transforms a robot's trajectory, motion, and environmental signals into sound, enhances users' comprehension of robot behavior. This improvement in understanding fosters more effective, safe, and reliable Human-Robot Interaction (HRI). Demonstrations of auditory data sonification's benefits are evident in real-world applications such as industrial assembly, robot-assisted rehabilitation, and interactive robotic exhibitions, where it promotes cooperation, boosts performance, and heightens engagement. Beyond conventional HRI environments, auditory data sonification shows substantial potential in managing complex robotic systems and intricate structures, such as hyper-redundant robots and robotic teams. These systems often challenge operators with complex joint monitoring, mathematical kinematic modeling, and visual behavior verification.

This dissertation explores the sonification of motion in hyper-redundant robots and teams of industrial robots. It delves into the Wave Space Sonification (WSS) framework developed by Hermann [9], applying it to the motion datasets of protein molecules modeled as hyper-redundant mechanisms with numerous rigid nanolinkages. This research leverages the WSS framework to develop a sonification methodology for protein molecules' dihedral angle folding trajectories. Furthermore, it introduces a novel approach for the systematic sonification of robotic motion across varying configurations. By employing localized wave fields oriented within the robots' configuration space, this methodology generates auditory outputs with specific timbral qualities as robots move through predefined configurations or along certain trajectories. Additionally, the dissertation examines a team of wheeled industrial/service robots, whose motion patterns are sonified using sinusoidal vibratory sounds, demonstrating the practical applications and benefits of this innovative approach.

CHAPTER I

Introduction

Sonification, the process of transforming data into sound, is increasingly recognized as a valuable tool in bridging the gap between human operators and machines, offering an intuitive and direct way to comprehend complex data and systems. In the realm of robotics, this technique holds immense potential, as it allows users to interpret information not solely through visual displays, but through the auditory modality, which is highly sensitive to changes in patterns and rhythm. The use of sonification has been applied across various domains, from assistive technologies to healthcare innovations, scientific research, and industrial automation, all of which benefit from its ability to present data in a form that can be processed in real time, while reducing the cognitive load typically associated with complex visual interfaces.

In the context of robotic systems, the application of sonification extends far beyond basic monitoring tasks. It enhances the user's ability to interact with and control highly complex, multi-dimensional systems in a manner that would otherwise be unattainable through traditional visual methods. One prominent example of this is its application in navigation assistance for the visually impaired (VIP). When robotic trajectories are sonified, auditory cues can guide VIPs through different environments, providing real-time feedback that facilitates navigation without reliance on visual data. Ahemetovic et al. [10] introduced several sonification techniques tailored to

navigation assistance for VIPs, demonstrating the effectiveness of auditory cues in providing guidance during turns and straight paths. This research highlights the practical value of sonification in overcoming the challenge of non-visual navigation, offering a highly effective solution to a traditionally difficult problem.

For example, Ahemetovic and his collaborators [11] proposed a novel sonification technique aimed at providing continuous guidance during rotations. This system was designed for Indoor Navigation Systems (INS), where VIPs rely on mobile devices that utilize location tracking and inertial sensors to follow routes to a given destination. By converting spatial and motion data into sound, the researchers created a system that offers continuous auditory feedback, allowing users to orient themselves and navigate complex environments safely. Similarly, Hu et al. [12] explored how image sonification techniques could be used to convey critical scene information to VIPs via Electronic Travel Aids (ETA). Their approach included depth image sonification, obstacle sonification, and path sonification, each of which mapped different types of spatial data into sound. By translating visual information into distinct auditory cues, these systems have empowered VIPs to navigate autonomously, even in environments where traditional assistive technologies might falter.

Beyond assistive technology, sonification has been widely adopted in healthcare and scientific research to enhance data interpretation and real-time monitoring. In healthcare, for instance, researchers have explored sonification as a tool for converting complex physiological data—such as heart rate variability or EEG recordings—into sound [13; 14; 15; 16; 17]. The conversion of these data streams into auditory signals provides an additional layer of insight for clinicians, who can detect anomalies, monitor patient health, and even assist in diagnosing conditions such as heart arrhythmias. Studies have shown that auditory patterns can reveal subtle irregularities in patient data that might otherwise go unnoticed with traditional visual monitoring techniques. By transforming multi-dimensional physiological data into sound, sonification has al-

lowed healthcare professionals to monitor patient conditions more effectively and in real time, enhancing diagnostic accuracy and improving patient outcomes.

Scientific research also benefits greatly from the application of sonification. In fields such as genomics and astrophysics, where data is often vast, multi-dimensional, and difficult to visualize, sonification provides a novel way to interpret and analyse complex datasets [18; 19],. For example, in genomic research [20; 21; 22], sonification has been employed to analyze large-scale datasets and uncover insights into genetic sequences. Similarly, in astrophysics [23; 24; 25], researchers have used sonification to explore celestial data, such as the movement of stars and galaxies, where traditional visualizations might not effectively convey the nuances of these phenomena. The ability to listen to data, rather than solely relying on visual interpretation, offers scientists a new dimension through which they can make discoveries and draw conclusions.

Sonification's potential is not confined to static data interpretation but also extends to real-time monitoring of dynamic systems, particularly in applications involving human kinematic movement [26; 27; 28]. One growing area of research is the sonification of kinematic data, where complex human movements are converted into auditory signals that can be used for rehabilitation, sports performance analysis, and training. In this context, sonification offers immediate feedback that helps individuals, whether patients or athletes, correct and improve their movements. By providing real-time auditory feedback [29; 30; 31], patients can receive ongoing cues that help them refine their motor skills, which is particularly valuable in rehabilitation settings where continuous feedback is critical for motor learning and recovery.

In rehabilitation, sonification can provide feedback on key aspects of movement such as joint angles, velocity, and trajectory. For patients recovering from a stroke, injury or other motor impairments, or even neurological disorder [32; 33]. For instance, a patient recovering from a stroke may need to focus on the smoothness and

coordination of limb movements, while an athlete recovering from an injury might need to pay attention to the speed and strength of their movements or improve their physical abilities by sharing sports-related information to increase the accuracy of the sport movements reproduction [34; 30; 35]. These auditory feedback allow them to make small adjustments to their movements, improving coordination and overall motor function. Unlike visual feedback, which often require focused attention on a screen, auditory feedback can be processed peripherally, allowing patients to focus entirely on their physical movements. This can lead to faster recovery times and more effective rehabilitation outcomes, as patients are able to make corrections in real time without interrupting the flow of their exercises. The flexibility of sonification also allows for the customization of auditory signals to meet the specific needs of different patients, whether they are focusing on regaining smooth movement in their limbs or increasing the strength and speed of their motions.

In addition to enhancing precision in movement correction, the use of sound in rehabilitation can significantly engage patients and maintain their motivation. Auditory feedback can be designed to be pleasant and encouraging, transforming the often monotonous and repetitive nature of rehabilitation exercises into a more engaging and enjoyable experience [36; 37; 38]. Studies have shown that sonification can lead to improved motor performance and increased engagement compared to traditional visual-only feedback systems [39; 40]. Patients are more likely to adhere to their rehabilitation programs when they find the process enjoyable and rewarding.

In addition, for therapists, sonification offers a novel and effective tool to monitor patient progress. The auditory signals can provide a continuous stream of information that is easier to interpret in real-time, enabling more precise adjustments to therapy plans. This dynamic feedback loop ensures that rehabilitation strategies can be promptly modified based on the patient's performance, thereby optimizing recovery outcomes.

Moreover, in the context of multi-robot systems, such as teams of mobile robots, sonification has the potential to be an invaluable tool for real-time monitoring and control. Teams of mobile robots generate vast quantities of motion data, much of which is too complex for traditional visual methods of monitoring. Sonification allows for the continuous tracking of the movements and interactions between robots, offering operators an auditory representation of system states that would otherwise be difficult to grasp visually. By converting this data into sound, operators can listen for deviations in the expected motion patterns of individual robots or the team as a whole, allowing for more effective management of these systems in dynamic environments. The auditory feedback provided by sonification enhances the operator's situational awareness, enabling them to detect anomalies, monitor performance, and make rapid adjustments to optimize system efficiency.

The benefits of sonification extend further into the realm of industrial automation, where robots are deployed for complex tasks such as material handling, assembly, and quality control. In such settings, the ability to monitor and control the behavior of robotic systems in real time is essential for maintaining productivity and ensuring the quality of output. Sonification offers a unique advantage in this context, as it allows operators to remain attuned to the performance of their systems without needing to constantly observe visual displays. By providing auditory cues that indicate changes in system behavior, sonification can alert operators to potential issues before they escalate into serious problems, thereby reducing downtime and enhancing operational efficiency.

In conclusion, the growing recognition of sonification as a critical tool in human-machine interaction highlights its potential to revolutionize the way complex systems are monitored and controlled. Whether in the fields of assistive technology, healthcare, scientific research, rehabilitation, or industrial automation, the ability to transform data into sound opens up new possibilities for interpreting and interacting with infor-

mation in real time. Sonification not only reduces the cognitive load associated with visual monitoring but also offers a more intuitive and accessible means of understanding complex, multi-dimensional data. As robotic systems become more advanced and the volume of data they generate increases, the role of sonification will only become more prominent, providing operators with the tools they need to effectively monitor and manage these systems in dynamic, fast-paced environments.

1.1 Motivation

The increasing complexity of modern robotic systems, particularly those with a large number of degrees of freedom, presents a significant challenge to traditional methods of monitoring and control. These robots, whether hyper-redundant or part of multi-robot teams, generate vast amounts of motion data, the interpretation of which is critical for ensuring smooth operation, detecting anomalies, and optimizing performance. As robotics continues to evolve and becomes more integral to industrial automation, healthcare, service industries, and advanced manufacturing, the need for effective monitoring grows. However, current approaches are largely reliant on visual methods—dashboards, screens, and graphical interfaces—which are proving insufficient in environments where high-dimensional, intricate motion data must be processed in real-time. The overarching motivation for this research is to explore and develop alternative, non-visual methods for system monitoring. Specifically, the focus is on the sonification of motion data from robots with large degrees of freedom, including hyper-redundant robots and teams of mobile robots, with the goal of providing real-time auditory feedback that aids in interpreting and managing their behavior, hence, enhancing Human-Robot Interaction.

Hyper-redundant robots—characterized by their numerous joints and linkages—pose unique challenges to system monitoring. Each of these robots' many degrees of freedom represents a distinct trajectory that must be tracked and monitored as the robot

operates. The sheer volume of motion data produced during the operation of such robots makes it difficult, if not impossible, for operators to fully comprehend the system's behavior using visual feedback alone. Traditional visualization tools, such as multi-dimensional graphs and time-series plots, become cluttered and hard to interpret, especially in dynamic and fast-paced environments where real-time monitoring is essential. In systems where many joints interact simultaneously, these traditional tools are prone to information overload, ultimately hindering the operator's ability to effectively monitor the robot. As such, there is an urgent need for alternative approaches that provide more intuitive, less cognitively demanding methods of monitoring and controlling robots with many degrees of freedom.

In this research, we propose the application of sonification as an innovative method for addressing these challenges. Sonification is the process of translating data into sound, providing users with an auditory representation of complex information that might otherwise be difficult to grasp visually. By converting motion data into non-speech auditory cues, sonification leverages the human auditory system's innate ability to detect changes, patterns, and anomalies in real time. This auditory feedback can complement or even replace traditional visual methods, providing an alternative means for users to monitor robotic systems that are too complex for effective visual interpretation alone. In particular, for hyper-redundant robots, where multiple degrees of freedom interact in a high-dimensional space, sonification offers an opportunity to represent the intricate and often non-linear behavior of the system in a more accessible and comprehensible format.

The motivation to explore sonification as a monitoring tool for hyper-redundant robots is driven not only by the practical challenges of real-time monitoring but also by the conceptual parallels between these robots and other high-dimensional systems, such as molecular structures. Specifically, hyper-redundant robots, with their large number of flexible joints, can be modeled similarly to protein molecules, which exhibit

complex folding pathways as they move from unfolded to folded states. Just as the molecular movements of protein folding are difficult to visualize in high-dimensional space, the motion of hyper-redundant robots presents similar challenges in visual monitoring. This analogy provides an interesting framework for exploring sonification as a tool to map these high-dimensional trajectories into an auditory domain, where users can intuitively track, understand, and respond to the system's behavior.

However, hyper-redundant robots are not the only type of robotic system that stands to benefit from a sonification-based monitoring approach. Teams of mobile robots, which are increasingly deployed in industrial and service environments, also generate complex motion data that can overwhelm traditional visual monitoring systems. In such scenarios, multiple robots operate simultaneously, coordinating their movements and interacting with each other in ways that are often difficult to monitor using only visual data. The need for real-time, intuitive feedback in these systems is critical, especially in environments where robots are tasked with complex, dynamic missions such as material transport, assembly, or inspection. The coordination of these robots requires careful monitoring to ensure that all units work together efficiently, avoiding collisions, task misalignments, or inefficiencies in execution.

The challenge in monitoring teams of mobile robots lies not only in the complexity of the motion data but also in the interaction dynamics between individual robots. Visual methods, although widely used, are limited in their capacity to provide real-time feedback on the behavior of these multi-agent systems, particularly when quick decisions must be made to avoid operational failures. By transforming the motion data from these robots into auditory feedback, sonification offers a solution that provides immediate, intuitive insight into the system's performance. It allows operators to track not only the movements of individual robots but also the coordination and collective behavior of the team. This is particularly important in environments where visual information can be incomplete, overwhelming, or difficult to process at the

speed required for effective decision-making.

Given the complexity of these systems, traditional monitoring methods are inadequate in capturing and conveying the full scope of robot behavior. This inadequacy underscores the importance of developing sonification techniques tailored to both hyper-redundant robots and teams of mobile robots. In systems with many degrees of freedom, the high-dimensional motion data requires a monitoring approach that is not only capable of representing intricate behaviors but also scalable and robust enough to handle real-time data streams. Sonification fills this need by providing an alternative means of conveying complex system states through sound, making it possible to track subtle variations in movement and performance that might otherwise go unnoticed through visual monitoring alone.

In the case of hyper-redundant robots, each joint or linkage operates within a multi-dimensional space, and their collective movements result in complex trajectories that describe the robot's behavior. Monitoring these trajectories through visual methods alone is impractical due to the sheer volume and intricacy of the data. Sonification, however, offers a way to map these trajectories to auditory signals, allowing operators to detect shifts in the robot's behavior, such as deviations from expected movements or the emergence of inefficiencies in the system. By converting motion data into sound, this approach enhances the user's ability to track and respond to changes in real time, providing a more accessible and efficient means of understanding the robot's performance.

Similarly, in teams of mobile robots, where each robot operates independently but in coordination with others, the collective motion data poses a significant challenge for visual monitoring. Sonification enables the auditory tracking of these interactions, allowing operators to assess the team's performance without having to parse through dense visual representations of the data. This auditory feedback is particularly useful in environments where robots must coordinate tightly to avoid collisions, complete

tasks, or navigate through complex spaces. The ability to monitor these interactions through sound provides an additional layer of feedback that complements visual monitoring, offering operators a more comprehensive understanding of the system's behavior.

Despite its promise, the field of robotic trajectory sonification is still in its early stages. Existing research has focused on simpler robotic systems, such as those used in human-robot interaction (HRI) studies, where sonification has been applied primarily to small-scale, low-dimensional systems. The application of sonification to robotic systems with large degrees of freedom or teams of robots operating collaboratively has remained largely unexplored. This research aims to address this gap by developing a systematic sonification framework that can be applied to both hyper-redundant robots and teams of mobile robots, offering a novel solution to the challenges posed by high-dimensional motion data and multi-agent coordination.

The motivation for this work is also grounded in the broader trend toward increasing automation and the deployment of robots in complex, real-world environments. As robots become more integral to tasks such as material handling, transportation, and assembly, the need for reliable, real-time monitoring will only grow. Sonification offers a powerful tool for addressing this need, providing an intuitive means of interpreting the behavior of these systems without over-reliance on visual feedback. In industrial settings, where robots often operate in close coordination and at high speeds, the ability to detect deviations or anomalies in real time is critical to ensuring safe and efficient operation. Sonification provides a way to augment traditional monitoring techniques, offering a new dimension of feedback that can enhance system performance and reliability.

In conclusion, this dissertation is motivated by the growing need for alternative approaches to system monitoring in complex robotic systems, particularly those with large degrees of freedom and multi-robot teams. Traditional visual methods are in-

creasingly inadequate in handling the scale and complexity of modern robotics, necessitating the development of new tools for real-time feedback and control. Sonification offers a promising solution to this challenge, transforming high-dimensional motion data into intuitive auditory signals that enhance the operator's ability to monitor and manage robotic systems. By applying sonification techniques to hyper-redundant robots and teams of mobile robots, this research seeks to develop a robust, scalable framework for auditory monitoring, contributing to the broader effort to improve the performance, safety, and efficiency of complex robotic systems.

1.2 Dissertation Organization

This dissertation is organized as follows: Chapter II begins by laying the necessary background on sonification and various sonification techniques. It explores the current state-of-the-art applications of sonification in robotics, highlighting its relevance in non-visual system monitoring. The chapter also examines how sonification has been applied to protein-related datasets, linking this work to robotics through a brief overview of the Kinetostatic Compliance Method (KCM)-based approach to protein folding. This provides a conceptual foundation that connects the sonification of protein folding pathways to robotic trajectory monitoring, setting the stage for the discussion of more complex robotic systems in subsequent chapters.

In Chapter III we provide an in-depth look at redundant robots. First, we focus on Hyper-redundant robots and their unique kinematic structure and their applications by emphasizing on their high degree of dexterity and flexibility due to their numerous degrees of freedom. Despite the structural differences between hyper-redundant robots and teams of mobile robots, the chapter draws parallels between these systems by emphasizing their shared fundamental principles of redundancy, coordination, and adaptability. It explores how the kinematic structures of both types of robots are essential for designing systems that can execute complex, coordinated tasks, paving

the way for the integration of sonification techniques.

Chapter IV, we discuss the importance of studying the folding pathways of protein molecules and how challenging is to represent the vast amount of data generated by protein folding simulations. This chapter presents the contributions of this research to the sonification of protein folding pathways, specifically addressing the unsolved problem of representing conformational changes in proteins through auditory feedback.

Thereafter, we formulate our problem statement related to the sonification of folding pathways of protein molecules modeled as hyper-redundant robots. We also provides our solution to the problem of sonification of datasets associated with conformational changes during protein folding. Then, in this chapter we present examples and results of the Wave Space Sonification (WSS)-based methodology developed for the backbone chain of a protein molecule with a dihedral angle space of dimension 82. Specifically, we utilize a canonical wave space function based on a sum-of-sinusoids with protein conformation-dependent frequencies and a sample-based wave space function based on Mozart's Alla Turca for sonification of the peptide chain folding trajectories. The chapter concludes with a discussion on how the proposed sonification method could be extended to other hyper-redundant robotic systems, demonstrating the interdisciplinary potential of this research.

In chapter V, the focus shifts to the sonification of the motion of teams of mobile robots using our developed data-driven localized WSS method. Despite the significance of sonification of the motion patterns of industrial/service robots as an important human-robot collaboration enabler, there is still no general method for real-time sonification of the motion of teams of these robots with any arbitrary number of team members. The chapter begins by outlining the formal problem of sonifying the real-time motion of multi-robot systems, which is a critical challenge in industrial and service environments. It describes the experimental settings used in this study

and presents the data-driven localized WSS methodology as a solution for monitoring the motion patterns of teams of mobile robots. The methodology is applied to a team of OMRON LD series autonomous mobile robots, showcasing how sonification can enhance real-time tracking of robot coordination and performance. The chapter emphasizes the importance of sonifying the motion of teams of robots, particularly in scenarios where human-robot collaboration is essential, and discusses the broader implications of this work in enabling more intuitive and responsive interaction with robotic systems.

Finally, Chapter VI concludes the dissertation by evaluating the overall significance of the proposed WSS-based sonification framework. This chapter reflects on the contributions of the research to the field of sonification, specifically in the context of hyper-redundant robots and teams of mobile robots. It also considers the potential for applying the developed methodology to other complex robotic systems, offering insights into future research directions. The chapter highlights the scalability and adaptability of sonification as a tool for real-time monitoring in robotics, proposing future advancements and applications of the techniques presented in this dissertation.

CHAPTER II

Background

In this section, we provide a brief background on sonification techniques and their applications to datasets resulting from studying protein molecules as well as robotic motion sonification. We further highlight the contributions of the method in the context of the state-of-the-art sonification techniques applied to these important problems. Finally, we conclude the chapter by providing an overview of the Kineto-static Compliance Method for modeling the folding of protein molecules.

2.1 Sonification

Sound, from Rene Laennec's stethoscope to the Geiger-Muller counter, has had longstanding importance in the process of scientific discovery and technological development [41]. Despite this significance, the utilization of non-speech audio for conveying information, which is known as sonification, is still in its developing phase (see, e.g., [42; 43; 44]). Formally, sonification can be defined as the technique of using datasets as input and generating sound signals as output, while satisfying the four conditions of: (i) reflecting the objective and/or relational properties in the input data; (ii) transforming datasets systematically; (iii) being reproducible; and (iv) applying to versatile datasets [45].

The Sonification Handbook [45] categorizes (see, also, [46]) the sonification techniques into five different structural classes, namely, earcons, auditory icons, parameter-mapping sonification, audification, and model-based sonification. Earcons refer to structured sounds serving as an index for abstract messages, such as the Windows abstract operating system sounds or the signature three-tone melody of the National Broadcasting Company (NBC). Auditory icons refer to short sound messages that convey information about an event, situation, or object [47] such as the sound of crumpling a piece of paper when deleting a document in Windows. Audification is a special case of WSS where data is directly translated into sound. Finally, in model-based sonification [48], the data is converted to a dynamical system that demonstrates acoustic behavior, e.g., utilizing the data to determine the mass-spring system parameters of an acoustic device.

2.2 Wave Space Sonification

2.2.1 Wave Space Sonification Overview

In addition to the five established classes of sonification, a new class known as the wave space sonification (WSS) has been recently proposed by Hermann [9]. This framework lies in the spectrum between parameter-mapping sonification and audification. WSS, whose essence is based on effective navigation of sound signal spaces by using high-dimensional data, has been utilized in a few applications such as the development of audiovisual dance displays [49].

WSS is a method for representing data acoustically by mapping it to the frequency, amplitude, and other characteristics of sound waves. The framework converts data points into sound parameters such as pitch, volume, and timbre, enabling auditory

exploration and interpretation of complex data sets belonging to the multidimensional space of sound waves.

Depending on the nature of the data and the desired auditory output, the data gets mapped based on mathematical algorithms, physical models, or subjective interpretation before it gets converted to sound waves.

The resulting acoustic signal lets users perceive patterns, trends, and anomalies in their data by listening. By leveraging the human ear's ability to detect subtle changes in sound, WSS provides a unique and intuitive way to explore complex datasets and complement traditional visualization techniques.

WSS demonstrates potential applicability across diverse domains and disciplines, including scientific research, data analysis, and artistic expression. In scientific research, it could be of huge help in discovering patterns and relationships in data, making it easier to create and test hypotheses. Providing Data analyst with another perspective on the dataset and revealing insights that are not evident through visual inspection alone. In art, it can be used to create immersive and interactive experiences.

Overall, WSS is a powerful tool for converting data into sound, providing a rich and expressive medium for data exploration and communication. This is the main reason behind utilizing the WSS framework for solving the problem of sonification of folding trajectories of protein molecules, which are modeled as hyper-redundant robotic mechanisms (see, e.g., the line of work in [49; 50; 51; 52] for such a robot kinematics-based point of view on the structure of proteins). This is the first time that Hermann's WSS framework [9] is utilized for navigating sound signal spaces by using high-dimensional data resulting from the folding process of protein molecules.

2.2.2 Wave Space Sonification Elements

The WSS framework requires defining the following three elements [9]: (i) a trajectory in the wave space; (ii) a suitable definition of a wave space function; and, (iii) a proper way of moving along the trajectory in the wave space.

In the context of sonification of folding pathways of protein molecules, the wave space is the configuration space $\mathbb{Q}$ to which the vector of dihedral angles (introduced in Section 2.5.1) belongs (see Equation 2.2). Furthermore, the dihedral angle vector trajectory $\theta(t)$ obtained from the protein folding process defines an embedded trajectory within the high-dimensional wave space $\mathbb{Q}$. Moreover, in the WSS framework, one needs to select a morphing function $M : t \longrightarrow M(t)$, which determines how the dihedral angle folding trajectory is traversed. Finally, one needs to construct a scalar field $V : \mathbb{Q} \longrightarrow \mathbb{R}$, which is also known as the wave space function (see, also, Figure 4.1). After determining the wave space function $V(.)$ (see Sections 4.5.1 and 4.5.2), the sound signal, which can be sent to the PC sound card for listening to the folding pathway, is given by

$$s(t) = V(\theta(M(t))) \tag{2.1}$$

Figure 4.1 depicts the WSS elements in the context of sonification of protein folding pathway datasets. In the figure, the morphing function is considered to be the identity mapping, i.e., M(t) = t.

2.3 Sonification Techniques Applied to Structural/Vibrational Protein Data

One of the very first endeavors to sonify the structure of proteins and their encoding gene sequences is due to Dunn and Clark [53] In their work, fixed pitches were assigned to each amino acid based on an absolute basis or more consonant intervals

were assigned to the more frequently occurring amino acids based on a relative basis. Furthermore, water solubility of amino acids was also considered as a third metric for pitch assignment. Another pioneering work on molecular data sonification is due to Delatour [54], where a process for the acoustic and musical conversion of vibrational spectra data was proposed. Following Dunn and Clark [53] and Delatour [54], many of the important methods in this area such as the innovative line of work by Buehler and collaborators [21; 55; 56; 57; 58] all within translation of either structural properties or vibrational spectra of proteins into sound/musical compositions. Of notable importance is the work by Franjou et al. [56] where a neural network model is trained on 'protein music' and gives rise to new musical structures. These novel musical compositions, in turn, can be utilized to generate new protein structures through proper translation mappings. In another notable work, Qin and Buehler [55] employ frequency spectra of proteins, which result from a high-throughput automatic computational method, to produce audible sound. Moreover, using the concept of transpositional equivalence in music theory, they overlay the vibration of molecular structures and translate them to the audible frequency range (see [55] for further details).

Despite all the previous developments for sonification of protein molecule structural/vibrational data, the problem of sonification of protein folding pathway datasets is still an open one. This challenge is mainly due to the existence of an overwhelming amount of data, which are generated using physics-based numerical simulations (see, e.g., [59; 60; 61; 62; 63; 64; 7; 65; 66]), associated with time-indexed dihedral angle trajectories. Indeed, it is not clear how one can assign sound/music signals to these trajectories lying in the high-dimensional conformation space of protein molecules. It is important to note that in the biochemistry literature, 'conformation' is the standard word for describing the geometric structure of a protein molecule. In the robotics literature, on the other hand, the terminology 'configuration' is frequently

used to describe the kinematic structures of robots.

2.4 Sonification of Robotic Motion/Gestures

Sonification of the motion of robots is a relatively new paradigm with many potentials for efficient communication of robotic motion/intentions to human users while relying less on visual engagement [67; 68; 69], [70; 71; 72; 73; 74]. A notable approach, which belongs to the family of Parameter Mapping Sonification methods, is proposed by Schwenk et al. [74]. In their approach, a robot sonification system based on sound modulation of a synthesizer has been developed, where joint state and sensor data are fed into the synthesizer. Another notable line of work is the SONAO project led by Frid, Bresin, and collaborators [67; 70; 71], where limitations in robot communicative channels with humans are compensated through mapping humanoid robot expressive gestures to non-speech audio. For instance, Frid and Bresin [71] used a rectangular oscillator with a short envelope duration while mapping the magnitude of the input to pitches in a C major scale to convey sensations of joy. In the context of virtual reality-based robot teleoperation, Bremner et al. [72] have decreased the stress and perceived workload of human operators working with remote robots in hazardous environments by using proper data sonification through the Parameter Mapping Sonification framework. Another relevant project is SonifyIt [73] that enables sample playback and live sound synthesis for robots using Robot Operating System (ROS) and a visual programming language for multimedia called Pure Data.

Despite the advancements in the field of robot motion sonification, one major limitation of the current state-of-the-art methods is that they are limited to robots with a low number of degrees-of-freedom (e.g., less than ten like the robot Daryl in [74]). On the other hand, hyper-redundant robots such as elephant trunk robotic arms or segmented space manipulators (see, e.g., [75; 76; 77]), which are useful for operation in highly constrained environments or executing novel types of locomo-

tive patterns, have a very large or infinite number of degrees-of-freedom. The KCM approach [59; 51; 78] for protein molecules also relies on modeling the proteins as hyper-redundant robotic mechanisms with each dihedral angle corresponding to one degree-of-freedom of the mechanism (see Section 2.5.1 for further details). Furthermore, each dihedral angle trajectory is a time series generated by the protein folding dynamical model. For instance, the backbone chain of the protein Triponin with 159 amino acids has 320 dihedral angles that change with time during the Triponin folding process. Consequently, Triponin folding results in 320 time-indexed trajectories. For the first time, we provide a systematic way of sonifying the high-dimensional data resulting from the motion of protein molecules that are modeled as hyper-redundant robotic mechanisms.

2.5 Protein Folding Pathways Prediction Method

To execute a variety of important biological functions such as force generation in motor proteins and protein-ligand binding, protein molecules go under conformational transitions between two or more native conformations through the processes of folding and unfolding [79]. Numerical algorithms, which can predict the three-dimensional structures of folded protein molecules and the pathways/transitions through which proteins fold/unfold, have an integral role in computer-aided drug discovery [80] and in designing protein-based nanomachines [81; 82].

2.5.1 Kinetostatic Compliance-Based Protein Folding

In this section, we provide an overview of the Kinetostatic Compliance Method (KCM) for modeling the folding of protein molecules in vacuo. For brevity, we limit our presentation to the protein main chain.

2.5.2 Nano-linkage-based kinematic model of protein molecules

The kinematic structure of protein molecules and hyper-redundant robots exhibits a striking resemblance. Figure 2.1 clearly illustrates the parallel kinematic similarities or the analogy between the kinematic structure of a protein molecule and a hyper-redundant robot by comparing their structural elements. In the upper part of the figure, the hyper-redundant robot is depicted, showing multiple rigid links connected through flexible joints. Each joint introduces degrees of freedom, represented by the rotational axes, allowing for a wide range of motion and adaptability in the robot's structure. These joints enable the robot to adjust its configuration dynamically, ensuring smooth and continuous movements. These joints are known as universal joints and are used to provide multi-axis rotational freedom. they allow two rigid links to rotate about multiple axes (typically two), which significantly increases the robot's flexibility and its ability to change configurations. This type of joint can rotate in different directions simultaneously, giving the robot a higher degree of adaptability in maneuvering through constrained spaces or performing intricate tasks.

In the lower part of the figure, the protein molecule is depicted with its kinematic components aligned to the robot's structure. The backbone comprises a series of rigid nano-linkages (analogous to the robot's rigid bodies). These rigid sections of the protein chain are made up of amino acid residues, while the peptide bonds act like the joints of the robot, providing rotational flexibility. The figure highlights the peptide bond angles, similar to joint angles in robotics, that enable the protein backbone to fold into various conformations. These bonds, much like the joints in the hyper-redundant robot, allow for flexibility and dynamic adjustments in the overall structure of the protein. This flexibility enables proteins to adopt a wide variety of configurations, giving rise to their ability to fold into specific shapes required for their biological functions, such as enzyme catalysis or molecular recognition. The degrees of freedom in this structure are largely dictated by the angles at the peptide bonds,

which define how one rigid segment rotates relative to the next.

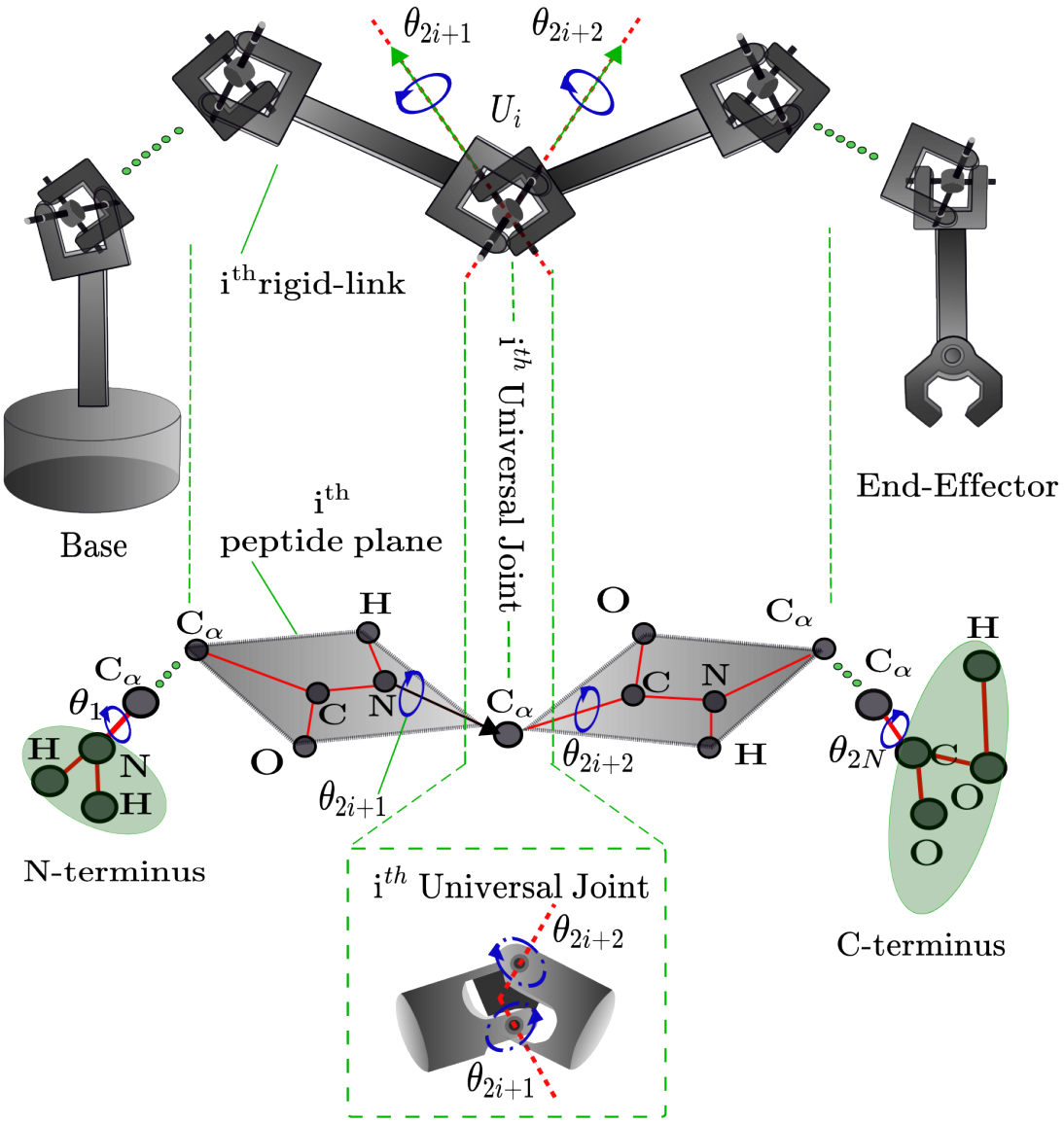

Figure 2.1: The kinematic structure of the protein backbone chain is similar to that of robotic mechanisms with hyper degrees of freedom. Specifically, C_α atoms play the role of hinges connecting peptide planes together. These C_α atoms are kinematically the same as universal joints with two degrees-of-freedom. In kinetostatic protein folding, the peptide linkages articulate with respect to each other through dihedral angular variations facilitated by the C_α atoms.

Both systems rely on their kinematic structure to accomplish their respective tasks—proteins rely on their structure to carry out biochemical functions, while hyper-redundant robots use theirs to achieve mechanical objectives. The similarity lies in the way rigid segments (nano linkages in proteins and rigid bodies in robots) are interconnected by flexible, universal joints (peptide bonds in proteins and mechanical joints in robots), resulting in a flexible, highly adaptable system with numerous degrees of freedom. This structural parallel allows both proteins and hyper-redundant robots to adapt to their environments and perform complex tasks with precision and flexibility.

Proteins, unlike mechanical systems, operate at a molecular scale where their flexibility directly influences their biological functions. The complexity of protein behavior is governed by the interactions and rotations at atomic levels, specifically around the peptide bonds connecting the amino acids. Understanding the kinematic chain of a protein involves analyzing these peptide planes, the specific atomic bonds, and the dihedral angles that dictate the spatial orientation of the protein backbone.

Protein molecules are long chains of peptide planes joined together via peptide bonds, where each plane consists of six coplanar atoms. As demonstrated in Figure 2.2, these planes can be considered as the linkages of the protein kinematic mechanism [50; 51]. Central carbon atoms, which are also known as the alpha-Carbon atoms denoted by C_α, play the role of inter-peptide plane hinges. Indeed, C_α atoms in protein molecules can be considered as the revolute joints in this kinematic mechanism. The red line segments in Figure 2.2 represent the covalent bonds between the peptide plane atoms.

The coplanarity assumption of the six atoms $C_\alpha - \mathrm{CO} - \mathrm{NH} - C_\alpha$, which constitute each of the peptide planes (see Figure 2.2), is based on the high-resolution X-ray crystallographic experimental observations of the structure of protein molecules (see, e.g., [79]). This coplanarity assumption has been the basis of various robotics-inspired

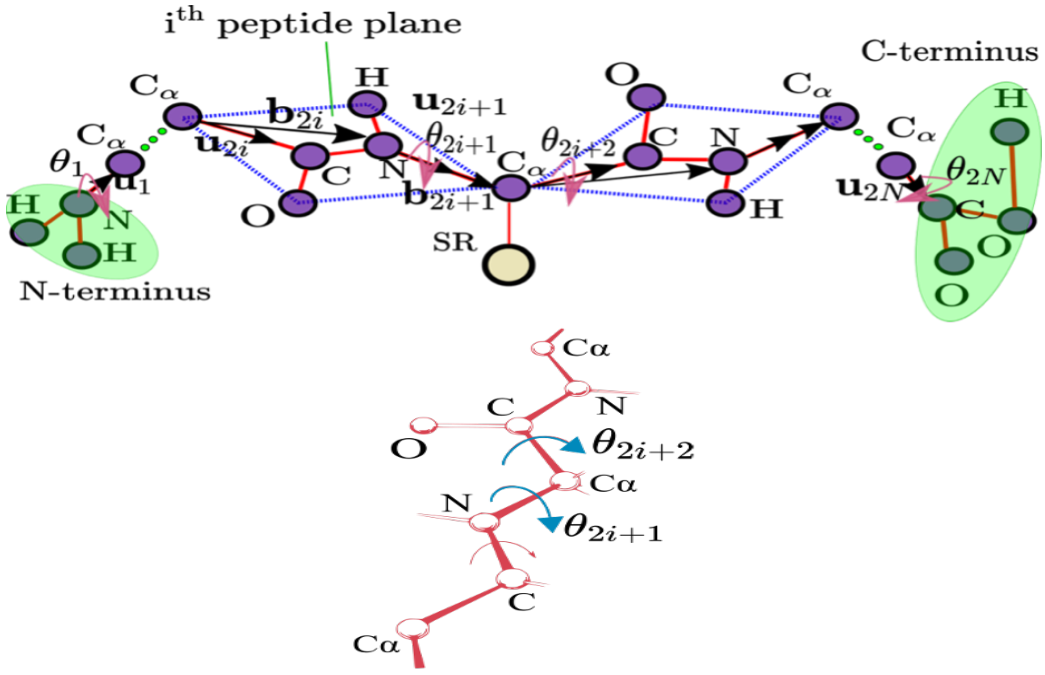

Figure 2.2: The protein molecule kinematic structure consisting of peptide planes (similar to robotic linkages) and C_α atom hinges (similar to robotic revolute joints). There also exists a hydrogen atom that is bonded to each alpha-Carbon atom using a covalent chemical bond but not shown in the figure. Bottom: Dihedral angles.

approaches in the literature that model protein molecules as hyper-redundant mechanisms (see, e.g., [59; 52]).

As it can be seen from Figure 2.2, each C_α is bonded to four other components, namely, a variable side chain denoted by SR and the three atoms C, N, and H. The first C_α of the protein chain structure is connected to N-terminus, which is an amino group, as well as one other peptide plane. Finally, the last C_α atom hinges to the C−terminus, which is a carboxyl group, as well as one other peptide plane. The backbone conformation of the protein molecule kinematic structure consisting of $-$ N $-$ C_α $-$ C $-$ atoms, is completely described by a set of bond lengths and a collection of pairs of dihedral angles, i.e., the rotation angles around C_α $-$ C and N $-$ C_α bonds (see Figure 2.2). A protein molecule dihedral angle can be defined as the

internal angle of the polypeptide backbone at which two adjacent planes meet (i.e., at each C_α atom). Therefore, the backbone conformation can be represented by two dihedral angles per residue, because the backbone residing between two juxtaposing alpha-Carbon atoms are all in a single plane (see Figure 2.2). Accordingly,

$$\theta := [\theta_1, \ldots, \theta_{2N}]^T \in \mathbb{Q} \tag{2.2}$$

is the configuration vector of the kinematic structure of a given protein backbone chain with N $-$ 1 peptide planes. As indicated by Equation 2.2, the dihedral angle vector θ belongs to the 2N-dimensional configuration space $Q := S^1 \times \cdots \times S^1$, where S^1 is the unit circle.

Each of the dihedral angles in the conformation vector θ in Equation 2.2 correspond to one degree-of-freedom (DOF) of the protein molecule kinematic chain. Associated with each DOF, one may consider a unit vector denoted by $u_j, 1 \leq j \leq 2N$. Each of these unit vectors is aligned with the rotation axis about which the protein kinematic chain can rotate. Therefore, as demonstrated in Figure 2.2, the vectors u_{2i} and u_{2i+1} are the unit vectors along the $C_\alpha -$ C and N $- C_\alpha$ bonds of the i^{th} peptide plane, respectively. Finally, u_1 and u_{2N} correspond to the unit vectors of the N-(the amino group) and C-termini (the carboxyl group), respectively.

In addition to the unit vectors u_j, one may utilize the so-called body vectors to complete the description of the spatial orientation of the rigid peptide nano-linkages in protein molecules. The body vectors, which are denoted by $b_j, 1 \leq j \leq 2N$, completely describe the relative position of any two coplanar peptide plane atoms. Specifically, the relative positions of any two atoms are determined by a linear combination of the form $k_{1m}b_{2i} + k_{2m}b_{2i+1}$, in which the coefficients k_{1m} and k_{2m}, $1 \leq m \leq 4$, are constant and the same across all peptide linkages (see, e.g., [83; 84] for further details). The unit vectors u_j and the body vectors b_j can be utilized to completely de-

scribe the conformation of a protein molecule using the conformation vector θ, which consists of the peptide dihedral angles. Indeed, after designating the zero-position configuration with $\theta = 0$, the transformations

$$u_j(\theta) = \Xi(\theta, u_j^0)u_j^0, \quad b_j(\theta) = \Xi(\theta, u_j^0)b_j^0 \tag{2.3}$$

where the transformation matrix $\Xi(\theta, u_j^0)$ is defined according to:

$$\Xi(\theta, u_j^0) := \prod_{r=1}^{j} R(\theta_j, u_j^0) \tag{2.4}$$

where the superscript 0 indicates the reference zero position (ZP) conformation. The zero-position conformation of the protein molecule refers to a linear structure in which all the amino acid peptide nano-linkages lie on the same plane (i.e., a completely stretched protein chain with dihedral angle vector $\theta = 0$). Therefore, using the ZP conformation, we are expressing all the possible directions of the unit vectors u_j and body vectors b_j in terms of rotational transformations applied to these vectors at the zero conformation where the protein chain is completely stretched.

The matrix $\Xi(\theta, u_j^0)$ determines the molecule's kinematic structure using the dihedral angle conformation vector θ.

In Equation 2.3, the rotation matrix $R(\theta_j, u_j^0) \in \mathrm{SO}(3)$ describes the rotation about the direction given by the unit vector u_j^0 with an angle equal to 0. It is remarked that the special orthogonal group SO(3) is the set of all rotational matrices about the origin of three-dimensional Euclidean space. Furthermore, any rotation matrix $R(\alpha, \hat{v})$, where α is an angle and $\hat{\mathbf{v}} = \begin{bmatrix} \hat{v}_x & \hat{v}_y & \hat{v}_z \end{bmatrix}^{\mathrm{T}}$ is a unit vector, can be written as:

$$R(\alpha, \hat{\mathbf{v}}) = \begin{bmatrix} \hat{v}_x^2 V_\alpha + C_\alpha & \hat{v}_x \hat{v}_y V_\alpha - \hat{v}_z S_\alpha & \hat{v}_x \hat{v}_z V_\alpha + \hat{v}_y S_\alpha \\ \hat{v}_x \hat{v}_y V_\alpha + \hat{v}_z S_\alpha & \hat{v}_y^2 V_\alpha + C_\alpha & \hat{v}_y \hat{v}_z V_\alpha - \hat{v}_x S_\alpha \\ \hat{v}_x \hat{v}_z V_\alpha - \hat{v}_y S_\alpha & \hat{v}_y \hat{v}_z V_\alpha + \hat{v}_x S_\alpha & \hat{v}_z^2 V_\alpha + C_\alpha \end{bmatrix}, \tag{2.5}$$

where $V_\alpha := 1 - cos(\alpha)$, $C_\alpha := cos(\alpha)$, and $S_\alpha := sin(\alpha)$.

After the body vectors $b_j(\theta)$ are determined from Equation 2.3 and assuming that the N-terminus atom is located at the origin, the position vectors of the atoms belonging to the backbone chain, which are located in the k^{th} peptide plane, are computed from

$$r_i(\theta) = \sum_{j=1}^{i} b_j(\theta), \quad 1 \leq i < 2N - 1, \tag{2.6}$$

where the indices i = 2k - 1 and i = 2k are associated with the N and alpha-Carbon atoms, respectively.

The zero position for the conformation of the protein molecule refers to a linear structure in which all the amino acid peptide nano-linkages lie on the same plane (i.e., a completely stretched protein chain with dihedral angle vector $\theta = 0 \in \mathbb{R}^{2N}$). On the other hand, the zero position for the N-terminus nitrogen atom means that this atom is treated as the fixed base of the mechanism located at $[0, 0, 0]^{\mathrm{T}}$. The reason for fixing the position of the N-terminus nitrogen atom at the origin is that it is only the changes in the conformation vector of the protein molecule that result in changes of the three-dimensional structure of the molecule independent of the choice of the N-terminus nitrogen atom base position.

2.5.3 Folding according to the KCM iteration

The KCM approach for modeling the protein folding process pioneered by Kazerounian and collaborators is based on the experimental fact that the inertial forces can be neglected in the folding process (see, e.g., [78; 85; 86; 87]). Instead, the pro-

tein chain dihedral angles vary under the kinetostatic influence of the van der Waals and electrostatic interatomic forces in the protein molecules. Consequently, in the KCM framework, the dihedral angle variation about the alpha-Carbon atoms at each molecule individual conformation is proportional to the effective torques acting on the peptide chain.

Considering a peptide chain with Na atoms and N - 1 peptide planes with the configuration vector $\theta \in Q$ and denoting the Cartesian position of any two single atoms a_i, a_j belonging to the molecule chain by $r_i(\theta)$, $r_i(\theta)$, their distance can be computed from $d_{ij}(\theta) := |r_i(\theta) - r_j(\theta)|$.

It is remarked that the number of atoms in the main backbone chain of the protein molecule (ignoring the side chains and the individual hydrogen atoms connected to alpha-Carbon atoms which are not in the peptide planes) is equal to Na = 5N + 8, where the added constant takes into account the number of atoms in the N-terminus and C-terminus.

Furthermore, we denote the respective electrostatic charges of a_i, a_j by q_i, q_j, their van der Waals radii by R_i, R_j, their van der Waals distance by $D_{ij} = R_i + R_j$, their dielectric constant by ϵ_{ij}, and their potential well depth as $\in_{ij}$.

Finally, we let w_{ij}^{elec} and w_{ij}^{vdw} represent the weight factors for the electrostatic and van der Waals forces between the two atoms a_i, a_j, respectively. All these parameters are provided in [84] and its references. Under these considerations, the molecule aggregated free energy can be computed from

$$\mathcal{G}(\theta) := \mathcal{G}_{\text{elec}}(\theta) + \mathcal{G}_{\text{vdw}}(\theta), \tag{2.7}$$

where,

$$\mathcal{G}^{\text{elec}}(\theta) = \sum_{i=1}^{N_a} \sum_{j \neq i} \frac{w_{ij}^{\text{elec}}}{4\pi\varepsilon_{ij}} \frac{q_i q_j}{d_{ij}(\theta)} \tag{2.8}$$

is the molecule potential energy resulting from the interatomic electrostatic interactions, and

$$\mathcal{G}^{vdW}(\theta) = \sum_{i=1}^{N_a} \sum_{j \neq i} w_{ij}^{vdW} \in_{ij} \left[\left(\frac{D_{ij}}{d_{ij}(\theta)} \right)^{12} - 2 \left(\frac{D_{ij}}{d_{ij}(\theta)} \right)^{6} \right] \tag{2.9}$$

is the molecule potential energy due to the van der Waals interactions. The resultant Coulombic and van der Waals forces on each atom a_i, $1 \leq i \leq N_a$, can be computed from $F_i^{elec}(\theta) = -\nabla_{r_i} \mathcal{G}^{elec}$ and $F_i^{vdw}(\theta) = -\nabla_{r_i} \mathcal{G}^{vdw}$, respectively. It is remarked that $\nabla_{r_i} \mathcal{G}_j$ where j = elec or j = vdw, is the gradient of the potential function $\nabla_{r_i} \mathcal{G}_j$ with respect to the position vector r_i.

The KCM-based folding process is performed according to a successive numerical iteration up to the moment that all the kinetostatic torques converge to a local minimum on the aggregated free energy landscape. To perform this numerical iteration, one can compute the effective forces and torques acting on each of the N - 1 peptide planes, which are the rigid nano-linkages of the protein kinematic mechanism and appending them in the generalized force vector $\mathcal{F}(\theta) \in \mathbb{R}^{6N}$.

Using a proper mapping, it is possible to map the generalized force $\mathcal{F}(\theta)$ to the equivalent torque vector influencing the configuration vector θ. Specifically, the vector $\tau(\theta) \in \mathbb{R}^{2N}$, which is the overall joint torques resulting from the interatomic forces in the protein kinematic structure, and can be computed according to

$$\tau(\theta) = \mathcal{J}^T(\theta) \mathcal{F}(\theta), \tag{2.10}$$

where the Jacobian matrix $\mathcal{J}^T(\theta) \in \mathbb{R}^{6N \times 2N}$ is determined by the kinematic structure of the protein chain at conformation θ (see [59; 78] for the calculation details). It is remarked that the vector $\mathcal{F}(\theta)$ is generated by the torques and forces acting on the peptide planes at each conformation vector θ.

Starting from the initial unfolded conformation θ_0, the difference equation

$$\textbf{KCM Iteration: } \boldsymbol{\theta}_{k+1} = \boldsymbol{\theta}_k + \frac{h}{|\boldsymbol{\tau}(\boldsymbol{\theta}_k)|_\infty}\boldsymbol{\tau}(\boldsymbol{\theta}_k), \tag{2.11}$$

describes the KCM-based numerical iteration due to Kazerounian and his collaborators, where the non-negative integer k determines the iteration number and h is a positive real constant equal to the maximum magnitude of the dihedral angle rotation in each step. Starting from an unfolded conformation, the KCM iteration in Equation 2.11 gives rise to the protein folding pathway data. A flowchart of the successive kinetostatic folding iteration is depicted in Figure 2.3. The most computationally intensive procedure at each conformation of the protein molecule (highlighted in red) consists of the electrostatic and van der Waals force computations.

In particular, the protein molecule backbone folding pathway trajectory is the dihedral angle vector series $\{\theta_k\}_{k=0}^{Ns}$, with $\theta_u := \theta_0$ corresponding to the initial unfolded conformation and $\theta_f := \theta_{Ns}$ corresponding to the final folded conformation.

The KCM framework also renders itself to control input synthesis interpretations. For instance, it has been shown in [7] that entropy-loss constraints during protein folding can be encoded in the KCM framework using nonlinear optimization-based control algorithms (see the flow chart in 2.3 here below).

In this method we consider the time series associated with the dihedral angle vector folding pathway generated by the robotics-based KCM numerical iteration in 2.11 or its variations (see, e.g., [7; 65]). The dihedral angle pathway datasets can also be generated by other means such as all-atom molecular dynamics simulations, e.g., GROMACS [88]. The sonification methodology proposed can also be applied to such pathway datasets.

The most computationally intensive step in each iteration of this process, occurring at every conformation of the protein molecule, involves the computation of

electrostatic forces and van der Waals interactions between atoms. These force calculations are critical for accurately simulating the folding pathways of protein molecules. When interatomic forces are computed exactly, the computational complexity for a molecule containing N_a atoms grows quadratically, i.e., it follows an order of $O(N_a^2)$ [89]. This quadratic growth in complexity is a direct result of the need to evaluate the interactions between every pair of atoms, which becomes increasingly expensive as the number of atoms increases.

The computational complexity of numerical algorithms can be defined using big O notation, as follows: consider any two real-valued functions $h_1(\cdot)$ and $h_2(\cdot)$; if there exists a real number $a_0 > 0$ and the real number z_0 such that the inequality $|h_1(z)| \leq a_0|h_2(z)|$ is satisfied for all $z \geq z_0$, then we say that $h_1(z) = O(h_2(z))$. Moreover, to encode more physical constraints in protein folding numerical simulations, such as entropy-loss constraints [7], it is necessary to solve a box-constrained convex quadratic program (QP) at each conformation of the protein molecule. The computational cost of such a convex QP using a state-of-the-art interior-point QP solver is of order $O(N^3)$ [90], where there are $N - 1$ peptide planes in the protein backbone chain.

Also, instead of using traditional methods for simulating protein folding, such as those using KCM which face computational inefficiencies when paired with explicit Euler integration methods, we can use one of the recent advancements in numerical integration, such as the development of the pseudo-transient continuation (ψTC) method [2], which offers a more efficient approach compared to those with integration step requiring intensive calculations of interatomic forces and the incorporation of physical constraints, which becomes computationally expensive. This method, which is an expansion of a preliminary version presented as a conference poster [1] adapts step sizes based on underlying dynamics and proximity to a steady state, significantly improving convergence and stability properties when applied to kinetostatic protein folding. Importantly, ψTC has proven to reduce the number of computational steps

required, offering a faster and more accurate way to simulate these complex kinematic motions compared to traditional KCM approaches reliant on fixed step sizes.

The explicit ψTC integration with fixed step size for solving the PFPCP can be described using the following flowchart:

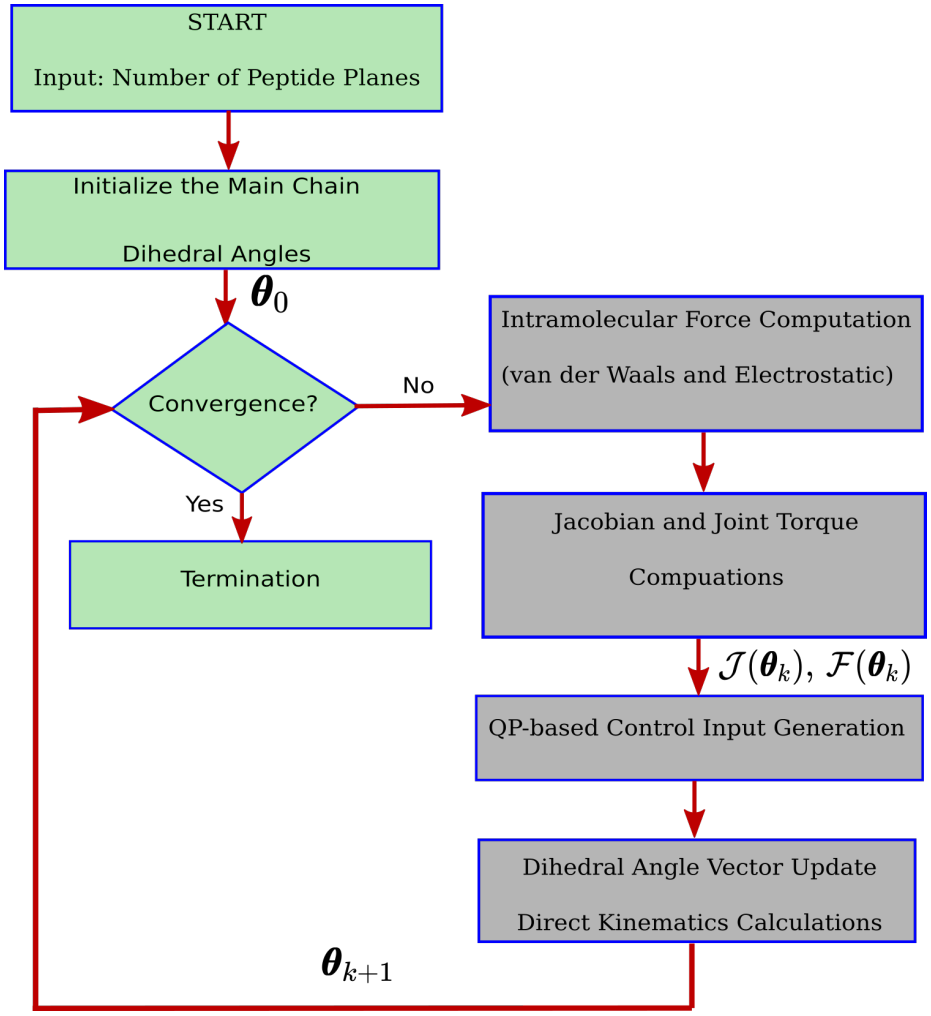

Figure 2.3: The flow chart associated with the KCM iteration with entropy-loss constraints encoded in the protein folding process (see [7] for further details). Such iterative KCM-based numerical algorithms give rise to the protein folding pathway datasets. The objective of this method is the sonification of such folding pathway dihedral angle trajectories.

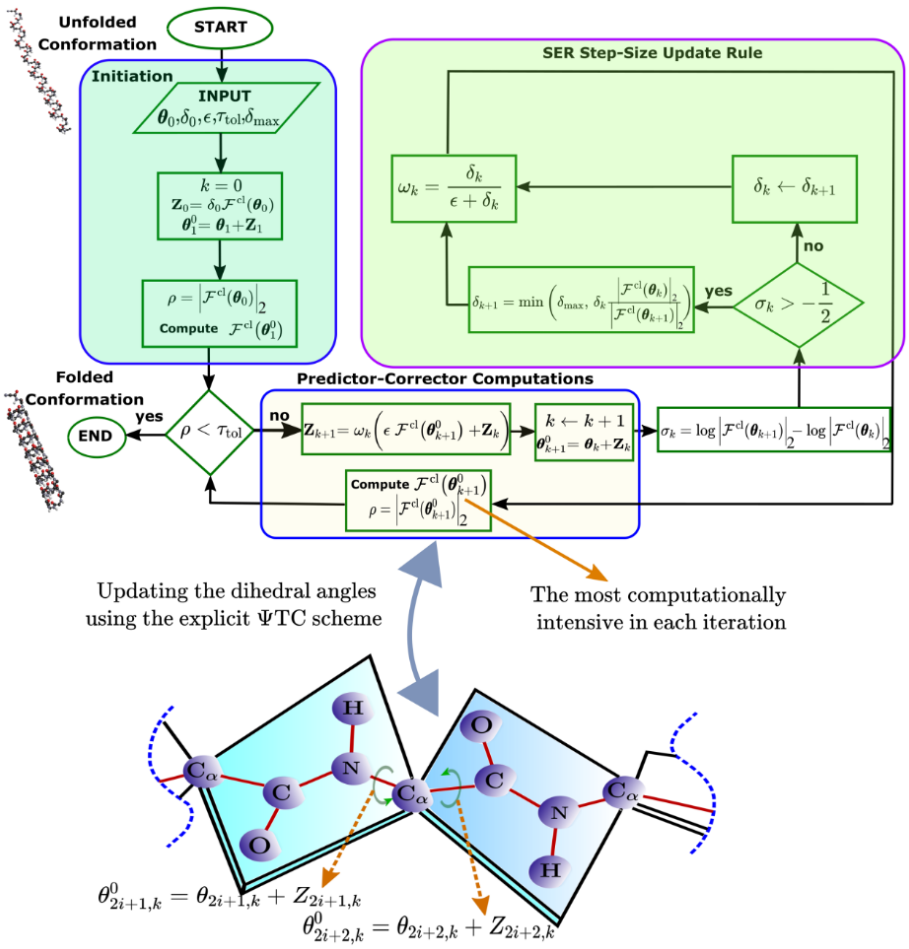

Figure 2.4: Flowchart of the proposed explicit ψTC integrator for computing protein folding pathways in kinetostatic folding simulations. The ψTC algorithm consists of four main steps: (Step 1) Initiation; (Step 2) Predictor–Corrector Computations; (Step 3) Checking Convergence; and, (Step 4) SER-based Step Size Update. In the ψTC integration scheme with a fixed step size, (Step 4) is skipped.

CHAPTER III

Redundant Robots, Robotic Teams, and Their Kinematic Structure

3.1 Introduction

In the field of robotics, redundancy serves as a fundamental design principle that significantly enhances a robot's ability to perform tasks with greater flexibility, adaptability, and fault tolerance. Redundancy refers to the presence of more degrees of freedom than are minimally required to achieve a specific task, which offers a multitude of advantages in terms of task versatility and robust performance in complex environments. This chapter explores two distinct forms of redundant robotic systems: hyper-redundant robots and teams of mobile robots.

3.2 Hyper-Redundant Robots

3.2.1 Introduction

Hyper-redundant robots [91], often referred to as snake-like robots, are characterized by their large or infinite number of degrees of freedom. This high degree of redundancy allows these robots to achieve remarkable flexibility and adaptability, making them suitable for navigating through constrained, and complex environments

where standard robots would encounter difficulties operating in such situations.

3.2.2 Kinematic Structure of Hyper-Redundant Robots

The kinematic structure of hyper-redundant robots is designed to mimic continuous and versatile movements such as snake and worm motion. These robots have typically a sequential chain-like structure from the base to the end-effector as shown in 3.1 composed of a series of interconnected rigid links denoted by $L_i, 0 \leq i \leq n$ joined together with universal joints $U_i, 0 \leq i \leq n$.

The kinematic structure of hyper-redundant robots is different from that of robot manipulators. While conventional robots often rely on a limited number of joints and links to achieve their movements, hyper-redundant robots utilize a large number of smaller, often identical, rigid links. These links are connected by universal joints, also known as U-joints, which provide two rotational degrees of freedom per joint allowing the rotation of each rigid link around two independent, perpendicular axes. The universal joints enable the links to rotate in multiple directions, allowing for smooth and continuous curvature along the length of the robot. This flexibility is essential for the robot's ability to operate through tight spaces and bend around obstacles.

The use of universal joints ensures that the robot can achieve a high degree of dexterity and range of motion. This is particularly important in many applications [92; 93] such as medical surgery [94], search and rescue missions [95], and industrial inspection [96; 97], where the robot must navigate through complex and variable environments.

Advanced algorithms and computational techniques are employed to solve the inverse kinematics problem [98; 99; 100], which involves determining the necessary joint angles to achieve a specific end-effector location or trajectory. However, designing and controlling hyper-redundant robots, managing their complexity, and ensuring smooth and precise overall behavior and movements remain a significant challenge. Current

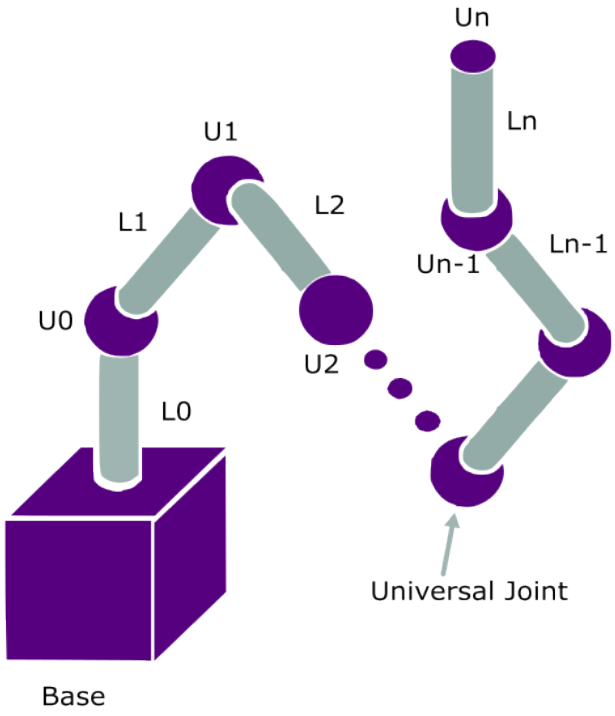

Figure 3.1: The kinematic Structure of a Hyper-Redundant robot manipulator consisting of rigid body links Li and universal joints Ui. Ui is the i-th 2DOF revolute joint.

research predominantly focuses on traditional visual feedback systems for monitoring and controlling these robots, allowing operators to visually track the robot's movements and make necessary adjustments based on visual data analysis. Yet, given the complex kinematic structures and the vast amount of real-time data generated by hyper-redundant robots, visual feedback systems often fail to maximize their effectiveness and performance. These robots are designed to navigate complex, constrained environments, such as inside pipes, around obstacles, or within the human body during surgery. In such scenarios, maintaining a clear line of sight for visual monitoring can be challenging, if not impossible. Due to the complex and obscured paths these robots must traverse, the operators may not always have access to comprehensive

visual data. This limitation can result in delays in movement correction, reduced precision and effectiveness, and a higher likelihood of errors, eventually impeding the robot's full potential. These limitations highlight the need for alternative feedback mechanisms, such as sonification, to enhance the robot's functionality and effectiveness in challenging environments.

Despite the extensive research on hyper-redundant robots for their distinctive kinematic structures and applications in complex environments, and the widespread utilization of sonification across various fields to enhance data interpretation and provide real-time feedback, the convergence of these two technologies remained largely unexplored in the past literature. No existing studies or applications have investigated the potential benefits and use of sonification that could be applied to hyper-redundant robots to improve their control and performance.

In summary, hyper-redundant robots represent a significant advancement in robotic design and functionality. Their kinematic structure, characterized by a large number of segments joined together with universal joints, provides exceptional flexibility and adaptability for their operation. These features enhance hyper-redundant robots' effectiveness in navigating complex environments and executing tasks requiring a high degree of dexterity and precision. As the development of these robots continues, their applications and capabilities are also expanding, offering innovative solutions to challenges across various fields such as science and engineering. Despite the extensive amount of data that hyper-redundant robots can generate, alternative feedback systems, such as sonification, hold promise for providing new insights into the exploration and advancement of these robots.

3.3 Team Of Mobile Robots

3.3.1 Introduction

A team of mobile robots (example shown in figure 3.2) employs a distributed form of redundancy. Instead of relying on a single robot with many joints or actuators to perform complex tasks, the team of mobile robots involves multiple robots, each operating with a smaller number of DOF, working together toward a shared objective or even distinct objectives. The redundancy in this system is not internal to any one robot but is distributed across the entire team, enabling a more flexible and scalable approach to problem-solving.

Figure 3.2: A team of OMRON Mobile robots: LD-250, LD-105CT, and LD-90.

3.3.2 Kinematic Structure of a Team of Mobile Robots

The kinematic structure of a team of mobile robots refers to how each robot in the group is engineered to move and interact within its environment, and how these movements are collectively coordinated to achieve a common goal. While the kinematics of a single robot typically involves a sequence of joints, links, and actuators

that define how it moves, in a team of robots, the kinematic structure is spread across multiple independent units. Each of these robots has its own kinematic design, but when working as a team, they combine their movements to perform complex, coordinated tasks.

In teams of mobile robots, the robots may differ in their specific kinematic structures depending on their type and function. For example, wheeled robots [101] often utilize differential drive systems, omnidirectional wheels, or car-like steering mechanisms. These systems enable the robot to move efficiently on flat surfaces. Wheeled robots typically have two degrees of freedom—translational movement along the ground plane and rotational movement around their vertical axis. Their ability to navigate smooth surfaces makes them ideal for tasks in structured environments like warehouses or factory floors [101].

On the other hand, legged robots [102] have more complex kinematic systems. Each leg can have multiple joints, allowing for greater freedom of movement. This higher number of joints provides these robots with enhanced flexibility and stability when navigating uneven or challenging terrain [103]. The kinematics of legged robots are designed to mimic the gait of animals, making them suitable for environments that are too rugged for wheeled robots.

Similarly, aerial robots [104] —such as drones—operate in three-dimensional space and typically have six degrees of freedom. These include three translational degrees (movement along the x, y, and z axes) and three rotational degrees (pitch, roll, and yaw). Their ability to move in all directions and rotate in space allows them to perform complex maneuvers, making them well-suited for tasks like aerial mapping, inspection, or delivering payloads [105].

When these different types of mobile robots collaborate, the overall kinematic structure of the team reflects the combined capabilities of each unit which is known as distributed kinematics. The multi-robot kinematics refers to the collective kinematic

behavior of multiple independent robotic units working together in a coordinated system, where each robot has its own kinematic structure and degrees of freedom, but the overall behavior of the group is defined by their combined movements and interactions This form of distributed kinematics allows the team to achieve behaviors that an individual robot might not be capable of. For instance, in a search-and-rescue mission, legged robots might navigate rough terrain while wheeled robots handle transportation tasks in flat areas, and drones provide aerial surveillance. The interaction and coordination between these robots, each with its distinct kinematic properties, create a robust and adaptable system.

This distributed nature of the kinematic structure in a team of mobile robots offers significant advantages. It allows the team to scale easily, adapting to larger or smaller tasks by simply adding or removing robots from the group. The team can also remain highly flexible, re-configuring itself to respond to dynamic environments or unexpected challenges. Additionally, because the robots are often able to function autonomously while coordinating with each other, these teams can operate with a degree of fault tolerance [106]. If one robot fails, the others can adjust their tasks and maintain overall mission performance.

Understanding the kinematic structure of a team of mobile robots is crucial for designing systems that are efficient, adaptable, and capable of working together in a range of coordinated tasks. Whether for exploration in unknown environments [107], transporting goods [108; 109], or performing distributed sensing over a large area [110; 111], the effectiveness of the team depends on the careful coordination of each robot's movements. By leveraging the strengths of different robotic types and optimizing their collaboration, such teams can perform tasks with a high level of autonomy and reliability, even in complex and uncertain conditions.

Additionally, the concept of sonification—the process of using sound to represent data—offers a novel and intuitive way to analyze and understand the complex dy-

namics within robotic systems. By converting key parameters such as movement, task execution, and coordination into sound, sonification transforms abstract or difficult-to-visualize data into auditory representations. This can provide valuable insights into the performance, redundancy, and interaction patterns of both individual robots and teams of robots.

In the next chapters, the potential of sonification as a tool for both hyper-redundant robots and teams of mobile robots is explored. By converting robotic behaviors and interaction patterns into sound, sonification offers an intuitive medium for interpreting complex robotic systems. It allows researchers and operators to perceive and monitor performance and behavior in a way that is immediate and often more accessible than visual data or numerical outputs, especially in dynamic or uncertain environments. This exploration demonstrates how sound can be exploited to enhance our understanding of redundancy, coordination, and overall system functionality, providing an additional layer of insight into robotic performance and interaction.

CHAPTER IV

Wave Space Sonification of The Folding Pathways of Protein Molecules Modeled as Hyper-Redundant Robotic Mechanisms

4.1 Introduction

To execute a variety of important biological functions such as force generation in motor proteins and protein-ligand binding, protein molecules go under conformational transitions between two or more native conformations through the processes of folding and unfolding [79]. Numerical algorithms, which can predict the three-dimensional structures of folded protein molecules and the pathways/transitions through which proteins fold/unfold, have an integral role in computer-aided drug discovery [80] and in designing protein-based nanomachines [81; 82].

Despite their high computational burden, physics-based approaches relying on physical first principles are still the preferred way to numerically compute the protein folding pathways [112]. To address the high computational times associated with the physics-based approaches, the promising framework of kinetostatic compliance method (KCM), pioneered by Kazerounian, Ilies, and collaborators, models protein molecules as mechanisms with a large number of rigid nano-linkages form-

ing a hyper-redundant robot, which fold under the nonlinear effect of interatomic forces [59; 60; 61; 62]. Since its advent, the KCM framework has been successfully applied to investigating the role of hydrogen bond formation in protein kinematic mobility problems [63] and design of peptide-based molecular nano-linkages [82]. Furthermore, using nonlinear optimization-based control algorithms, it has been shown that entropy-loss constraints during protein folding (see, e.g., [64] for the importance of these constraints) can be encoded in the KCM framework [7]. Finally, Chetaev instability analysis can be utilized for synthesizing unfolding control inputs (e.g., computing proper optical tweezer forces for unfolding in desired directions) for the KCM-based model of protein molecules [65].

Numerical simulation of protein folding for computing the molecule conformational changes generates an overwhelming amount of data. Accordingly, one is still left with the problem of representing these large folding pathway datasets. Despite the recent advent of visualization techniques developed for representing the protein folding pathway datasets (see, e.g., [66]), their sonification, where non-speech audio is utilized for conveying information, has remained an unaddressed question. In the presented method, we employ the recent Wave Space Sonification (WSS) paradigm due to Hermann [9] to answer the challenging question of generating a non-speech auditory representation of large datasets associated with protein folding pathways (see Figure 4.1). WSS is a class of sonification techniques developed for high-dimensional data (indexed by time or space), which relies on generating auditory data representation by scanning a scalar field along a data-driven trajectory of interest. In this method, we demonstrate that WSS provides a novel approach for creating non-speech auditory representations of protein folding pathway datasets through a data-driven audio signal sampling, which is afforded by a high-dimensional scalar sound field defined on the dihedral angle space of protein conformations.

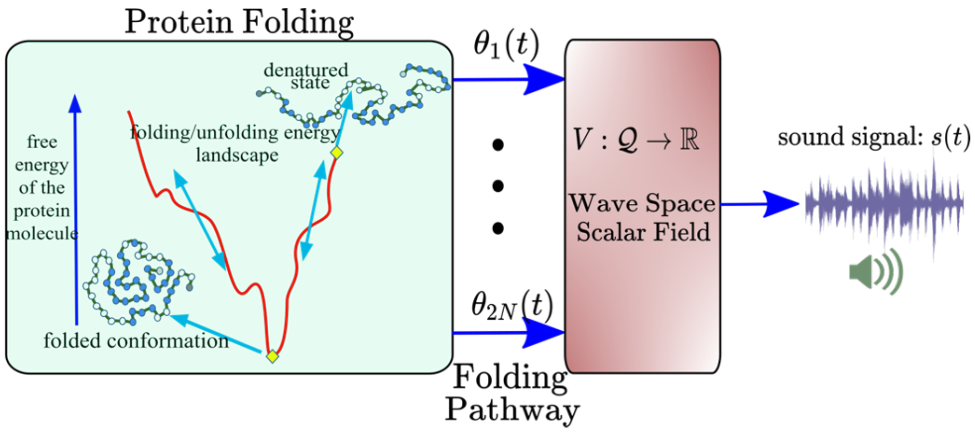

Figure 4.1: A novel WSS-based technique for creating non-speech auditory representations of protein folding pathway datasets is proposed. Such sonification is achieved through a data-driven audio signal sampling, which is afforded by a high-dimensional scalar sound field defined on the dihedral angle space of protein conformations.

4.2 Contributions of the Method

The contributions of this method are as follows. First, despite the innovative application of numerous sonification techniques to the problem of translating protein structural/vibrational data to musical compositions (see, e.g., [21; 55; 56; 57; 58]), the problem of folding pathway sonification is still an open problem. This article, relying on the WSS framework, provides a solution to this problem for the first time. Our non-speech auditory representation framework for protein folding processes complements the recent line of work by Ferina and Daggett for visualization of folding [66]. Second, this method contributes to the field of robotic trajectory sonification, which is still in its early development stages. Despite the application of sonification techniques to several human-robot interaction (HRI) problems [67; 68; 69], the problem of sonification of joint space trajectories for robots with a very large number of degrees of freedom has remained unaddressed. The proposed sonification methodology

paves the path for the sonification of robotic trajectories in other contexts such as soft robotics [113; 114] and industrial collaborative multi-robot systems [5; 115; 116], where the robotic system operation generates an overwhelming amount of motion data.

Notation: Given the real vector $\mathbf{x} \in \mathbb{R}^M$, we denote the Euclidean and the maximum norms of the vector by $\|\mathbf{x}\| := \sqrt{\mathbf{x}^\top \mathbf{x}}$ and $\|\mathbf{x}\|_\infty := \max_{1 \leq i \leq M} |x_i|$, respectively. Given a function $f \colon U \to V$ with domain U and codomain V, we let $f \colon u \mapsto v$ denote $f(u) = v$ for all $u \in U$ and $v = f(u) \in V$. Finally, by $f(\cdot)$, we mean that f is a function without identifying its domain and codomain.

4.3 Wave Space Sonification of the folding Pathways of Protein Molecules Methods

In this section we provide our solution to the problem of sonification of datasets associated with conformational changes of protein molecules during folding. Our solution to this problem is based on the Wave Space Sonification (WSS) framework due to Hermann [85]. After providing the problem statement and the formal definition of WSS, we elaborate on the three WSS elements needed in the context of protein folding. Next, we present two WSS-based solutions to this problem, namely, canonical WSS and sample-based WSS in Sections 4.5.1 and 4.5.2, respectively.

4.4 Problem statement

Consider a protein molecule with a backbone chain consisting of N - 1 peptide planes modeled as a hyper-redundant robotic mechanism (see Section 2.5.1 for such a robotics-inspired modeling approach). Consider the protein molecule backbone

folding pathway trajectory, namely, the dihedral angle vector time-indexed trajectory $\theta(\mathrm{t})$, with $\theta_u := \theta(0)$ corresponding to the initial unfolded conformation and $\theta_f := \theta(T_f)$ corresponding to the final folded conformation. Find a non-speech auditory representation of the folding pathway trajectory given by $\theta(\cdot)$.

4.5 Solution To The Sonification of the folding Pathways of Protein Molecules Problem

In this section we present our wave space sonification solution to the Sonification of the folding Pathways of Protein Molecules stated in Section 4.4 by presenting two classes of WSS functions. The first class uses explicit algebraic expression for embedding the folding trajectories of the protein molecules, whereas, the second class defines the wave space function through available samples from recorded sound signals.

4.5.1 Canonical wave space sonification Solution

In this section we present a canonical WSS-based scalar field for solving the stated sonification problem in Section 4.4. Canonical wave space functions, according to Hermann [9], are explicit algebraic expressions that utilize the data-driven trajectory under study for embedding in the wave space. In our context, these trajectories are given by time-indexed vectors of the form $\theta(\mathrm{t})$, which are the dihedral angle vector folding pathway trajectories. For solving the sonification problem using the canonical WSS approach, we utilize a canonical wave space function $V_c : \mathrm{Q} \to \mathrm{R}$, which is a sum-of-sinusoids with conformation-dependent frequencies. In particular, we let

$$V_c(\theta) := \frac{A_0}{2N} \sum_{i=1}^{2N} \sin\left(2\pi f_0 h(\theta)\theta_i\right) \tag{4.1}$$

where the positive constant f_0 represents a desired base frequency, A_0 is a positive design parameter, and

$$h(\theta) = \exp\left(-\frac{\|\theta - \theta_f\|}{\sigma_0^2 \|\theta_u - \theta_f\|}\right) \tag{4.2}$$

is a frequency weighting function, where $\sigma 0 \in (0, 1)$ is some positive constant less than one. We are using an exponential frequency resolution function $h(\theta)$ given by 4.2 because of the logarithmic nature of the way that the human auditory system perceives sounds (see, e.g., [117] for further information on how humans perceive sound). Indeed, two pure-tone sounds, which slightly differ from each other in their frequencies are not heard as separate notes by a single human ear. Since we are interested in making the listener clearly perceive the protein folding process from an unfolded conformation to a folded one, such an exponential frequency resolution function is utilized within the proposed wave space function.

The significance of the proposed canonical wave space function in 4.1 and 4.2 is the generation of sounds with conformation-dependent frequencies. In particular, as the protein conformation approaches the final folded configuration θ_f from its unfolded initial conformation θ_u, sounds with higher frequency contents will be generated. The only design parameters for controlling the canonical wave space function in 4.1 and 4.2 are the base frequency f_0 and the parameter σ_0. To generate a sound file of duration T_s from a folding pathway of time duration T_f, we use the linear morphing function $M(t) = \frac{T_f}{T_s} t$. Therefore, the generated sound signal takes the following form

$$s(t) = \frac{A_0}{2N} \sum_{i=1}^{2N} \sin\left(2\pi f_0 h\left(\theta\left(\frac{T_f}{T_s}t\right)\right)\theta_i\left(\frac{T_f}{T_s}t\right)\right) \tag{4.3}$$

In Hermann's original work [9], the canonical wave space functions, which are written as sums-of-sinusoids, do not depend on the function $h(\theta)$ (or, equivalently, $h(\theta) = 1$ in Hermann's work). In this work, we are introducing the novel element of dependency of frequency components on the distance to desired locations in the dataset (here, folded and unfolded conformations of protein molecules). From this

perspective, our proposed wave space function in 4.1 and 4.2 can also be viewed as a hybrid of Hermann's canonical wave space function (because of being written in terms of algebraic functions) and of Hermann's data-driven localized wave space function (because of dependency on designated points in a given dataset).

4.5.2 Sample-Based Wave Space Sonification Solution

In this section we present a sample-based WSS scalar field for solving the stated sonification problem in Section 4.4. The key idea behind sample-based scalar fields is that instead of merely relying on mathematical functions as in their canonical counterparts in Section 4.5.1, one can define the wave space function through available samples from recorded sound signals [9]. Indeed, this point of view on wave space functions is motivated by the desire to generate acoustically more artistic and appealing sounds.

In the context of protein folding, datasets are given by time-indexed vectors of the form $\theta(t)$, which are the trajectories of the dihedral angle vector obtained from the folding process. For solving the sonification problem using the sample-based WSS approach, we utilize a sample-based wave space function $V : \mathcal{Q} \to \mathbb{R}$, which relies on recorded sounds, e.g., pieces of classical music. In particular, considering the collection of sound files $\dot{x}_i : t \mapsto \dot{x}_i(t), \quad 1 \leq i \leq 2N$, we let

$$V_\circlearrowleft(\boldsymbol{\theta}) := \frac{1}{2N} \sum_{i=1}^{2N} \circlearrowleft_i(c_i(\boldsymbol{\theta})) \tag{4.4}$$

where $c_i : \mathcal{Q} \to \mathbb{R}, \quad 1 \leq i \leq 2N$, are nonlinear scaling functions. In this article, we let these mappings have the conformation-dependent form

$$c_i(\boldsymbol{\theta}) := \alpha_i \Big\{ \lambda_{0,i} \exp\Big(\frac{-\|\boldsymbol{\theta} - \boldsymbol{\theta}_f\|}{\sigma_{0,i}^2 \|\boldsymbol{\theta}_u - \boldsymbol{\theta}_f\|} \Big) + \beta_i \Big\}, \tag{4.5}$$

where $\lambda_{0,i}$ and $\sigma_{0,i}$ are some positive constants to be chosen by the sound designer.

Having selected the design parameters $\lambda_{0,i}$ and $\sigma_{0,i}$ the constants α_i and β_i are given by

$$\beta_i = -\lambda_{0,i} \exp\big(\frac{-1}{\sigma_{0,i}^2}\big), \alpha_i = \frac{T_{s,i}}{\lambda_{0,i} + \beta_i}, \tag{4.6}$$

where $T_{s,i}$ is the duration of the file $\mathscr{s}_i(\cdot)$. the equality constraints in 4.6. ensure that $c_i(\boldsymbol{\theta}_u) = 0$ and $c_i(\boldsymbol{\theta}_u) = T_{s,i}$. In other words, the nonlinear scaling functions are guaranteed to map the initial unfolded conformation to time instant 0 in the sound file and the final folded conformation to time instant $T_{s,i}$, which corresponds to the duration of the i-th sound file $\mathscr{s}_{\mathscr{M}}(\cdot)$.

The significance of the proposed sample-based wave space function in equations 4.4–4.6 is the generation of sounds from available recordings $\mathscr{s}_i(\cdot)$ by scanning the scalar field $V_{\mathscr{s}}(\cdot)$ along the data-driven conformation trajectories of protein molecules during the folding process. Each of the sound files $\mathscr{s}_i$ is chosen arbitrarily and specific to the artistic flavor of the application at hand. For instance, they could be recorded by the sound designer in an ad hoc manner or as demonstrated in Section 4.6 sourced via other means (e.g., a piece of classical music). The nonlinear scaling functions $c_i(\cdot)$ in 4.5, $1 \leq i \leq 2N$, based on which the data-driven audio signal sampling is performed, guide the scanning process of the scalar field $V_{\mathscr{s}}(\cdot)$ using the molecule conformations during folding.

In Hermann's original work [9], the static sample-based wave space functions utilize linear scaling mappings of the form $c_i(\boldsymbol{\theta}) = c_i \cdot \theta_i$, $1 \leq i \leq 2N$. In this article, we are introducing a new type of nonlinear scaling function depending on designated conformations of protein molecules, namely, the folded $\boldsymbol{\theta}_f$ and the unfolded $\boldsymbol{\theta}_u$ conformations. From this perspective, our proposed sample-based wave space function in equations 4.4–4.6 can also be considered as a hybrid of Hermann's static sampling-based method (because of relying on recorded sound signals) and Hermann's

data-driven localized method (because of dependency on designated points in a given dataset).

4.6 Results

In this section, the results associated with the proposed sonification methodology applied to a peptide backbone chain with a dihedral angle space of dimension 82 is presented. All of the numerical implementation has been carried out in MATLAB R2018b by utilizing the PROTOFOLD I framework [78; 84] on an Intel® Core™ i7-6770HQ CPU@2.60GHz. Figure 4.2 depicts the folding process resulting from our numerical simulations. As expected from the KCM-based folding iteration the molecule aggregated free energy converges to a local minimum located on the folding energy landscape (see [78; 89] for further details). Furthermore, as can be seen from 4.2a, the protein molecule conformation converges to a helix from its unfolded initial configuration. We are interested in generating non-speech auditory representation of this process according to the problem statement in Section 4.4. Finally, 4.2b depicts two sample projected folding pathway curves with the red and green diamonds corresponding to the unfolded and folded conformations, respectively. Indeed, these two three-dimensional curves are the projections of the original folding pathway, which is embedded in a configuration space of dimension 82.

4.6.1 Canonical WSS Results

The canonical wave space sonification method proposed in 4.5.1 is applied to the folding pathway dataset associated with the protein backbone peptide chain whose folding process is depicted in Figure 4.2.

The five sound signals generated by the proposed canonical wave space function in Equation 4.1 and Equation 4.2 are depicted in Figure 4.3. The base frequency in all these canonical wave space functions is chosen to be $f_0 = 250$ Hz. Furthermore,

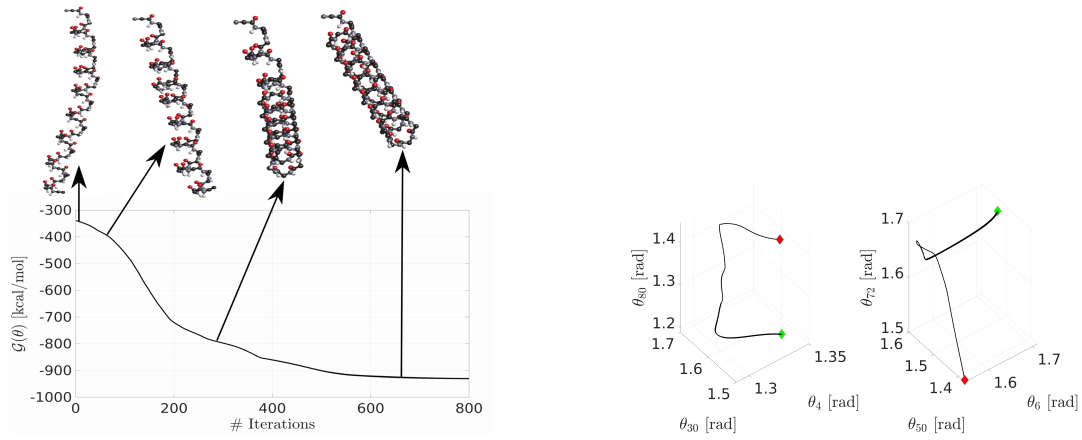

(a) (b)

Figure 4.2: The folding process of a protein peptide backbone chain with 82 DOFs: (a) the free energy of the molecule with its corresponding conformations along the folding pathway; and, (b) two sample 3D curves obtained by projecting the protein folding pathway on lower-dimensional spaces with the red and green diamonds corresponding to the unfolded and folded conformations, respectively.

the duration of the sound files, which is a tunable parameter, is selected as $T_s = 5$ seconds. Moreover, the design parameters σ_0 for generating these sounds signals (see 4.2 are chosen to be $\sigma_0 = 0.1$, $\sigma_0 = 0.15$, $\sigma_0 = 0.2$, $\sigma_0 = 0.3$, and $\sigma_0 = 0.4$, respectively. Finally, the parameter A_0 is set equal to 1 in all these sound signals.

The sepctrograms of the five sound signals generated by the proposed canonical wave space function are depicted in Figure 4.4. As expected from our sonification design methodology, while the conformation of the protein molecule approaches its final folded state, the frequency of the generated sound by the scalar field $V_c(\cdot)$ in Equation 4.1 increases according to the frequency weighting function given by Equation 4.2.

All the code used to generate the results of the Canonical WSS method presented in this section can be found in Appendix C. This includes the scripts for data processing, implementation of the sonification methodology, and the simulations carried out. Detailed comments and instructions are provided within the code to facilitate understanding and replication.

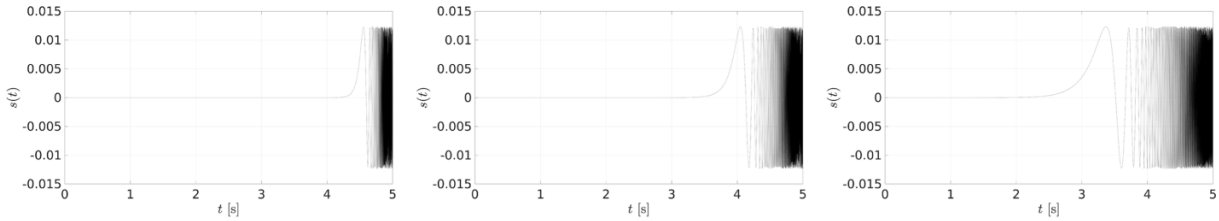

(a) $\sigma_0 = 0.1,\ f_0 = 250$ (b) $\sigma_0 = 0.15,\ f_0 = 250$ (c) $\sigma_0 = 0.2,\ f_0 = 250$

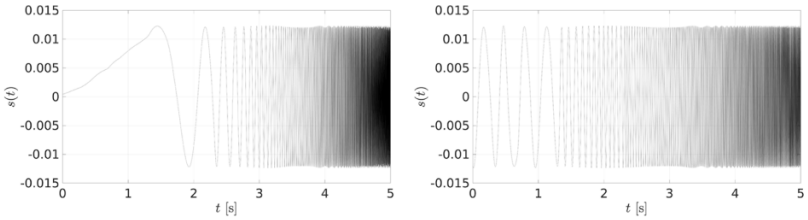

(d) $\sigma_0 = 0.3,\ f_0 = 250$ (e) $\sigma_0 = 0.4,\ f_0 = 250$

Figure 4.3: The sound signals generated by the proposed canonical wave space function in Equation 4.1 applied to a protein backbone peptide chain with 82 DOFs. As the conformation of the protein molecule approaches its final folded state, the frequency of the generated sound increases. The generated sound files (in .wav format) can be downloaded from https://dralirezamoha.github.io/proteinpathway/wssFoldingSoundFiles.zip

4.6.2 Sample-Based WSS Results

The sample-based wave space sonification method proposed in Section 4.5.2 was applied to the folding pathway dataset whose folding process is depicted in Figure 4.2. We have chosen a piece of Mozart's Alla Turca for applying our sample-based WSS method. This piece has been performed by Walter Gieseking and is available from his "Historic Broadcast Performances (1944–1950)" collection [8]. The original sound signal $\mathfrak{s}_{\mathscr{M}}(\cdot)$ and its spectrogram are depicted in Figure 4.5.

To determine the sample-based wave space function given by Equations 4.4-4.6, we need to determine the sound files $\mathfrak{s}_i(\cdot)$ and the scaling functions $c_i(\cdot)$. We have chosen all the sound files to be given by $\mathfrak{s}_i(\cdot) = \mathfrak{s}_{\mathscr{M}}(\cdot)$, where $\mathfrak{s}_i(\cdot)$ is the piece of Mozart's Alla Turca demonstrated in Figure 4.5. Furthermore, we have chosen all

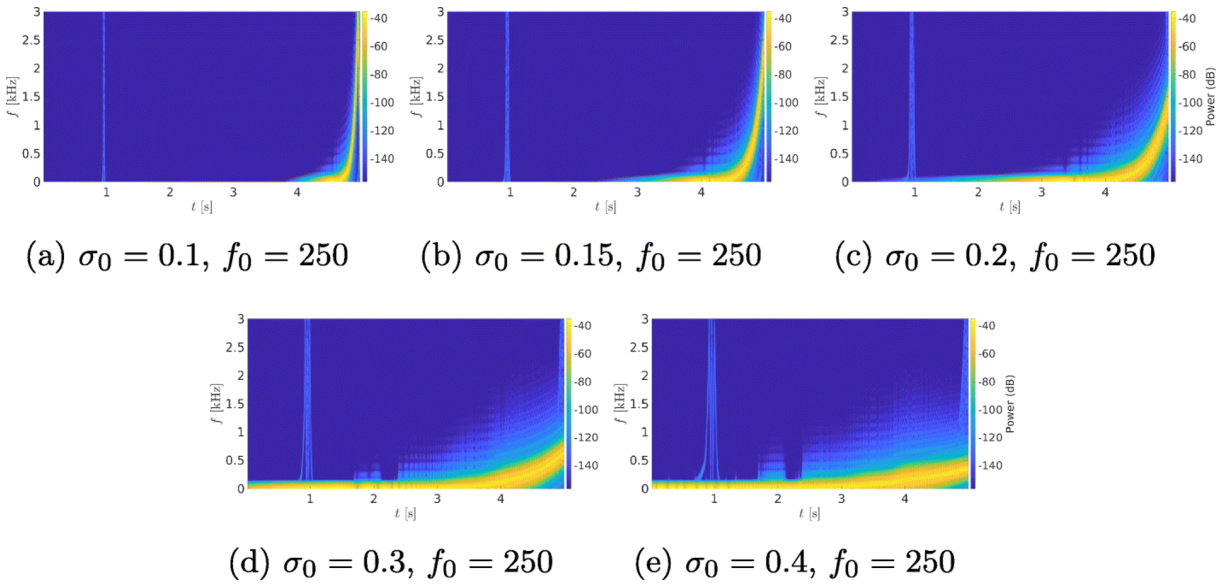

(a) $\sigma_0 = 0.1,\ f_0 = 250$ (b) $\sigma_0 = 0.15,\ f_0 = 250$ (c) $\sigma_0 = 0.2,\ f_0 = 250$

(d) $\sigma_0 = 0.3,\ f_0 = 250$ (e) $\sigma_0 = 0.4,\ f_0 = 250$

Figure 4.4: The spectrograms of the sound signals generated by the proposed canonical wave space function in (12) applied to a protein backbone peptide chain with 82 DOFs. As the conformation of the protein molecule approaches its final folded state, the frequency of the generated sound increases

the tuning parameters $f_{s,i}$ and $\sigma_{s,i}$ to be the same for the nonlinear scaling functions, which results in $c_i(\cdot) = c_0(\cdot)$, $1 \leq i \leq 2N$. Therefore, in this example, our scalar field takes the form $V_\jmath(\boldsymbol{\theta}) = \jmath_{\mathscr{M}}(c_0(\boldsymbol{\theta}))$, where $c_0(\boldsymbol{\theta}) := \alpha_0\{\lambda_0 \exp\left(\frac{-\|\boldsymbol{\theta}-\boldsymbol{\theta}_f\|}{\sigma_0^2\|\boldsymbol{\theta}_u-\boldsymbol{\theta}_f\|}\right) + \beta_0\}$.

Figure 4.6 depicts the result of applying our sample-based WSS method to the chosen piece of Mozart's Alla Turca. The resulting sound signals1 and the nonlinear scaling function $c_0(\cdot)$ along the protein folding pathway are demonstrated in the figure. In all the plots in Figure 4.6, the parameter λ_0 is chosen to be equal to 1. We have chosen three different values for σ_0, namely, 0.25, 0.5, 0.75, and 1. The spectrograms of the sound signals generated by the proposed sample-based wave space function are depicted in Figure 4.7. In the beginning, when the conformation of the peptide chain is far away from the final folded conformation, the scaling function $c_0(\cdot)$ varies very slowly resulting in sound patterns not familiar to the ear. This is specifically evident in the case of $\sigma_0 = 0.25$ and $\sigma_0 = 0.5$. This unnatural sound corresponds to the low-

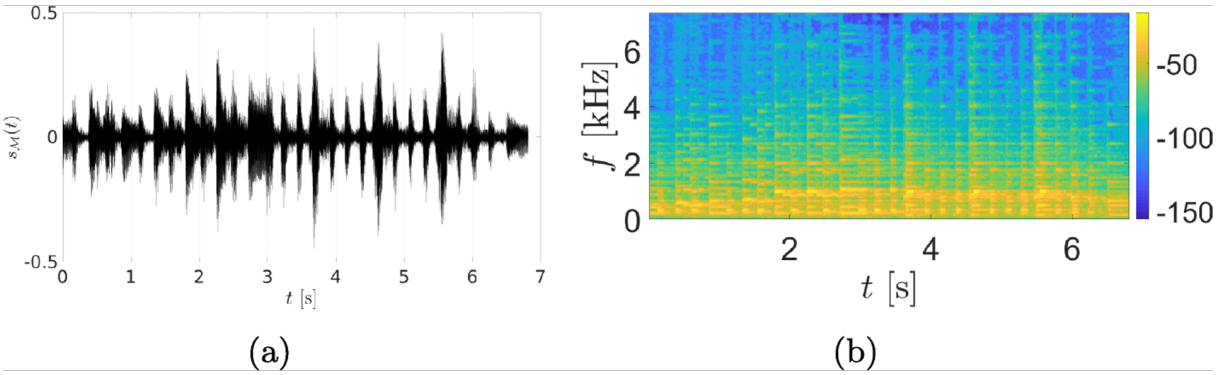

Figure 4.5: The music piece taken from Mozart's Alla Turca: (a) the original sound signal; and, (b) the spectrogram associated with the sound signal

frequency content of the generated sound as demonstrated by the spectrograms in Figure 4.7. As the peptide chain starts approaching its final folded conformation, the heard sound begins taking the familiar form of Mozart's All Turca. In other words, the listener hears a sound file that gradually takes a familiar auditory form as the protein backbone peptide chain approaches its final folded conformation. The transition to a familiar sound and emergence of an ordered music pattern also corresponds to the protein configurational entropy loss while the molecule converges to its native folded state (see, e.g., [87] for further details on entropy loss during protein folding).

All the code used to generate the results of the Sample Based WSS method presented in this section can be found in Appendix D. This includes the scripts for data processing, implementation of the sonification methodology, and the simulations carried out. Detailed comments and instructions are provided within the code to facilitate understanding and replication.

4.7 Discussion on the application of the proposed sonification method to other hyper-redundant robotic mechanisms

Sonification could provide an auditory means of conveying complex motion data, allowing users to perceive and interpret the robot's configuration changes in real-time. This would be especially useful for monitoring and controlling hyper-redundant robots, where visual feedback alone may be insufficient due to the large number of joints and the intricate nature of their movements. As discussed in Section 2.5.1, the KCM-based folding framework relies on describing the motion of protein molecules by modeling them as hyper-redundant robotic mechanisms consisting of numerous rigid nano-linkages that fold under the nonlinear effect of the protein molecule interatomic forces. The justification for such a modeling approach is the experimental observations verifying that the six atoms $C_\alpha - \mathrm{CO} - \mathrm{NH} - C_\alpha$ are coplanar in each of the protein-peptide planes (see Figure 2.2). Another notable fact is that each alpha-Carbon atom acts as a 2 DOF revolute joint playing the role of hinges in the kinematic mechanism as shown in Figure 2.1. Modeling the peptide planes as rigid links and treating the alpha-carbon atoms as revolute joints have been the basis for various robotics-inspired approaches in the literature that model protein molecules as hyper-redundant mechanisms. For instance, the robotic kinematics-based point of view on the structure of proteins can be seen in the line of work by Kavraki and collaborators (see, e.g., [52; 50]), and Kazerounian and collaborators (see, e.g., [51; 89]), to name a few. Another interesting fact is that the protein kinematic model described in Section 2.5.1 has the exact same kinematic structure as robotic manipulators with hyper degrees-of-freedom as described in the work of Mochiyama et al. (see, e.g., [118]). This type of kinematic modeling has also been used for multisection continuum robots (see, e.g., [119]). Indeed, considering a hyper-redundant robotic mechanism with configuration vector $\boldsymbol{\theta} \in \mathcal{Q}$, where $\mathcal{Q}$ is a manifold of dimension

N0, the time-indexed configuration vector $\boldsymbol{\theta(t)} \in \mathcal{Q}$ represents the joint time profile trajectories of the hyper-redundant robot. Therefore, the same problem statement presented in Section 4 can also be considered for such robots. The only difference with the protein folding setting presented in this application is the choice of designated configurations in the joint space of the robot. These designated configurations given by $\boldsymbol{\theta^*}$, instead of $\boldsymbol{\theta_u}$ and $\boldsymbol{\theta_f}$ in the case of protein molecules, can be generated by proper trajectory planning and obstacle avoidance algorithms designed for these hyper-redundant robotic mechanisms (see, e.g., [75]).

By mapping different aspects of the robot's motion—such as joint angles, speed, or proximity to obstacles—into distinct sound patterns, operators could develop an intuitive understanding of the robot's state without relying on detailed visualizations. This technique could streamline operations in environments where rapid decision-making is crucial, such as in medical robotics, search-and-rescue missions, or industrial applications, where the robot's ability to navigate and manipulate within tight spaces is vital. Additionally, integrating sonification with trajectory planning and obstacle avoidance algorithms could further enhance the robot's functionality by providing auditory cues that assist in anticipating or avoiding collisions, making the system more efficient and safer to operate. Thus, sonification has the potential to significantly improve both the real-time control and monitoring of hyper-redundant robotic systems.

4.8 Conclusion

In this project, we proposed a Wave Space Synthesis (WSS)-based solution to the sonification of protein folding pathway datasets. Sonification, or the process of transforming data into sound, provides a powerful alternative to visual representations, particularly for understanding complex, multi-dimensional systems like protein folding. By utilizing the WSS framework, we developed a systematic and structured

method to generate sounds from the dihedral angle folding trajectories of protein molecules. These folding pathways describe the angular movements between bonds within a protein as it transitions from an unfolded to a folded state. Given the complexity and high dimensionality of protein folding, we modeled these molecules as hyper-redundant robotic mechanisms—a type of robotic system known for its numerous degrees of freedom and flexibility, similar to the many rigid nano-linkages that define a protein's structure. This analogy allows us to treat protein molecules in a manner similar to highly flexible robots, where each bond in the molecule corresponds to a joint or linkage in the robotic model, and the folding pathways represent the trajectories of movement.

To demonstrate this sonification methodology, we applied it to the backbone chain of a protein molecule, which features a dihedral angle space with 82 dimensions. This means the folding process involves tracking a highly complex and multi-dimensional set of angular movements, making it challenging to visualize or represent through traditional means. To sonify this folding process, we employed two distinct wave space functions, each providing a different auditory perspective on the protein's behavior.

The first method used a canonical wave space function based on a sum of sinusoids. In this approach, the frequencies of the sound waves were directly influenced by the conformation, or shape, of the protein as it folded. By adjusting the sound frequencies based on the real-time dihedral angles of the molecule, we were able to audibly represent the dynamic transitions of the protein, with changes in pitch or tone reflecting specific shifts in the folding pathway. This provided an immediate auditory cue to the different stages of folding and allowed for a more intuitive understanding of the protein's structural transformations.

The second method employed a sample-based wave space function, where we used a well-known piece of classical music—Mozart's Alla Turca—to sonify the folding trajectories. In this case, the protein's angular movements were translated into variations

within the musical framework of the piece, creating an auditory experience that tied molecular motions to recognizable musical motifs. This artistic approach not only provided a unique way to interpret the data but also allowed for a more engaging and familiar sonification, linking molecular complexity to the world of music.

By combining both the canonical and sample-based approaches, we demonstrated the versatility of the WSS framework in representing highly complex molecular systems through sound. Sonifying the protein folding pathways not only provided a novel way to monitor the dynamic process of folding but also opened the door to new insights, enabling researchers to detect patterns and behaviors in protein folding that might be difficult to spot using traditional visual methods. Ultimately, this project highlights the potential of sonification as a tool for understanding the intricate behaviors of molecular systems, offering a fresh perspective on how we interpret and interact with high-dimensional biological data.

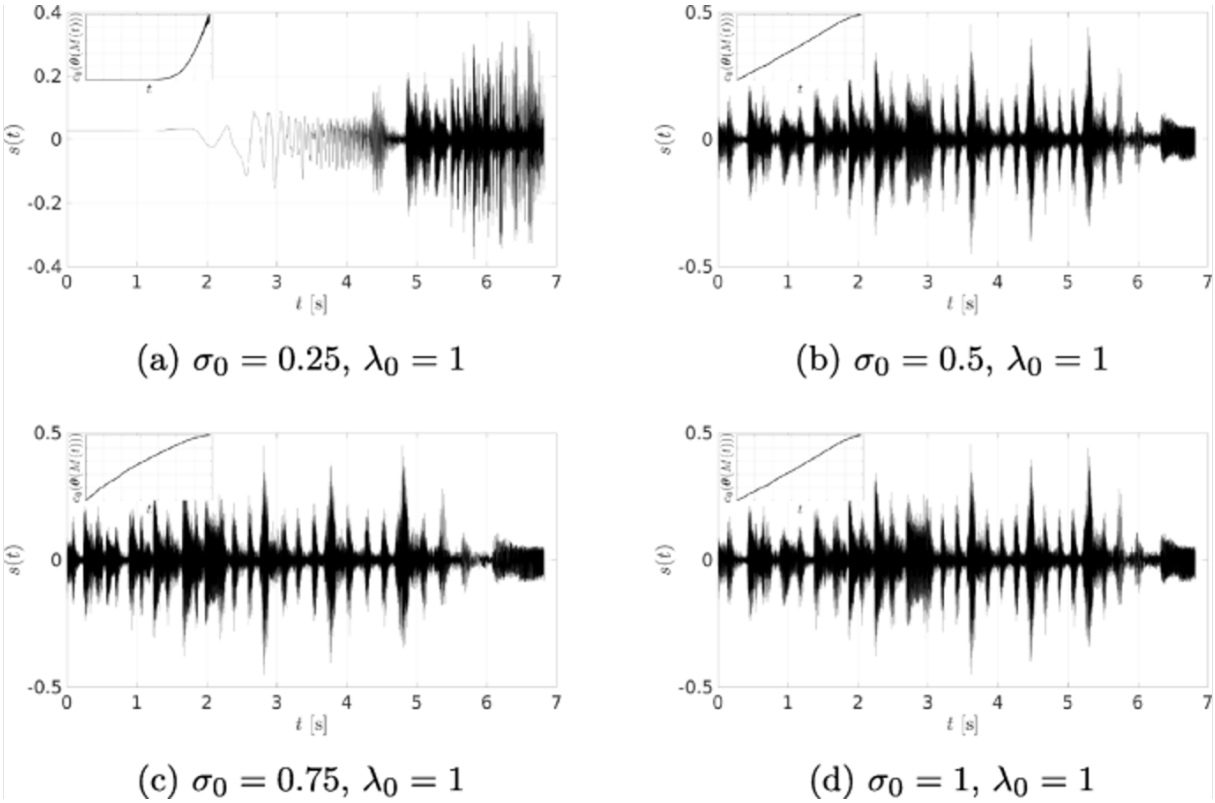

Figure 4.6: The sound signals generated by the proposed sample-based wave space function in 4.4-4.6) with sound samples taken from Mozart's All Turca [8] applied to a protein backbone peptide chain with 82 DOFs. The embedded smaller plots demonstrate how the nonlinear scaling function $c_0(\cdot)$ varies along the protein folding pathway. The generated sound files (in .wav format) can be downloaded from https://dralirezamoha.github.io/proteinpathway/wssFoldingSoundFiles.zip

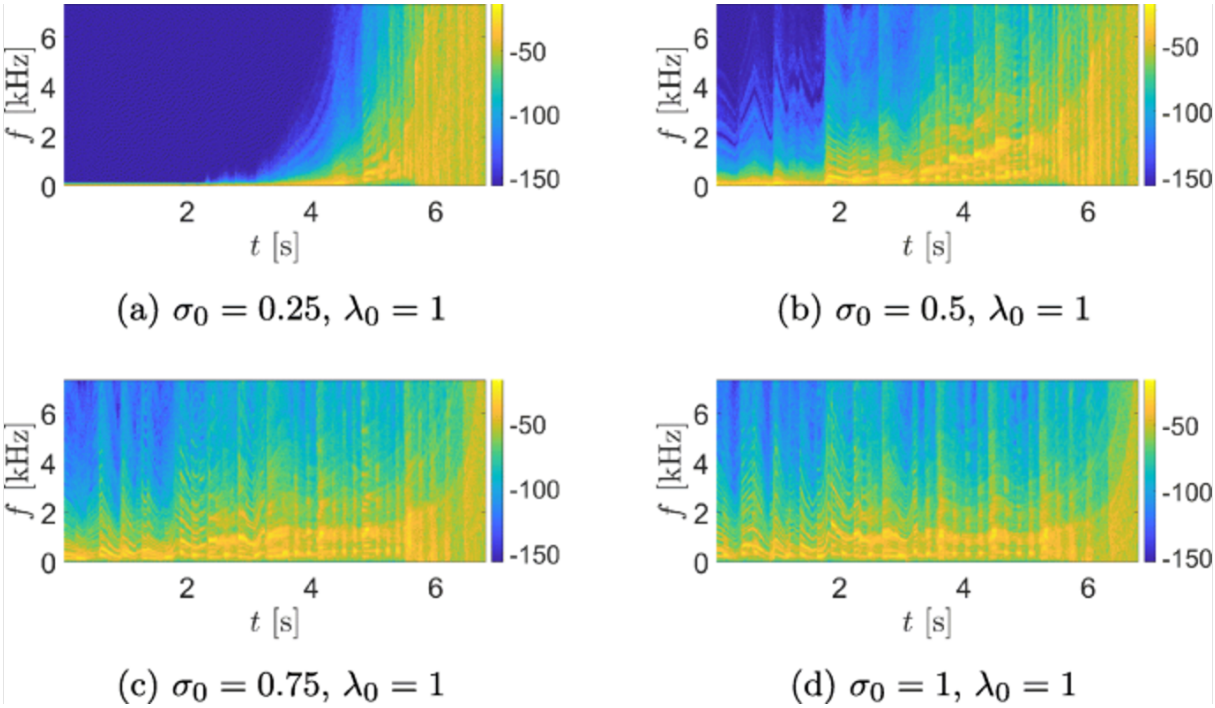

Figure 4.7: The sepctrograms of the sound signals generated by the proposed sample-based wave space function in 4.4-4.6 with sound samples taken from Mozart's All Turca [8] applied to a protein backbone peptide chain with 82 DOFs

CHAPTER V

Transforming Motion Into Sound: A Novel Sonification Approach for Teams of Mobile Robots

5.1 Introduction

Sonification refers to the translation of data into non-speech audible information, hence allowing to experience data by listening [45]. The emerging paradigm of robot motion sonification, which converts robotic motion data to non-speech audio for communicating information, presents significant potential for enhancing the efficiency of human-robot interaction (HRI) by reducing reliance on visual engagement and a reduction in stress and perceived workload for human operators working with robots [120; 73; 121; 71].

Herman et al. [45] classify sonification techniques into five broad categories: earcons, auditory icons, parameter-mapping sonification, audification, and model-based sonification. In audification, data is directly mapped to sound features, while model-based approaches translate data into dynamic systems exhibiting desired acoustic behaviors. For example, data can be used to manipulate the parameters of a mass-spring system generating sound waves. For further details on these classifications and specific techniques, readers are directed to Hermann et al [45].

Within the realm of parameter-mapping sonification for robotic motion, Schwenk

et al. [74] propose a notable approach. Their system leverages a synthesizer modulated by joint state and sensor data, effectively sonifying robot movement. Conversely, the SONAO project, led by Frid and collaborators, explores compensating for limited human-robot communication channels through non-speech audio mapped to expressive gestures [67; 70; 71]. For instance, Frid and Bresin [71] employed a rectangular oscillator with a short envelope, manipulating its pitch within a C major scale based on input magnitude, to convey joy. Bremner et al. [72] investigated the impact of parameter-mapping sonification in virtual reality-based telerobotics, demonstrating a reduction in stress and perceived workload for human operators controlling robots in hazardous environments. Similarly, the SonifyIt project [73] leverages Robot Operating System (ROS) and the multimedia visual programming language Pure Data to enable both sample playback and live sound synthesis for robots, expanding potential avenues for sonification implementation.

While advancements in robot motion sonification have yielded promising results, current state-of-the-art methods largely face the limitation of being designed for robots with a low number of degrees of freedom (DOFs), as exemplified by Daryl in Schwenk et al.'s work [74]. This poses a challenge for a diverse range of robotic systems possessing significantly higher or even infinite DOFs. Examples include elephant trunk arms and snake robots (e.g., [76; 122]), essential for navigating constrained environments and diverse locomotion patterns, as well as industrial collaborative multi-robot systems (e.g., [5; 115; 116]).

In addition to the five conventional sonification methods, a novel approach termed Wave Space Sonification (WSS) was recently proposed by Hermann [123]. WSS, designed for high-dimensional data, relies on creating an audible representation of the data by exploring a scalar field using a data-driven trajectory. This novel framework, which falls within the spectrum of sonification techniques that map parameters to sound and techniques that directly convert data into sound, has only been applied to

very few applications, such as the creation of audiovisual dance performances [124] and sonification of protein folding pathways modeled as mechanisms with numerous rigid nano-linkages [3].

We employ the WSS paradigm due to Hermann [123] to answer the challenging question of generating *non-speech auditory representation* of the motion of robotic systems with any number of mobile robots. The motion data generated by the robotic system consisting of a team of industrial mobile robots is fed into a properly designed wave space sonification function that performs a data-driven audio signal sampling and generates pure tonal sounds from the robotic motion data. The generated sounds using our WSS-based approach exhibit selected timbre when passing close to the designated configurations and/or along desired directions in the robot configuration space.

5.2 Contributions of the Method

Despite the utilization of sonification techniques in several HRI settings [67; 68; 69], the problem of robotic motion sonification for systems consisting of teams of mobile robots has remained unaddressed. This article, relying on the WSS framework [123], provides a novel data-driven solution to the problem of systematic sonification of motion data generated by robotic systems consisting of any number of mobile robots. Our WSS-based algorithm generates sounds from the motion data of mobile robots so that the generated audio signal exhibits a chosen timbre when the mobile robots pass near designated configurations or move along desired directions. Our general solution contributes to the field of robotic trajectory sonification, which is still in its early development stages, and paves the path for sonification of robotic trajectories in other emerging areas such as soft robotics [113; 114]. To demonstrate its versatility, our WSS-based sonification algorithm is applied to a team of OMRON LD series autonomous mobile robots, sonifying their motion patterns with pure tonal

sounds.

5.3 Sonification of Robotic Motion

In this section, we provide the formal problem statement and the experimental setting of the robotic motion sonification problem. Our solution investigates the problem of designing sonification algorithms that translate the motion of teams of industrial mobile robots to non-speech sounds. Our proposed solution leverages the WSS framework and utilizes localized wave fields with specific orientations within the system configuration space. Therefore, in this section, we also elaborate on the three WSS elements needed in the context of robotic motion.

5.4 Problem statement

Let us consider a robotic system with configuration vector

$$\mathbf{q} := \left[q_1, \cdots, q_N\right]^\top \in \mathcal{Q}, \tag{5.1}$$

where $\mathcal{Q} \subset \mathbb{R}^N$ is the configuration manifold of dimension N. Assume that the time evolution of the robotic system configuration during a certain maneuver is given by the smooth function $\mathbf{q} : t \mapsto \mathbf{q}(t)$ (i.e., a curve on the configuration manifold $\mathcal{Q}$).

5.4.1 Robotic Motion Sonification Problem

The **Robotic Motion Sonification Problem (RMSP)** is concerned with generating a non-speech auditory representation (i.e., a sound signal $s(t)$) associated with this evolving configuration.

To state the RMSP for a team of mobile robots, we consider a group of M industrial wheeled mobile robots with possibly different underlying kinematics/dynamics. Assuming planar motion and ignoring the DOFs internal to the robots and their

wheels, the chassis coordinates with respect to a common global reference frame are given by [125]

$$\boldsymbol{\xi}_i = [x_i,\, y_i,\, \theta_i]^\top, 1 \leq i \leq M, \tag{5.2}$$

where x_i, y_i are the Cartesian coordinates of the robot chassis center of mass, and θ_i is the planar orientation of the chassis. Consequently, the motion data of the team of M robots is given by $\mathbf{q}(t) = [\boldsymbol{\xi}_1(t), \boldsymbol{\xi}_2(t), \cdots, \boldsymbol{\xi}_M(t)]^\top$. The RMSP for a team of mobile robots is concerned with generating a sound signal $s(t)$ from the motion data $\mathbf{q}(t)$.

In our experiments (Section 5.6), we consider a subset of the configuration space containing the vectors

$$\mathbf{q} = [x_1,\, y_1,\, \cdots, x_M,\, y_M]^\top \in \mathbb{R}^{2M}, \tag{5.3}$$

by ignoring the chassis orientations in (5.2). Accordingly, a configuration trajectory $\mathbf{q}(t)$ describes the movement of the chassis centers of the industrial wheeled mobile robot with respect to a common global reference frame. We would like to sonify this motion pattern in real-time, where at each moment of time t_0, a sound signal sample $s(t_0)$ is generated based on $\mathbf{q}(t_0)$ at that particular instance of time.

We utilize the wave space sonification (WSS) framework due to Hermann [123] to provide an answer to the RMSP. WSS, which relies on generating an auditory data representation by scanning a scalar field along a data-driven trajectory of interest, requires defining the following *three elements* (see Figure 5.1): (i) a trajectory in the *wave space*; (ii) a suitable definition of a *wave space function*; and, (iii) a *proper way of moving along the trajectory* in the wave space. In the context of the RMSP, the wave space is the configuration manifold $\mathcal{Q}$ to which the vector of robot configurations $\mathbf{q}$ given by (5.1) belongs. The configuration vector trajectory $\mathbf{q}(\cdot)$ obtained from the motion of the robotic system defines an embedded curve within the wave space $\mathcal{Q}$.

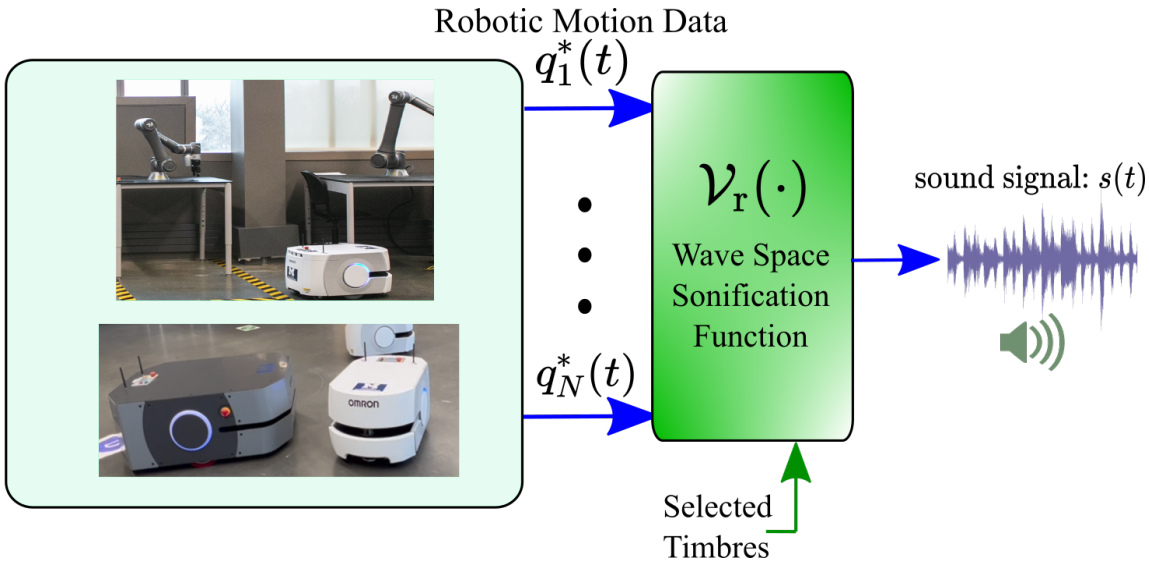

Figure 5.1: The proposed approach for converting the motion data of robotic systems consisting of industrial mobile robots to non-speech auditory information. The motion data generated by the robotic system is fed into a wave space sonification function that performs a data-driven audio signal sampling and generates pure tonal sounds from the robotic motion data.

Moreover, in the WSS framework, one needs to select a morphing function $M : t \mapsto M(t)$, which determines how the configuration trajectory $\mathbf{q}(\cdot)$ is traversed. Finally, a scalar field $\mathcal{V}_{\mathrm{r}}(\cdot)$, which is known as the *WSS function*, needs to be constructed. Figure 5.1 depicts these elements, where the morphing function is considered to be the identity mapping, i.e., $M(t) = t$.

RMSP is solved when the WSS function $\mathcal{V}_r(\cdot)$ is constructed. As depicted in Figure 5.1, the sound signal $s(\cdot)$, which can be sent to a sound card for listening to the non-speech auditory representation of the robot motion, is given by

$$s(t) = \mathcal{V}_{\mathrm{r}}\big(\, t, \mathbf{q}(\, M(t)\,)\,\big). \tag{5.4}$$

Here, the WSS function $\mathcal{V}_{\mathrm{r}}(\cdot)$ maps the motion data generated by the robotic system to sound signals for HRI purposes.

5.5 Solution to The Robotic Motion Sonification Problem

In this section we present our wave space sonification solution to the RMSP stated in Section 5.4.1 by presenting two classes of WSS functions. The first class utilizes the information of the absolute position of the mobile robots whereas the second class utilizes the information of the relative position of the mobile robots with respect to each other.

5.5.1 WSS Function Utilizing the Absolute Position of the Mobile Robots

Let us consider the robotic motion configuration trajectory $\mathbf{q}(t)$ in an N-dimensional configuration manifold $\mathcal{Q}$. Figure 5.2 depicts a collection of K designated configurations $\{\boldsymbol{\mu}_k\}_{k=1}^{K} \subset \mathcal{Q}$ (also called the anchor points), a set of K designated N-dimensional unit vectors $\{\hat{\mathbf{u}}_k\}_{k=1}^{K} \subset \mathbb{R}^N$, and a group of K sound signals $s_k : t \mapsto s_k(t)$, $1 \leq k \leq K$.

Each sound $s_k(\cdot)$ can either utilize algebraic expressions, e.g., sinusoidal vibratory sounds, or pre-recorded sound files, e.g., pieces of classical music. Since we are interested in creating alarm systems similar to industrial chemical process settings (see, e.g., [126]), we choose sinusoidal vibratory sounds as described later in this section.

A localized data-driven WSS function $\mathcal{V}_{\mathrm{r}}(\cdot)$ that anchors each of the sound signals $s_k(\cdot)$ to the designated robotic configuration $\boldsymbol{\mu}_k$ within $\mathcal{Q}$ and aligned to the desired direction $\hat{\mathbf{u}}_k$ is given by the sum (see, also, Figure 5.2)

$$\mathcal{V}_{\mathrm{r}}(t, \mathbf{q}) = \sum_{k=1}^{K} \mathcal{S}_k(t, \mathbf{q}) K_\sigma\big(\|\boldsymbol{\Xi}_k (\mathbf{q} - \boldsymbol{\mu}_k)\|\big), \tag{5.5}$$

where $K_\sigma(y) = \exp(\frac{-y^2}{2\sigma_0})$ is a window function with σ_0 being a positive constant design parameter, and the matrix is

$$\boldsymbol{\Xi}_k = \mathbf{I}_N - \hat{\mathbf{u}}_k \hat{\mathbf{u}}_k^\top, \; 1 \leq k \leq K, \tag{5.6}$$

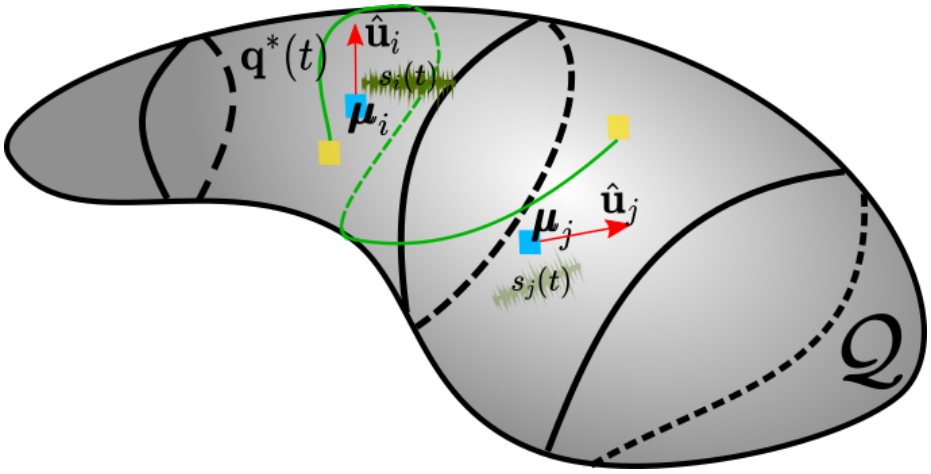

Figure 5.2: Construction of the data-driven localized WSS function $\mathcal{V}_{\mathrm{r}}(\cdot)$ on the configuration manifold $\mathcal{Q}$. The WSS function anchors each of the sound signals to a designated robotic configuration (called the sonification anchor points) within $\mathcal{Q}$ aligned with a desired direction.

where $\mathbf{I}_N \in \mathbb{R}^{N\times N}$ is the identity matrix. Furthermore, $\mathcal{S}_k$, $1 \leq k \leq N$, is some smooth function encoding the sound signals $s_k(\cdot)$ in a proper way. In its simplest form, one can choose $\mathcal{S}_k(t, \mathbf{q}) = s_k(t)$. As a more complicated example, one can choose $\mathcal{S}_k(t, \mathbf{q}) = g_k\, s_k\big(\hat{\mathbf{u}}_k^\top(\mathbf{q} - \boldsymbol{\mu}_k)\big)$, where g_k is a constant sound signal gain. In (5.6), $\boldsymbol{\Xi}_k$ is a symmetric projection matrix, i.e., $\boldsymbol{\Xi}_k^2 = \boldsymbol{\Xi}_k$ and $\boldsymbol{\Xi}_k^\top = \boldsymbol{\Xi}_k$.

As it can be seen from (5.5), data-driven localized WSS scalar fields can be defined through available samples from recorded sound signals. The generated sounds exhibit selected timbre encoded in $\mathcal{S}_k$ when passing close to the designated configurations/anchor points $\big\{\boldsymbol{\mu}_k\big\}_{k=1}^K$ and/or along desired directions $\big\{\hat{\mathbf{u}}_k\big\}_{k=1}^K$ (see Figure 5.2).

For the team of M industrial mobile robots, we construct a WSS function for each of the M mobile robots utilizing the scalar function given by (5.5). In particular, for the i$^{\text{th}}$ robot, $1 \leq i \leq M$, we define the WSS function

$$\mathcal{V}_{\mathrm{r},i}(t, \mathbf{q}) = \sum_{k=1}^{K} \mathcal{S}_{k,i}(t, \mathbf{q}) K_\sigma\big(\|\boldsymbol{\Xi}_{k,i}\left([x_i, y_i]^\top - \boldsymbol{\mu}_{k,i}\right)\|\big), \tag{5.7}$$

where $\boldsymbol{\mu}_{k,i} \in \mathbb{R}^2$, $1 \leq k \leq K$, are the designated positions/anchor points in the

common workspace of the robots (e.g., the location of conveyor belts and charging stations on the manufacturing floor). Furthermore, $\mathbf{\Xi}_{k,i} = \mathbf{I}_2 - \hat{\mathbf{u}}_{k,i}\hat{\mathbf{u}}_{k,i}^\top$, where the unit vector $\hat{\mathbf{u}}_{k,i} \in \mathbb{R}^2$ is a designated direction in the plane (e.g., a pre-specified line on the manufacturing floor).

For the timbres $\mathcal{S}_{k,i}(t, \mathbf{q})$ of the WSS function in (5.7), we are choosing sinusoidal vibratory sounds since we are interested in creating alarm systems similar to industrial chemical process settings (see, e.g., [126]). In particular, we choose

$$\mathcal{S}_{k,i}(t, \mathbf{q}) = g_{k,i} \sin\left(2\pi r_{k,i}\hat{\mathbf{u}}_{k,i}^\top([x_i, y_i]^\top - \boldsymbol{\mu}_{k,i}) + \alpha_{k,i}\right), \tag{5.8}$$

where $g_{k,i}$, $r_{k,i}$, and $\alpha_{k,i}$ are amplitude, frequency, and phase constant design parameters, respectively.

The intuition behind the choice of $\mathcal{S}_{k,i}(t, \mathbf{q})$ in (5.8) is that the motion pattern of each of the mobile robots, which is given by the position vector trajectory $[x_i(t), y_i(t)]^\top$, would generate a desired vibratory sinusoidal timbre depending on their direction of movement $[x_i, y_i]^\top - \boldsymbol{\mu}_{k,i}$, the designated direction $\hat{\mathbf{u}}_{k,i}$, and their proximity to the anchor $\boldsymbol{\mu}_{k,i}$. For instance, if the phase parameter $\alpha_{k,i}$ is set to zero and the i$^{\text{th}}$ robot is moving in a direction almost perpendicular to $\hat{\mathbf{u}}_{k,i}$, then a diminishing sound associated with the motion of the i$^{\text{th}}$ robot will be generated.

Using (5.7) and (5.8), which are defined for each of the mobile robots, we can construct the WSS function

$$\mathcal{V}_{\text{r}}(t, \mathbf{q}) = \sum_{i=1}^{M} \mathcal{V}_{\text{r},i}(t, \mathbf{q}), \tag{5.9}$$

for sonification of the motion patterns of the robots.

5.5.2 WSS Function Utilizing the Relative Position of the Mobile Robots

In addition to the WSS function given by (5.7)–(5.9), it is possible to use the relative position of the mobile robots to construct yet another class of WSS functions. In contrast with the WSS function in the previous section, which utilizes fixed designated anchor points and directions, we use the relative positions of the robot team members to define the anchor points and directions.

Let us consider the i$^{\text{th}}$ robot and utilize the position vectors of the other $M-1$ robots in the team as the designated positions. In other words, the k$^{\text{th}}$ anchor point for the i$^{\text{th}}$ robot, where $1 \leq k \leq M$ and $k \neq i$, is given by $\boldsymbol{\mu}_{k,i}(t) = [x_k(t), y_k(t)]^\top$. Furthermore, we can choose the k$^{\text{th}}$ designated direction $\hat{\mathbf{u}}_{k,i}$ for the i$^{\text{th}}$ robot, where $1 \leq k \leq M$ and $k \neq i$, to be the unit vector

$$\hat{\mathbf{u}}_{k,i}(t) = \frac{[x_k(t) - x_i(t), y_k(t) - y_i(t)]^\top}{\sqrt{(x_k(t) - x_i(t))^2 + (y_k(t) - y_i(t))^2}}, \tag{5.10}$$

which points from the i$^{\text{th}}$ robot to the k$^{\text{th}}$ robot. It is remarked that the unit direction vectors given by (5.10) are always well-defined. Because the denominator in (5.10) is always bounded away from zero, since the chassis centers never coincide with each other even in the case of a collision between the robots.

Under the choice of anchor points and designated directions given by (5.10), it can be easily seen that $K_\sigma\big(\boldsymbol{\Xi}_{k,i}\left([x_i(t), y_i(t)]^\top - \boldsymbol{\mu}_{k,i}(t)\right)\big) = 1$. Accordingly, the WSS function $\mathcal{V}_{\text{r,i}}(\cdot)$ given by (5.9) takes the position-dependent form

$$\mathcal{V}_{\text{r,i}}(\mathbf{q}) = \sum_{k=1,\, k\neq i}^{M} g_{k,i} \sin\big(2\pi r_{k,i} \|(\mathbf{E}_i - \mathbf{E}_j)\mathbf{q}\| + \alpha_{k,i}\big), \tag{5.11}$$

in which $\mathbf{E}_i \in \mathbb{R}^{2\times 2M}$, $1 \leq i \leq M$, is the projection matrix

$$\mathbf{E}_i := \begin{bmatrix} 0 & \cdots & 1 & 0 & \cdots & 0 \\ 0 & \cdots & 0 & 1 & \cdots & 0 \end{bmatrix}, \tag{5.12}$$

satisfying $\mathbf{E}_i\,\mathbf{q} = [x_i, y_i]^\top$. Indeed, the projection matrix $\mathbf{E}_i$ can be used to extract the position of the i$^{\text{th}}$ robot from the aggregate vector $\mathbf{q} \in \mathbb{R}^{2M}$ given by (5.3).

Using the functions in (5.11), we construct the WSS function

$$\mathcal{V}_{\text{r}}(\mathbf{q}) = \sum_{1\leq i,\, j\leq M} g_{i,j} \sin\big(2\pi r_{i,j}\|(\mathbf{E}_i - \mathbf{E}_j)\mathbf{q}\| + \alpha_{i,j}\big), \tag{5.13}$$

for motion pattern sonification of the wheeled mobile robots.

5.6 Results

In our experimental setting, we are using the family of OMRON LD autonomous mobile robots. These differential-drive industrial/service mobile robots are designed for moving material in settings such as manufacturing floors and warehouses with confined passageways while in the presence of other dynamically moving objects/humans [127; 128]. The utilized OMRON robots are LD-90 and LD-250 that scan the environment with a 240-degree laser scanner for primary navigation and are capable of transporting payloads up to 90 and 250 kilograms, respectively.

To control the motion of and gather data from these two robots, we have developed a Python-based interface for interacting with the OMRON Advanced Robotics Command Language (ARCL). ARCL, which is a text-based and command-and-response operating system, can be utilized to integrate a fleet of OMRON LD mobile robots with external automation systems. More details are found in Appendix E. The block diagram of our in-house Python interface is depicted in Figure 5.3. In all of our experiments, we are collecting data with a sample rate of 25 Hz. The detailed experimental

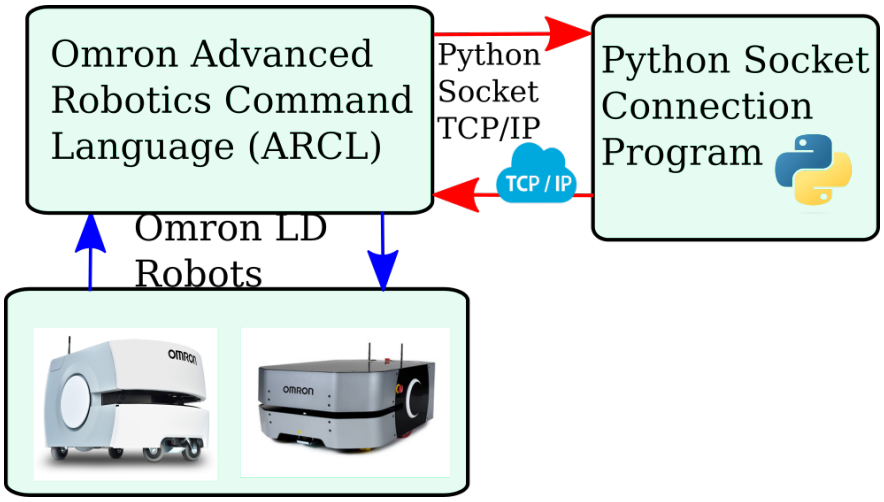

Figure 5.3: The block diagram of our in-house Python interface for interacting with the Omron LD robots and performing the sonification experiments. LD-90 and LD-250 are the robots with the white and gray chassis, respectively.

results can be viewed at https://youtu.be/Aqtf6ImaIWo.

Figure 5.4 depicts the trajectories of LD-90 and LD-250 utilized within our sonification experiments. As demonstrated in Figure 5.4, the designated anchor points for LD-90 are chosen to be $\boldsymbol{\mu}_{1,1} = [x_{\mathbf{D}}, y_{\mathbf{D}}]^\top$ and $\boldsymbol{\mu}_{2,1} = [x_{\mathbf{C}}, y_{\mathbf{C}}]^\top$, where $i = 1$ is the index associated with LD-90. The designated sonification directions for LD-90 are chosen to be the unit vectors $\hat{\mathbf{u}}_{1,1}$ and $\hat{\mathbf{u}}_{2,1}$ that point along the directions connecting **D** to **C** and **C** to **A**, respectively. Furthermore, in (5.8), we have chosen $g_{k,1} = 10$, $r_{k,1} = 0.25$, and $\alpha_{k,1} = 0$, for $k = 1, 2$. Finally, we set $g_{k,2} = 0$ for LD-250 in the first set of our experiments.

Figures 5.5 and 5.6 depict the snapshots of the movement of the robots, the generated sound time profile (the upper left embedded plots in Figure 5.5), and the associated spectrogram, respectively. As expected from the way of construction of the WSS function in (5.7), (5.8), and (5.9), the generated sound within the time interval between $t \approx 12$ and $t \approx 15$ completely fades away. This is due to the fact that the direction of movement of LD-90 is almost perpendicular to both of the designated

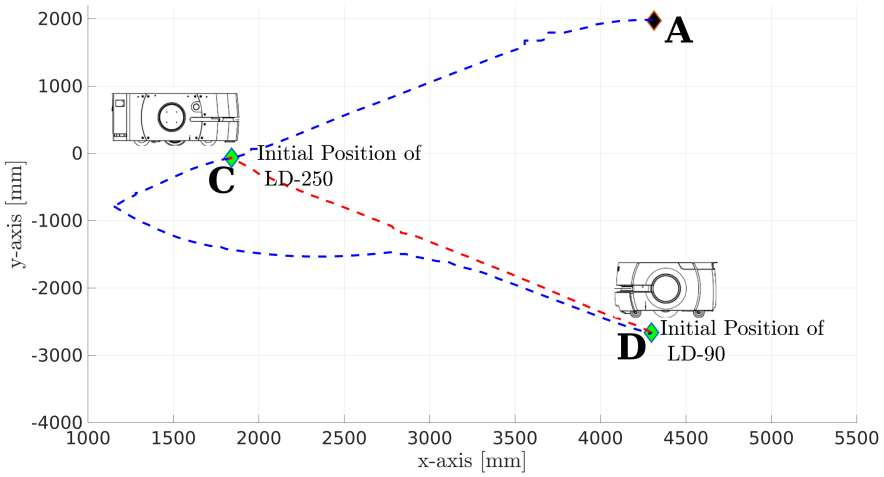

Figure 5.4: The trajectories of LD-90 (dashed blue) and LD-250 (dashed red) in the two experiments. The points **A**, **C**, and **D** are used to define the anchor points and designated directions for constructing the generic WSS function for each of the robots.

directions $\hat{\mathbf{u}}_{1,1}$ and $\hat{\mathbf{u}}_{2,1}$.

In our sonification experiments with the custom WSS function in (5.13), we set the phase design parameters as $\alpha_{i,j} = 0$. Consequently, when $i = j$, the sinusoidal term will become equal to zero. Furthermore, we set the amplitude design parameters as $g_{1,2} = g_{2,1} = 5$. Finally, we choose the frequency design parameters to be $r_{1,2} = r_{2,1} = 0.05$.

Under the choice of the aforementioned design parameters, we apply the WSS function in (5.13) to the trajectories of LD-90 and LD-250 given by the vector $\mathbf{q}(t)$ (see Figure 5.4). Furthermore, we use a linear morphing function of the form $M(t) = t$ that results in sound signal samples be given by $s(t) = \mathcal{V}_{\mathrm{r}}(\mathbf{q}^*(t))$. Figures 5.5 and 5.7 depict the snapshots of the movement of the robots, the generated sound time profile (the embedded plots in the upper middle part of Figure 5.5), and the associated spectrogram, respectively. As expected from the way of construction of the custom position-dependent WSS function in (5.13), the generated sound volume when the two robots start approaching each other keeps decreasing. Indeed, the sound signal

amplitude in the interval between $t \approx 7$ and $t \approx 15$ seconds is the smallest. As the robots start moving away from each other at around $t \approx 15$ seconds, the sound volume starts increasing.

5.7 Conclusion

Motivated by the growing need to translate complex motion data from robotic systems into audible information, we developed a Wave Space Sonification (WSS)-based solution aimed at creating sonification algorithms that can convert the movements of teams of industrial mobile robots into non-speech sounds. Sonification, as an auditory representation of data, offers an innovative and intuitive way to understand the dynamics and interactions of robotic systems, particularly in environments where visual monitoring is challenging or impractical. In this project, we focused on applying this methodology to a team of OMRON LD autonomous mobile robots, where the motion data from multiple independent units working collaboratively was converted into sound, providing an auditory pathway to monitor and analyze their behaviors in real-time.

The sonification of mobile robotic systems presents unique challenges, especially when dealing with teams of robots that exhibit complex, multi-agent behaviors. In our proposed solution, we utilized the WSS framework to systematically map the motion data of these robots—such as their paths, speeds, and coordination patterns—into sound. By capturing the underlying kinematic patterns of the robots' motion, the sonification provided a way to monitor not only the movement of individual robots but also the overall interaction and coordination within the team. This method can help operators and researchers detect anomalies, optimize performance, and ensure the robots are working effectively as a group. The resulting non-speech sounds reflect the movement, task execution, and interaction of the robots in an easily interpretable form, offering an alternative means of analyzing complex robotic systems.

One of the key advantages of this approach is its potential to provide real-time feedback on the operational status of the robotic system. In environments where visual data might be overwhelming or difficult to process, the auditory cues generated through sonification can alert operators to changes in performance, potential malfunctions, or deviations from expected behavior. This auditory feedback adds an extra layer of monitoring and control, making it especially useful in industrial settings where teams of robots are deployed for tasks like material handling, transportation, and assembly.

In conclusion, the WSS-based sonification solution we developed for teams of mobile robots represents an innovative approach to monitoring and analyzing robotic systems through sound. By translating complex motion data into non-speech auditory feedback, we have created a powerful tool for interpreting robotic behavior in real-time. As the field of robotics continues to evolve, particularly with the rise of soft robots and collaborative robotic arms, expanding the use of sonification will open up new possibilities for managing and understanding increasingly complex robotic systems in dynamic and data-rich environments.

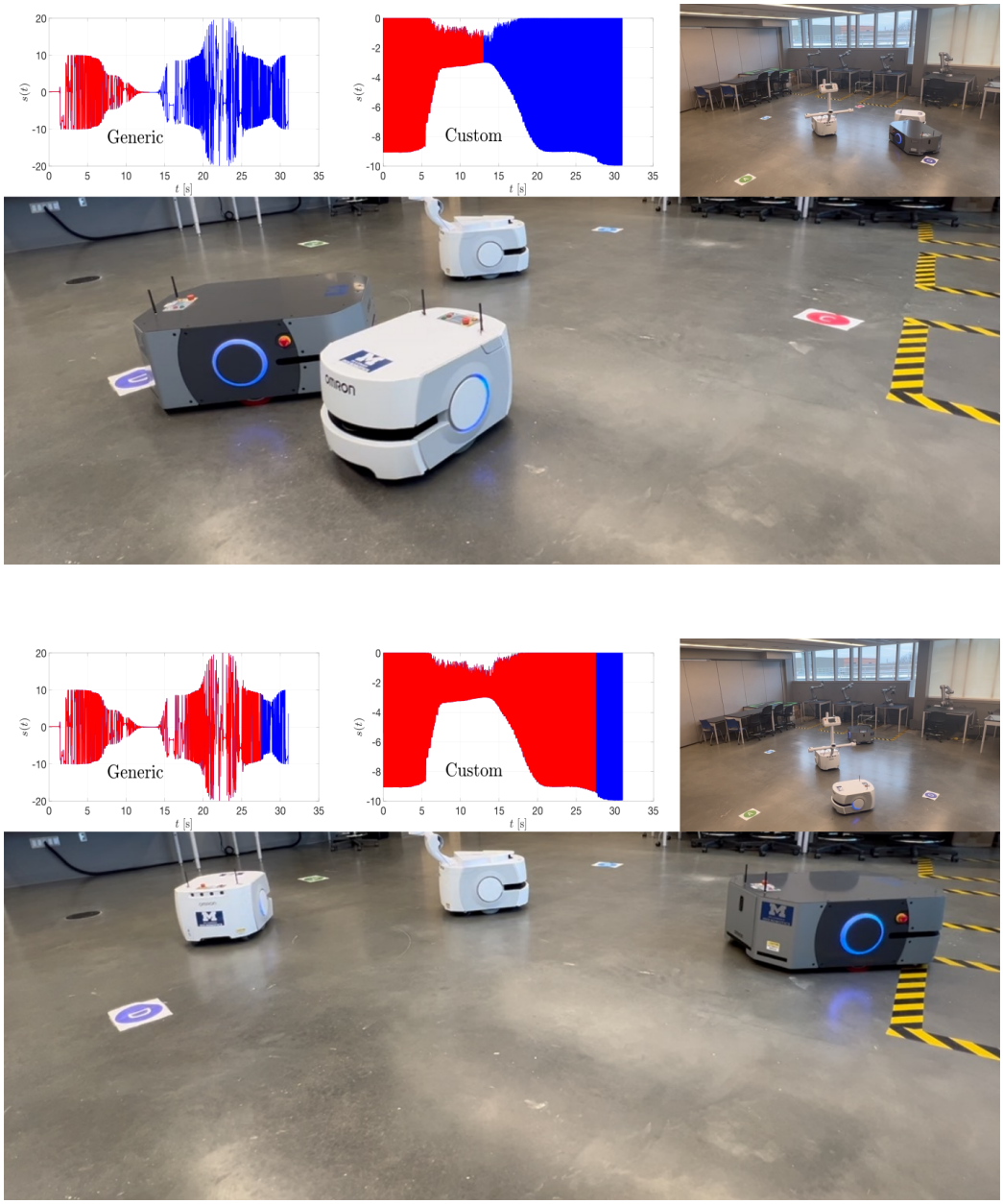

Figure 5.5: Applying the proposed sonification method with the WSS function given by (5.7)–(5.9) (embedded plot in the upper left) and the WSS function given by (5.13) (embedded plot in the upper middle) to a team of wheeled mobile robots. The embedded plots in the two snapshots demonstrate the generated sound signal using our sonification technique. The detailed experimental results can be viewed at `https://youtu.be/Aqtf6ImaIWo`.

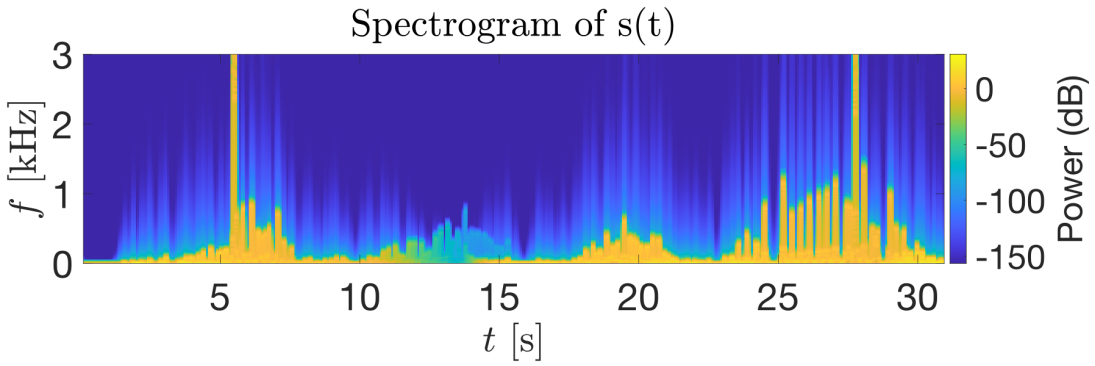

Figure 5.6: Generated sound spectrogram resulting from the WSS function given by (5.7)–(5.9).

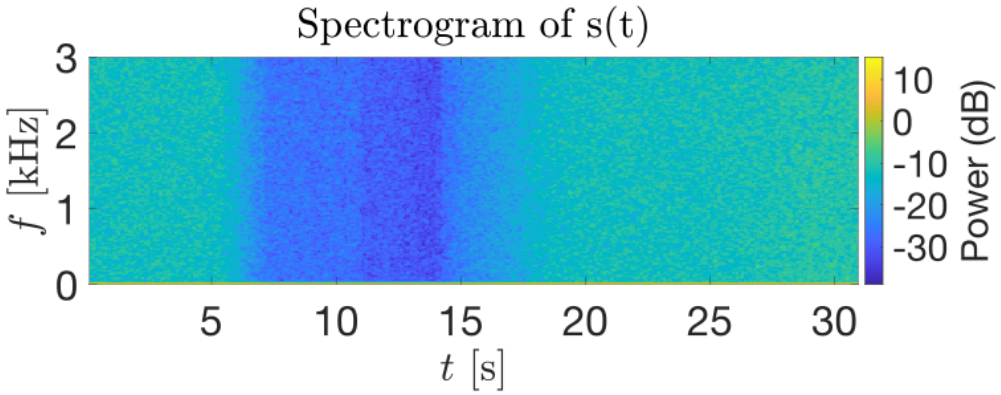

Figure 5.7: Generated sound spectrogram resulting from the WSS function given by (5.13).

CHAPTER VI

Concluding Remarks and Future Research Directions

In this dissertation, we explored the potential of Wave Space Sonification framework as a powerful tool for translating complex, multi-dimensional data into auditory representations, offering new ways to interpret and monitor systems that are challenging to analyze visually. We first applied this methodology to the sonification of protein folding pathway datasets, where the intricate folding trajectories of protein molecules were modeled as hyper-redundant robotic mechanisms. These mechanisms, with their numerous degrees of freedom and rigid nano-linkages, mirrored the flexibility and complexity found in high-dimensional robotic systems. By converting the dihedral angle folding trajectories into sound using two distinct wave space functions—a canonical sum of sinusoids and a sample-based approach incorporating Mozart's Alla Turca—we demonstrated the effectiveness of WSS in capturing and representing the dynamic transitions of protein folding. This sonification not only offered an alternative way to visualize the folding process but also provided auditory cues that allowed researchers to detect previously hidden patterns and behaviors, ultimately opening up new avenues for understanding high-dimensional biological systems.

We then extended the use of WSS framework to the motion of teams of industrial mobile robots, focusing specifically on OMRON LD autonomous mobile robots. In

this context, the sonification of the robots' motion data—such as their paths, speeds, and coordination patterns—allowed for real-time monitoring of their behaviors. By converting the complex, multi-agent dynamics into non-speech sounds, this approach enabled us to better understand and manage the interactions and coordination within the team. This auditory feedback proved to be particularly useful in industrial environments where visual data might be overwhelming or impractical, offering a novel means of detecting anomalies, optimizing performance, and ensuring smooth operation.

Looking toward future applications, both projects highlight the potential for expanding sonification to more advanced systems. For instance, in the domain of robotics, the sonification framework could be adapted to soft robots, which exhibit continuous deformation and generate vast amounts of motion data that are difficult to track visually. By providing real-time auditory feedback on the fluid, adaptive movements of soft robots, sonification could enhance our ability to monitor and interpret their complex behaviors. Additionally, teams of industrial collaborative robotic arms, which produce overwhelming amounts of data as they work in coordination with humans and other robots, could benefit from sonification to ensure safety, efficiency, and smooth performance. The auditory monitoring of these systems could help operators detect deviations or issues in real time, ensuring the seamless operation of such collaborative environments.

In conclusion, the WSS-based sonification techniques developed in this dissertation offer a novel and versatile solution for representing complex, high-dimensional data through sound. Whether applied to protein folding pathways or the motion of teams of mobile robots, sonification provides an intuitive and engaging way to interpret intricate systems, making it a valuable tool for both biological and robotic applications. As technology continues to advance, expanding the use of sonification to emerging fields such as soft robotics and collaborative robotic systems will open

new possibilities for managing and understanding complex, data-rich environments, further enhancing our ability to interact with and control these advanced systems.

APPENDICES

APPENDIX A

Data Availability

The datasets codes generated during and/or analyzed during the current study are available in the GitHub repository, https://dralirezamoha.github.io/proteinpathway/wssFoldingSoundFiles.zip, https://dralirezamoha.github.io/proteinpathway/wssFoldingSoundFiles.zip, https://dralirezamoha.github.io/proteinpathway/2023MTAP_Canonical_WaveSpaceSonification.zip and https://dralirezamoha.github.io/proteinpathway/2023MTAP_MatlabFiles_SampleBasedWSS.zip.

APPENDIX B

Sound Files

The generated sound files (in .wav format) based on our WSS-based proposed method can be downloaded from https://dralirezamoha.github.io/proteinpathway/wssFoldingSoundFiles.zip. See Chapter IV for further details.

APPENDIX C

Canonical WSS MATLAB Code

```
% MTAPCANONICALWSS.m:
% Canonical WSS M-File for sonification of the folding trajectories
% of the backbone chain of the example protein molecule using
% sinusoidal functions
%
% MATLAB M-File associated with the article: "Wave Space Sonification of
% Folding Pathways of Protein Molecules Modeled as Hyper-Redundant Robotic
% Mechanisms" Multimedia Tools and Applications (Springer Nature)
%
% Note: Contact the corresponding author Dr. Alireza Mohammadi
% (amohmmad@umich.edu) for any further assistance/information.
%
%
% This version: 02-11-2023
%~~~~~~~~~~~~~~~~~~~~~~~~~~~~~~~~~~~~~~~~~~~~~~~~~~~~~~~~~~~~~~~~~~~~~~~~~~~~~~~
%
clear; close all; clc;
%~~~~~~~~~~~~~~~~~~~~~~~~~~~~~~~~~~~~~~~~~~~~~~~~~~~~~~~~~~~~~~~~~~~~~~~~~~~~~~~
% Step-0: Set the figure/sound file names for writing the final results to.
%
```

```
% Choose flagNum to be an integer between 1 and 5.
flagNum = 1; %1->sigma0=0.1; 2->sigma0=0.15; 3->sigma0=0.2; 4->sigma0=0.3;
                %5->sigma0=0.4;
%
figStr2  = 'canonicalSt';
figStr3  = 'canonicalSpectro';
%
figStr2  = [figStr2 ,num2str(flagNum)];
figStr3  = [figStr3 ,num2str(flagNum)];
fileStr  = 'simulResult';
fileStr2  = {'1.mat','2.mat','3.mat','4.mat','5.mat'};
audioStr = 'canonicalWSS';
audioStr = [audioStr,num2str(flagNum),'.wav'];
%
fileStr  = [ fileStr , fileStr2 {flagNum}];
sigma0Mat = [0.1; 0.15; 0.2;  0.3;  0.4];
%
disp(' ')
disp('Your chosen sigma0 parameter for the frequency scaling function:')
disp(' ')
disp(sigma0Mat(flagNum))
disp('Sonification in process. Please wait ... ')
%
%~~~~~~~~~~~~~~~~~~~~~~~~~~~~~~~~~~~~~~~~~~~~~~~~~~~~~~~~~~~~~~~~~~~~~~~~~~~~~~~~
% Step-1: Load the folding pathway trajectory dataset
% provided in the data file "sonificationData.mat".
%
% Load the protein folding pathway dataset.
load("sonificationData.mat");
thVec = thVec(2:end-1,:);
% Extract the information about the folded and unfoled conformations
xStart = thVec(:,1);
xFinish = thVec(:,end);
```

```
mu_unf = xStart ; % The unfolded protein conformation
mu_fol = xFinish; % The folded protein conformation
%~~~~~~~~~~~~~~~~~~~~~~~~~~~~~~~~~~~~~~~~~~~~~~~~~~~~~~~~~~~~~~~~~~~~~~~~~~~~~~~
% Step-2: Load the folding pathway trajectory dataset provided in the
% data file "sonificationData.mat".
%
% The design parameters that are chosen by the use
Fs = 6000; %Sampling frequency
F0 = 250;  %Fundamental frequency
sigma0 = sigma0Mat(flagNum);
%
% Set the duration of the desired canonical WSS-based sound file
duration = 5;  % in seconds
% Set L, i.e., the length of the generated WSS-based sound vector
L = Fs*duration;
%~~~~~~~~~~~~~~~~~~~~~~~~~~~~~~~~~~~~~~~~~~~~~~~~~~~~~~~~~~~~~~~~~~~~~~~~~~~~~~~
% Step-3: The main computations for generating the canonical WSS-based
% sound file.
%
% The linear interpolation function.
Nsmax = length(thVec(1,:));
Ns = (Nsmax-1)/(L-1);
%
N = 1:Nsmax;
NN = 1:Ns:Nsmax;
%
 fi  = zeros(length(thVec(:,1)),L);
% Create a spline object for faster computations.
thVecNew = spline(N,thVec);
%
for k=1:length(thVec(:,1))
    sigma(k) = (sigma0^2)*norm(mu_fol(k) - mu_unf(k));
end
```

```
%
thVec_new = ppval(thVecNew,NN);
%
for k =1:length(thVec(:,1))
    for m=1:L
        fi(k,m) = F0*exp(-(norm(thVec_new(k,m)-mu_fol(k))/sigma(k)));
    end
end
%
V = zeros(1,L);
%
% The canoncial WSS summation
for i=1:length(thVec(:,1))
    V = (1/82) * (V + sin(2*pi*fi(i,:) .*thVec_new(i,:)));
end
%
%~~~~~~~~~~~~~~~~~~~~~~~~~~~~~~~~~~~~~~~~~~~~~~~~~~~~~~~~~~~~~~~~~~~~~~~~~~~~~~~~
% Step-4: Draw the final results and generate the WSS-based sound. Save the
% generated data in files defined in Step-0.
%
fig1 = figure('units','normalized','outerposition',[0 0 1 1]);
plot(linspace(0,duration,length(V)),V,'k','linewidth',0.01)
grid on
xlabel('$$t$$ [s]','interpreter','latex','fontSize',40)
ylabel('$$s(t)$$','interpreter',...
    'latex','fontSize',40)
set(gca,'FontSize',40)
%
% Uncomment to print the figure to a png file.
% print(fig1,figStr2,'-dpng','-r300')
%
fig2 = figure('units','normalized','outerposition',[0 0 1 1]);
%
```

```
120 subplot(1,2,1)
121 plot3(thVec(3,:),thVec(29,:),thVec(79,:),'k','LineWidth',2)
122 hold on
123 plot3(thVec(3,1),thVec(29,1),thVec(79,1),'d','MarkerSize', 20,...
124     'MarkerFaceColor', 'r')
125 plot3(thVec(3,end),thVec(29,end),thVec(79,end),'d','MarkerSize', 20,...
126     'MarkerFaceColor', 'g')
127 xlabel('$$\theta_4$$ [rad]','interpreter','latex','fontSize',40)
128 ylabel('$$\theta_{30}$$ [rad]','interpreter',...
129     'latex','fontSize',40)
130 zlabel('$$\theta_{80}$$ [rad]','interpreter','latex','fontSize',40)
131 set(gca,'FontSize',40)
132 grid on
133 %
134 subplot(1,2,2)
135 plot3(thVec(5,:),thVec(49,:),thVec(71,:),'k','LineWidth',2)
136 hold on
137 plot3(thVec(5,1),thVec(49,1),thVec(71,1),'d','MarkerSize', 20,...
138     'MarkerFaceColor', 'r')
139 plot3(thVec(5,end),thVec(49,end),thVec(71,end),'d','MarkerSize', 20,...
140     'MarkerFaceColor', 'g')
141 xlabel('$$\theta_6$$ [rad]','interpreter','latex','fontSize',40)
142 ylabel('$$\theta_{50}$$ [rad]','interpreter',...
143     'latex','fontSize',40)
144 zlabel('$$\theta_{72}$$ [rad]','interpreter','latex','fontSize',40)
145 grid on
146 set(gca,'FontSize',40)
147 %
148 % Uncomment to print the figure to a png file.
149 % print(fig2,'canonicalProjectedPath','-dpng','-r300')
150 % clear fig1
151 %
152 fig3 = figure('units','normalized','outerposition',[0 0 1 1]);
```

```
153 pspectrum(V,Fs,'spectrogram')
154  title ('')
155 xlabel('$$t$$ [s]','interpreter','latex','fontSize',40)
156 ylabel('$$f$$ [kHz]','interpreter' ,...
157       'latex','fontSize',40)
158 set(gca,'FontSize',40)
159 %
160 % Uncomment to print the  figure  to a png  file .
161 % print(fig3, figStr3,'-dpng','-r300')
162 % clear  fig2
163 %
164 % Uncomment to save the results in a  .mat  file .
165 % save( fileStr )
166 %To Play the output sound uncomment this line
167  sound(V,Fs);
168 %
169 % Uncomment to write the generated sound to a .wav file.
170 % audiowrite(audioStr,V,Fs)
```

APPENDIX D

Sample Based WSS MATLAB Code

```
% MTAPSAMPLEBASEDWSS.m:
% Sample-Based WSS M-File for sonification of the folding trajectories
% of the backbone chain of the example protein molecule using
% Mozart's Alla Turca
%
% MATLAB M-File associated with the article: "Wave Space Sonification of
% Folding Pathways of Protein Molecules Modeled as Hyper-Redundant Robotic
% Mechanisms" Multimedia Tools and Applications (Springer Nature)
%
% Note: Contact the corresponding author Dr. Alireza Mohammadi
% (amohmmad@umich.edu) for any further assistance/information.
%
%
% This version: 02-11-2023
%~~~~~~~~~~~~~~~~~~~~~~~~~~~~~~~~~~~~~~~~~~~~~~~~~~~~~~~~~~~~~~~~~~~~~~~~~~~~~~~
%
clear;  close all;
%~~~~~~~~~~~~~~~~~~~~~~~~~~~~~~~~~~~~~~~~~~~~~~~~~~~~~~~~~~~~~~~~~~~~~~~~~~~~~~~
% Step-0: Set the figure/sound file names for writing the final results to.
figStr1   = 'sampleBasedcFun';
```

```
figStr2   = 'sampleBasedst';
figStr3   = 'sampleBasedSpectro';
audioStr = 'mozartSampleBased';
%
% Choose flagNum to be an integer between 1 and 4.
flagNum = 1; %1->sigma0=0.25; 2->sigma0=0.5; 3->sigma0=0.75; 4->sigma0=1
figStr1  = [figStr1 ,num2str(flagNum)];
figStr2  = [figStr2 ,num2str(flagNum)];
figStr3  = [figStr3 ,num2str(flagNum)];
audioStr = [audioStr,num2str(flagNum),'.wav'];
fileStr  = 'simulResult';
fileStr2  = {'1.mat','2.mat','3.mat','4.mat','5.mat','6.mat'};
%
fileStr  = [ fileStr , fileStr2 {flagNum}];
% Set the sample based sonification parameters.
lambda0= 1;
sigma0Mat = [0.25; 0.5; 0.75;  1];
sigma0 = sigma0Mat(flagNum);
flagInnerPlot  = 1;
%
disp(' ')
disp('Your chosen sigma0 parameter for the scaling function:')
disp(' ')
disp(sigma0Mat(flagNum))
disp('Sonification in process. Please wait ... ')
%
%~~~~~~~~~~~~~~~~~~~~~~~~~~~~~~~~~~~~~~~~~~~~~~~~~~~~~~~~~~~~~~~~~~~~~~~~~~~~~~~~
% Step-1: Create a spline object from the folding pathway trajectory
% provided in the data file "sonificationData.mat"
%
load("sonificationData.mat");
Nfolding = length( thVec(1,:) );
thVecSpline = spline(linspace(0,1,Nfolding),thVec );
```

```
%
% Compute the nonlinear scaling function for later use in sample-based WSS
% sonification.
cscale = zeros(1,Nfolding);
%
mu_unf = thVec(:,1);   % Unfolded protein conformation
mu_fol = thVec(:,end); % Folded protein conformation
%
% Set the denominator of the nonlinear scaling function.
denominator = (sigma0^2) * ( norm(mu_unf - mu_fol) );
%
% Compute the samples of the nonlinear scaling function
for ii = 1 : Nfolding
    cscale(ii) = lambda0 * exp( -( ...
        norm( thVec(:,ii)-mu_fol )/ denominator ) );
    %
    if ~sigma0 % Use sigma0 = 0 for playing the base sound file (i.e.,
               % Mozart's Alla Turca in this example)
        cscale(ii) = (ii-1)/Nfolding;
    end
end
%
% Create a spline object from the nonlinear scaling function for sampling
% from Mozart's Alla Turca.
%
cscale = ( cscale - min(cscale) ) / max(cscale);
cscale = cscale/max(cscale);
cscaleSpline = spline( linspace(0,1,Nfolding), cscale);
%
%~~~~~~~~~~~~~~~~~~~~~~~~~~~~~~~~~~~~~~~~~~~~~~~~~~~~~~~~~~~~~~~~~~~~~~~~~~~~~~~
% Step-2: Pre-process the original sound file 'moz.wav'.
NumLow = 3; % NumLow = 1 --->  sound with original quality
Fs0 = 44000; % Base music playback frequency
```

```
87  %
88  yMozart = audioread('moz.wav')';
89  NMozartMusic = length(yMozart);      % NMozartMusic
90  yMozart = yMozart(:,1:NMozartMusic);
91  %
92  % Sample the original sound file for a faster computation.
93  yMozart = yMozart(1:NumLow:NMozartMusic);
94  % Create a spline object from the sampled sound file.
95  mozSpline   = spline(linspace(0,1, length(yMozart)) , yMozart) ;
96  %
97  % Set the frequency for playback of the protein folding pathway sonified
98  % dataset on the PC speakers
99  %
100 Fs  = floor(Fs0 / NumLow) ;
101 Nmozart = length(yMozart);
102 Tmozart = Nmozart / Fs;
103 %
104 % Uncomment to hear the original piece of music.
105 % sound(yMozart,Fs);
106 %~~~~~~~~~~~~~~~~~~~~~~~~~~~~~~~~~~~~~~~~~~~~~~~~~~~~~~~~~~~~~~~~~~~~~~~~~~~~~~~
107 % Step-3: Use the sample-based WSS function to sonify the folding pathway
108 % of the protein molecule.
109 %
110 % Pre-assign the variable for accelerating the loop computations.
111 yMozartWSS = zeros(1,Nmozart);
112 %
113 % The main computational loop for the generation of the WSS-based sound
114 % from the protein folding pathway.
115 %
116 for ii = 1 : Nmozart
117     tii = (ii-1)/Nmozart;
118     yMozartWSS(ii) = ppval(mozSpline , ppval(cscaleSpline,tii));
119 end
```

```
%
%~~~~~~~~~~~~~~~~~~~~~~~~~~~~~~~~~~~~~~~~~~~~~~~~~~~~~~~~~~~~~~~~~~~~~~~~~~~~~~~~
% Step-4: Draw the final results and generate the WSS-based sound. Save the
% generated data in files defined in Step-0.
%
fig1 = figure('units','normalized','outerposition',[0 0 1 1]);
plot(linspace(0,Tmozart,length(yMozartWSS)),yMozartWSS,'k',...
    'linewidth',0.01)
hold on
grid on
xlabel('$$t$$ [s]','interpreter','latex','fontSize',30)
ylabel('$$s(t)$$','interpreter',...
    'latex','fontSize',30)
set(gca,'FontSize',30)
if ~flagInnerPlot
    ylabel('$$s_{\mathcal{M}}(t)$$','interpreter',...
    'latex','fontSize',40)
else
    axes('Position',[.16 .72 .2 .2])
    box on
    plot(linspace(0,Tmozart,Nfolding), cscale,'k','LineWidth',2)
    hold on
    grid on
    ylabel('$$c_0($${\boldmath$\theta$}$$(M(t)))$$','interpreter',...
        'latex','fontSize',25)
    xlabel('$$t$$','interpreter',...
        'latex','fontSize',25)
    set(gca,'YTickLabel',[]);
    set(gca,'XTickLabel',[]);
    %
end
%
% Uncomment to print the figure to a png file.
```

```
153 % print(fig1, figStr2,'-dpng','-r150')
154 % clear fig1
155 %
156 fig2 = figure('units','normalized','outerposition',[0 0 1 1]);
157 pspectrum(yMozartWSS,linspace(0,Tmozart,...
158     length(yMozartWSS)),'spectrogram')
159 %
160 title ('')
161 xlabel('$$t$$ [s]','interpreter','latex','fontSize',40)
162 ylabel('$$f$$ [kHz]','interpreter',...
163     'latex','fontSize',40)
164 set(gca,'FontSize',40)
165 %
166 % Uncomment to print the figure to a png file.
167 % print(fig2, figStr3,'-dpng','-r150')
168 % clear fig2
169 %
170 sound(yMozartWSS,Fs);
171 % Uncomment to write the generated sound to a .wav file.
172 % audiowrite(audioStr,yMozartWSS,Fs)
173 %
174 % Uncomment to save the results in a .mat file.
175 % save( fileStr )
```

APPENDIX E

Gathering Data From OMRON LD Series Through ARCL

To control the motion of and gather data from the OMRON mobile robots, we have developed a Python-based interface for interacting with the OMRON Advanced Robotics Command Language (ARCL). ARCL, which is a text-based and command-and-response operating system, can be utilized to integrate a fleet of OMRON LD mobile robots with external automation systems. The block diagram of our in-house Python interface is depicted in Figure 5.3

We are employing the ARCL to gather data from the OMRON LD series mobile robots. The first step in our data-gathering process involves configuring the ARCL parameters within MobilePlanner, the software provided by OMRON for controlling, configuring, and communicating with their mobile robots. This software serves as a critical interface for setting up the necessary parameters that facilitate effective interaction with the OMRON LD series robots.

In MobilePlanner, we begin by defining the ARCL server address, port number, and password parameters. These settings are essential for establishing a secure and reliable connection to the mobile robots. After inputting these core parameters, we proceed to configure additional ARCL settings tailored to our specific research needs,

ensuring that the communication between our system and the robots is optimized for data gathering.

Once the ARCL parameters are correctly set, we connect to the ARCL using a Telnet client. This connection allows us to initiate real-time communication with the mobile robots, enabling us to send commands and retrieve data efficiently. The Telnet protocol provides a versatile and straightforward method for remote access, making it easier to interact with the robots' systems.

We are utilizing a terminal interface in conjunction with the Telnet protocol. This approach is particularly important because OMRON mobile robots, designed for industrial applications, often present challenges in terms of data collection and control due to their advanced functionalities and configurations.

Through this carefully structured setup, we can effectively utilize ARCL to command the robots and gather valuable data regarding their operations. This systematic approach not only simplifies the control process but also enhances our ability to monitor and analyze the performance of OMRON's mobile robots in various environments.

Once connected, we utilize the terminal interface to input ARCL commands, which are specifically designed to interact with the robot's internal systems and functions.

The use of ARCL enables us to send a variety of commands to the robots, allowing us to access real-time data regarding their operational status, performance metrics, and environmental interactions. This data includes information on the robot's position, velocity, battery status, and any errors or alerts that may arise during operation. Also, through the ARCL it is very simple to reconstruct the map of the robot's environment which captures the stationary obstacles present in the robot's surroundings.

As we execute these commands, the output generated by the robots is systematically recorded. We save this output in a text file, which serves as a repository for the data collected. This method not only ensures that we capture a comprehensive dataset but also allows for easy retrieval and analysis in subsequent phases of our

research.

By implementing this structured approach of data gathering, we can effectively monitor the performance of the OMRON LD series robots and gain valuable insights into their operation within industrial environments. This process is crucial for advancing the study on converting the robot's movement into auditory representations.

The following code was used to extract data from MobilePlanner software as well as computes the distance to a specific, predefined goal in the map:

```
import telnetlib
import getpass
from turtle import heading
import numpy as np
import matlab.engine
import matplotlib.pyplot as plt
import time

def toc():
    import time
    if 'startTime' in globals():
        t = time.time() - startTime
        print('elapsed time is: ', str(t), 'seconds')

def tic():
    import time
    global startTime
    startTime = time.time()

host = '192.168.1.63'
port = '1996'
lookfor = 'Location'
LocalizationScore = 'LocalizationScore:'
password = 'admin'
```

```
numberOfIterations = 150
threshold = 8

'Call a matlab script to extract the locations of the goals in the map file'
eng = matlab.engine.start_matlab()
eng.DataExtracFromMatlab(nargout=0)
a= eng.DataExtracFromMatlab()

goalpos = a[2]
xgoal = goalpos[0]
ygoal = goalpos[1]
print(xgoal) #5325
print(ygoal) #8146

# Establish the connection to the robot and run a macro
tn = telnetlib.Telnet(host,port)
tn.read_until(b'assword:')
tn.write(password.encode('ascii') + b'\n')
tn.write(b'goto Goal3 \n')
time.sleep(2)
tn.write(b'executeMacro Macro2 \n')
tn.write(b'dsfv RobotX \n')

def getData():

 tic()

    tn.write(b'dsfv RobotX \n')
    tn.read_until(b'RobotX')
    X = tn.read_some().decode('ascii')
    X = X.split()
    X = X[0]
    print('X =', int(X))
```

```
58
59
60      tn.write(b' \n')
61      tn.write(b'dsfv RobotY \n')
62      tn.read_until(b'RobotY')
63      Y = tn.read_some().decode('ascii')
64      print('y = ', int(Y))
65
66      tn.write(b' \n')
67      tn.write(b'dsfv RobotTh \n')
68      tn.read_until(b'RobotTh')
69      theta = tn.read_some().decode('ascii')
70      theta = float(theta)
71      print('heading = ', (theta))
72
73      tn.write(b' \n')
74      tn.write(b'dsfv RotVel \n')
75      tn.read_until(b'RotVel')
76      rotVel = tn.read_some().decode('ascii')
77      print('rotVel = ', int(rotVel))
78
79      tn.write(b' \n')
80      tn.write(b'dsfv LeftVel \n')
81      tn.read_until(b'LeftVel')
82      leftVel = tn.read_some().decode('ascii')
83      print('LeftVel = ', int(leftVel))
84
85      tn.write(b' \n')
86      tn.write(b'dsfv RightVel \n')
87      tn.read_until(b'RightVel')
88      rightVel = tn.read_some().decode('ascii')
89      print('RightVel = ', int(rightVel))
90
```

```
    #tn.write(b'dsfv batterystateofcharge \n')
    #tn.read_until(b'BatterySateOfCharge')
    #Bat = tn.read_some().decode('ascii')
    #print('Battery = ')
    #print(Bat)

    #tn.write(b'Odometer \n')
    #tn.read_until(b'Odometer: ')
    #time = tn.read_some().decode('ascii')
    #print(time)
    toc()
    return int(X) ,int(Y), (theta), int(rotVel), int(leftVel), int(rightVel)

xpos = np.empty(numberOfIterations)
ypos = np.empty(numberOfIterations)
heading = np.empty(numberOfIterations)
leftVel = np.empty(numberOfIterations)
rightVel = np.empty(numberOfIterations)
rotVel = np.empty(numberOfIterations)

i = 0
xpos[i], ypos[i], heading[i], rotVel[i], leftVel[i], rightVel[i] = getData()
dist = (((xpos[i]-xgoal)**2 + (ypos[i]-ygoal)**2)**0.5)
c =((((xpos[i]-xgoal)**2 + (ypos[i]-ygoal)**2)**0.5) > threshold )
#print(c)
print(dist)
c = True

while c:
    xpos[i], ypos[i], heading[i], rotVel[i], leftVel[i], rightVel[i] = getData()
    dist = (((xpos[i]-xgoal)**2 + (ypos[i]-ygoal)**2)**0.5)
    print('Distance to goal: ',dist)
    c =((((xpos[i]-xgoal)**2 + (ypos[i]-ygoal)**2)**0.5) > threshold )
```

```
124     print(c)
125     i = i+1
126
127     if c == False:
128         break
129
130 # Print the positions up to the end goal
131 print('number of iterations = ',i ,'\n')
132 print('x position: ' )
133 print(xpos[1:i] , '\n')
134 print('y position: ')
135 print(ypos[1:i], '\n')
136 print('Heading: , ')
137 print(heading[1:i], '\n')
138
139 print('Rotation Velocity: ' )
140 print(rotVel[1:i], '\n')
141 print('Left wheel Velocity: ')
142 print( leftVel [1:i], '\n')
143 print('Right Wheel Velocity: ')
144 print(rightVel[1:i], '\n')
145
146 xpos = xpos[0:i]
147 ypos = ypos[0:i]
148
149 # Plot path of the Robot
150 plt.plot(xpos,ypos)
151 plt.show()
152
153 plt.plot(heading)
154 plt.show()
155
156 tn.write(b'quit\n')
```

```
157 tn.write(b'exit\n')
158 tn.close()
```

BIBLIOGRAPHY

BIBLIOGRAPHY

[1] A. Kacem, K. Zbiss, and A. Mohammadi, "A numerical integrator for forward dynamics simulations of folding process for protein molecules modeled as hyper-redundant robots," in *2023 IEEE/RSJ International Conference on Intelligent Robots and Systems (IROS 2023)*, 2023.

[2] A. Kacem, K. Zbiss, and A. Mohammadi, "A numerical integrator for kinetostatic folding of protein molecules modeled as robots with hyper degrees of freedom," *Robotics*, vol. 13, no. 10, p. 150, 2024.

[3] A. Kacem, K. Zbiss, P. Watta, and A. Mohammadi, "Wave space sonification of the folding pathways of protein molecules modeled as hyper-redundant robotic mechanisms," *Multimed. Tools Appl.*, vol. 83, no. 2, pp. 4929–4949, 2024.

[4] A. Kacem, K. Zbiss, and A. Mohammadi, "Transforming motion into sound: A novel sonification approach for teams of mobile robots," in *International Symposium on Flexible Automation*, vol. 87882, p. V001T07A005, American Society of Mechanical Engineers, 2024.

[5] K. Zbiss, A. Kacem, M. Santillo, and A. Mohammadi, "Automatic collision-free trajectory generation for collaborative robotic car-painting," *IEEE Access*, vol. 10, pp. 9950–9959, 2022.

[6] K. Zbiss, A. Kacem, M. Santillo, and A. Mohammadi, "Automatic optimal robotic base placement for collaborative industrial robotic car painting," *Applied Sciences*, vol. 14, no. 19, p. 8614, 2024.

[7] A. Mohammadi and M. W. Spong, "Quadratic optimization-based nonlinear control for protein conformation prediction," *IEEE Control Systems Letters*, vol. 6, pp. 373–378, 2021.

[8] W. A. Mozart *et al.*, "Piano sonata no. 11 in a major, k. 331," 1953.

[9] T. Hermann, "Wave space sonification," in *Proceedings of the 24th International Conference on Auditory Display (ICAD 2018)*, 2018.

[10] D. Ahmetovic, F. Avanzini, A. Baratè, C. Bernareggi, M. Ciardullo, G. Galimberti, L. A. Ludovico, S. Mascetti, and G. Presti, "Sonification of navigation instructions for people with visual impairment," *International Journal of Human-Computer Studies*, vol. 177, p. 103057, 2023.

[11] D. Ahmetovic, F. Avanzini, A. Baratè, C. Bernareggi, G. Galimberti, L. A. Ludovico, S. Mascetti, and G. Presti, "Sonification of rotation instructions to support navigation of people with visual impairment," in *2019 IEEE International Conference on Pervasive Computing and Communications (PerCom*, pp. 1–10, IEEE, 2019.

[12] W. Hu, K. Wang, K. Yang, R. Cheng, Y. Ye, L. Sun, and Z. Xu, "A comparative study in real-time scene sonification for visually impaired people," *Sensors*, vol. 20, no. 11, p. 3222, 2020.

[13] T. Hermann, P. Meinicke, H. Bekel, H. Ritter, H. M. Müller, and S. Weiss, "Sonifications for eeg data analysis," Georgia Institute of Technology, 2002.

[14] G. Baier, T. Hermann, and U. Stephani, "Event-based sonification of eeg rhythms in real time," *Clinical Neurophysiology*, vol. 118, no. 6, pp. 1377–1386, 2007.

[15] M. Elgendi, B. Rebsamen, A. Cichocki, F. Vialatte, and J. Dauwels, "Real-time wireless sonification of brain signals," in *Advances in Cognitive Neurodynamics (III) Proceedings of the Third International Conference on Cognitive Neurodynamics-2011*, pp. 175–181, Springer, 2013.

[16] T. Hermann, G. Baier, U. Stephani, and H. Ritter, "Vocal sonification of pathologic eeg features," 2006.

[17] G. Baier and T. Hermann, "The sonification of rhythms in human electroencephalogram," in *Proceedings of the International Conference on Auditory Display*, 2004.

[18] S. Pauletto and A. Hunt, "Interactive sonification of complex data," *International Journal of Human-Computer Studies*, vol. 67, no. 11, pp. 923–933, 2009.

[19] N. Sawe, C. Chafe, and J. Treviño, "Using data sonification to overcome science literacy, numeracy, and visualization barriers in science communication," *Frontiers in Communication*, vol. 5, p. 46, 2020.

[20] M. S. Staege, "A short treatise concerning a musical approach for the interpretation of gene expression data," *Scientific reports*, vol. 5, no. 1, p. 15281, 2015.

[21] C.-H. Yu, Z. Qin, F. J. Martin-Martinez, and M. J. Buehler, "A self-consistent sonification method to translate amino acid sequences into musical compositions and application in protein design using artificial intelligence," *ACS nano*, vol. 13, no. 7, pp. 7471–7482, 2019.

[22] R. Braun, M. Tfirn, and R. M. Ford, "Listening to life: Sonification for enhancing discovery in biological research," *Biotechnology and Bioengineering*, 2023.

[23] W. L. Diaz-Merced, R. M. Candey, N. Brickhouse, M. Schneps, J. C. Mannone, S. Brewster, and K. Kolenberg, "Sonification of astronomical data," *Proceedings of the International Astronomical Union*, vol. 7, no. S285, pp. 133–136, 2011.

[24] S. A. Hughes, "Listening to the universe with gravitational-wave astronomy," *Annals of Physics*, vol. 303, no. 1, pp. 142–178, 2003.

[25] A. Zanella, C. Harrison, S. Lenzi, J. Cooke, P. Damsma, and S. Fleming, "Sonification and sound design for astronomy research, education and public engagement," *Nature Astronomy*, vol. 6, no. 11, pp. 1241–1248, 2022.

[26] H. Brock, G. Schmitz, J. Baumann, and A. O. Effenberg, "If motion sounds: Movement sonification based on inertial sensor data," *Procedia Engineering*, vol. 34, pp. 556–561, 2012.

[27] A. O. Effenberg, A. Weber, K. Mattes, U. Fehse, and H. Mechling, "Motor learning and auditory information: Is movement sonification efficient?," *Journal of Sport & Exercise Psychology*, vol. 29, 2007.

[28] A. O. Effenberg, "Movement sonification: Effects on perception and action," *IEEE multimedia*, vol. 12, no. 2, pp. 53–59, 2005.

[29] T. A. Rushton and P. R. Kantan, "A real-time embodied sonification model to convey temporal asymmetry during running," in *Proceedings of the 7th Interactive Sonification Workshop (ISon)*, p. 23, CITEC, Bielefeld University, 2022.

[30] A. Effenberg, U. Fehse, and A. Weber, "Movement sonification: Audiovisual benefits on motor learning," in *BIO web of conferences*, vol. 1, p. 00022, EDP Sciences, 2011.

[31] A. O. Effenberg, U. Fehse, G. Schmitz, B. Krueger, and H. Mechling, "Movement sonification: effects on motor learning beyond rhythmic adjustments," *Frontiers in neuroscience*, vol. 10, p. 195230, 2016.

[32] T. Nown, "Creating a real-time movement sonification system for hemiparetic upper limb rehabilitation for survivors of stroke," 2024.

[33] J. Reh, "Gait sonification for rehabilitation: adjusting gait patterns by acoustic transformation of kinematic data," 2024.

[34] F. Sors, M. Murgia, I. Santoro, T. Agostini, *et al.*, "Audio-based interventions in sport," *The Open Psychology Journal*, vol. 8, pp. 212–219, 2015.

[35] A. O. Effenberg, "Using sonification to enhance perception and reproduction accuracy of human movement patterns," in *Internation Workshop on Interactive Sonification*, vol. 2004, pp. 1–5, 2004.

[36] P. R. Kantan, S. Dahl, E. G. Spaich, and R. Bresin, "Sonifying walking: A perceptual comparison of swing phase mapping schemes," in *Proceedings of the 7th Interactive Sonification Workshop (ISon)*, p. 37, CITEC, Bielefeld University, 2022.

[37] J. Danna, V. Paz-Villagrán, A. Capel, C. Pétroz, C. Gondre, S. Pinto, E. Thoret, M. Aramaki, S. Ystad, R. Kronland-Martinet, *et al.*, "Movement sonification for the diagnosis and the rehabilitation of graphomotor disorders," in *Sound, Music, and Motion: 10th International Symposium, CMMR 2013, Marseille, France, October 15-18, 2013. Revised Selected Papers 10*, pp. 246–255, Springer, 2014.

[38] N. Nikmaram, D. S. Scholz, M. Großbach, S. B. Schmidt, J. Spogis, P. Belardinelli, F. Müller-Dahlhaus, J. Remy, U. Ziemann, J. D. Rollnik, *et al.*, "Musical sonification of arm movements in stroke rehabilitation yields limited benefits," *Frontiers in neuroscience*, vol. 13, p. 454144, 2019.

[39] A. O. Effenberg and T.-H. Hwang, "Movement sonification: Intermodal transformation of movement data to enhance motor learning," in *Sports Technology: Technologies, Fields of Application, Sports Equipment and Materials for Sport*, pp. 185–195, Springer, 2024.

[40] J. Danna, M. Fontaine, V. Paz-Villagrán, C. Gondre, E. Thoret, M. Aramaki, R. Kronland-Martinet, S. Ystad, and J.-L. Velay, "The effect of real-time auditory feedback on learning new characters," *Human movement science*, vol. 43, pp. 216–228, 2015.

[41] P. Thagard, "Creative combination of representations: Scientific discovery and technological invention," *Psychology of science: Implicit and explicit processes*, pp. 389–405, 2012.

[42] T. Hermann and H. Ritter, "Listen to your data: Model-based sonification for data analysis," *Advances in intelligent computing and multimedia systems*, vol. 8, pp. 189–194, 1999.

[43] S. Barrass and G. Kramer, "Using sonification," *Multimedia systems*, vol. 7, no. 1, pp. 23–31, 1999.

[44] J. G. Neuhoff, G. Kramer, and J. Wayand, "Sonification and the interaction of perceptual dimensions: Can the data get lost in the map?," Georgia Institute of Technology, 2000.

[45] T. Hermann, A. Hunt, J. G. Neuhoff, *et al.*, *The sonification handbook*, vol. 1. Logos Verlag Berlin, 2011.

[46] T. Hermann, "Taxonomy and definitions for sonification and auditory display," *Applied ergonomics*, 2008.

[47] J. P. Cabral and G. B. Remijn, "Auditory icons: Design and physical characteristics," *Applied ergonomics*, vol. 78, pp. 224–239, 2019.

[48] T. Hermann and H. Ritter, "Model-based sonification revisited—authors' comments on hermann and ritter, icad 2002," *ACM Transactions on Applied Perception (TAP)*, vol. 2, no. 4, pp. 559–563, 2005.

[49] S. Kalonaris and I. Zannos, "High-order surrogacy for the audiovisual display of dance," in *Proceedings of the 26th international conference on auditory display (ICAD), Virtual*, 2021.

[50] M. L. Teodoro, G. N. Phillips, and L. E. Kavraki, "Molecular docking: A problem with thousands of degrees of freedom," in *Proceedings 2001 ICRA. IEEE International Conference on Robotics and Automation (Cat. No. 01CH37164)*, vol. 1, pp. 960–965, IEEE, 2001.

[51] K. Kazerounian, K. Latif, K. Rodriguez, and C. Alvarado, "Nano-kinematics for analysis of protein molecules," 2005.

[52] N. Haspel, M. Moll, M. L. Baker, W. Chiu, and L. E. Kavraki, "Tracing conformational changes in proteins," *BMC structural biology*, vol. 10, pp. 1–11, 2010.

[53] J. Dunn and M. A. Clark, "Life music: the sonification of proteins," *Leonardo*, vol. 32, no. 1, pp. 25–32, 1999.

[54] T. Delatour, "Molecular music: the acoustic conversion of molecular vibrational spectra," *Computer Music Journal*, vol. 24, no. 3, pp. 48–68, 2000.

[55] Z. Qin and M. J. Buehler, "Analysis of the vibrational and sound spectrum of over 100,000 protein structures and application in sonification," *Extreme Mechanics Letters*, vol. 29, p. 100460, 2019.

[56] S. L. Franjou, M. Milazzo, C.-H. Yu, and M. J. Buehler, "Sounds interesting: Can sonification help us design new proteins?," *Expert Review of Proteomics*, vol. 16, no. 11-12, pp. 875–879, 2019.

[57] C.-H. Yu and M. J. Buehler, "Sonification based de novo protein design using artificial intelligence, structure prediction, and analysis using molecular modeling," *APL bioengineering*, vol. 4, no. 1, 2020.

[58] S. L. Franjou, M. Milazzo, C.-H. Yu, and M. J. Buehler, "A perspective on musical representations of folded protein nanostructures," *Nano Futures*, vol. 5, no. 1, p. 012501, 2021.

[59] P. Tavousi, M. Behandish, K. Kazerounian, and H. T. Ilieş, "An improved free energy formulation and implementation for kinetostatic protein folding simulation," in *International Design Engineering Technical Conferences and Computers and Information in Engineering Conference*, vol. 55935, p. V06AT07A006, American Society of Mechanical Engineers, 2013.

[60] M. Behandish, P. Tavousi, H. T. Ilieş, and K. Kazerounian, "Gpu-accelerated computation of solvation free energy for kinetostatic protein folding simulation," in *International Design Engineering Technical Conferences and Computers and Information in Engineering Conference*, vol. 55850, p. V02AT02A009, American Society of Mechanical Engineers, 2013.

[61] C. Madden, P. Bohnenkamp, K. Kazerounian, and H. T. Ilieş, "Residue level three-dimensional workspace maps for conformational trajectory planning of proteins," *The International Journal of Robotics Research*, vol. 28, no. 4, pp. 450–463, 2009.

[62] R. Subramanian and K. Kazerounian, "Kinematic mobility analysis of peptide based nano-linkages," *Mechanism and machine theory*, vol. 42, no. 8, pp. 903–918, 2007.

[63] Z. Shahbazi, H. T. Ilieş, and K. Kazerounian, "Hydrogen bonds and kinematic mobility of protein molecules," 2010.

[64] B. A. Shoemaker, J. Wang, and P. G. Wolynes, "Structural correlations in protein folding funnels," *Proceedings of the National Academy of Sciences*, vol. 94, no. 3, pp. 777–782, 1997.

[65] A. Mohammadi and M. W. Spong, "Chetaev instability framework for kinetostatic compliance-based protein unfolding," *IEEE Control Systems Letters*, vol. 6, pp. 2755–2760, 2022.

[66] J. Ferina and V. Daggett, "Visualizing protein folding and unfolding," *Journal of molecular biology*, vol. 431, no. 8, pp. 1540–1564, 2019.

[67] E. Frid, R. Bresin, and S. Alexanderson, "Perception of mechanical sounds inherent to expressive gestures of a nao robot-implications for movement sonification of humanoids," *Sound and music computing*, pp. 43–51, 2018.

[68] E. Triantafyllidis, C. Mcgreavy, J. Gu, and Z. Li, "Study of multimodal interfaces and the improvements on teleoperation," *IEEE Access*, vol. 8, pp. 78213–78227, 2020.

[69] T. H. Nown, P. Upadhyay, A. Kerr, I. Andonovic, C. Tachtatzis, and M. A. Grealy, "A mapping review of real-time movement sonification systems for movement rehabilitation," *IEEE Reviews in Biomedical Engineering*, vol. 16, pp. 672–686, 2022.

[70] R. Bresin, E. Frid, A. Latupeirissa, and C. Panariello, "Robust non-verbal expression in humanoid robots: New methods for augmenting expressive movements with sound," in *Workshop on Sound in Human-Robot Interaction, ACM/IEEE International Conference on Human-Robot Interaction*, 2021.

[71] E. Frid and R. Bresin, "Perceptual evaluation of blended sonification of mechanical robot sounds produced by emotionally expressive gestures: Augmenting consequential sounds to improve non-verbal robot communication," *International Journal of Social Robotics*, vol. 14, no. 2, pp. 357–372, 2022.

[72] P. Bremner, T. J. Mitchell, and V. McIntosh, "The impact of data sonification in virtual reality robot teleoperation," *Frontiers in Virtual Reality*, vol. 3, p. 904720, 2022.

[73] B. J. Zhang, N. Sigafoos, R. Moffit, I. Syed, L. S. Adams, J. Fick, and N. T. Fitter, "SonifyIt: Towards transformative sound for all robots," *IEEE Robot. Autom. Lett.*, vol. 7, no. 4, pp. 10566–10572, 2022.

[74] M. Schwenk and K. O. Arras, "R2-d2 reloaded: A flexible sound synthesis system for sonic human-robot interaction design," in *The 23rd IEEE international symposium on robot and human interactive communication*, pp. 161–167, IEEE, 2014.

[75] M. S. Menon, V. Ravi, and A. Ghosal, "Trajectory planning and obstacle avoidance for hyper-redundant serial robots," *Journal of Mechanisms and Robotics*, vol. 9, no. 4, p. 041010, 2017.

[76] Y. Zhao, L. Jin, P. Zhang, and J. Li, "Inverse displacement analysis of a hyper-redundant elephant's trunk robot," *Journal of Bionic Engineering*, vol. 15, pp. 397–407, 2018.

[77] Z. Hu, H. Yuan, W. Xu, T. Yang, and B. Liang, "Equivalent kinematics and pose-configuration planning of segmented hyper-redundant space manipulators," *Acta Astronautica*, vol. 185, pp. 102–116, 2021.

[78] K. Kazerounian, K. Latif, and C. Alvarado, "Protofold: A successive kinetostatic compliance method for protein conformation prediction," 2005.

[79] A. V. Finkelstein and O. Ptitsyn, *Protein physics: a course of lectures*. Elsevier, 2016.

[80] F. Bergasa-Caceres and H. A. Rabitz, "Interdiction of protein folding for therapeutic drug development in sars cov-2," *The journal of physical chemistry b*, vol. 124, no. 38, pp. 8201–8208, 2020.

[81] C. Mundrane, M. Chorsi, O. Vinogradova, H. Ilies, and K. Kazerounian, "Exploring electric field perturbations as the actuator for nanorobots and nanomachines," in *International Symposium on Advances in Robot Kinematics*, pp. 257–265, Springer, 2022.

[82] M. T. Chorsi, P. Tavousi, C. Mundrane, V. Gorbatyuk, H. Ilies, and K. Kazerounian, "One degree of freedom 7-r closed loop linkage as a building block of nanorobots," in *Advances in Robot Kinematics 2020*, pp. 41–48, Springer, 2021.

[83] C. Alvarado and K. Kazerounian, "On the rotational operators in protein structure simulations," *Protein engineering*, vol. 16, no. 10, pp. 717–720, 2003.

[84] P. Tavousi, "On the systematic design and analysis of artificial molecular machines," 2016.

[85] D. B. Adolf and M. D. Ediger, "Brownian dynamics simulations of local motions in polyisoprene," *Macromolecules*, vol. 24, no. 21, pp. 5834–5842, 1991.

[86] Y. Arkun and B. Erman, "Prediction of optimal folding routes of proteins that satisfy the principle of lowest entropy loss: dynamic contact maps and optimal control," *PloS One*, vol. 5, no. 10, p. e13275, 2010.

[87] Y. Arkun and M. Gur, "Combining optimal control theory and molecular dynamics for protein folding," *PLoS One*, vol. 7, no. 1, p. e29628, 2012.

[88] A. T. Bogetti, B. Mostofian, A. Dickson, A. Pratt, A. S. Saglam, P. O. Harrison, J. L. Adelman, M. Dudek, P. A. Torrillo, A. J. DeGrave, *et al.*, "A suite of tutorials for the westpa rare-events sampling software [article v1. 0]," *Living journal of computational molecular science*, vol. 1, no. 2, 2019.

[89] P. Tavousi, M. Behandish, H. T. Ilieş, and K. Kazerounian, "Protofold ii: Enhanced model and implementation for kinetostatic protein folding," *Journal of Nanotechnology in Engineering and Medicine*, vol. 6, no. 3, p. 034601, 2015.

[90] Y. Wang and S. Boyd, "Fast evaluation of quadratic control-lyapunov policy," *IEEE Transactions on Control Systems Technology*, vol. 19, no. 4, pp. 939–946, 2010.

[91] G. S. Chirikjian and J. W. Burdick, "The kinematics of hyper-redundant robot locomotion," *IEEE transactions on robotics and automation*, vol. 11, no. 6, pp. 781–793, 1995.

[92] G. S. Chirikjian, *Theory and applications of hyper-redundant robotic manipulators*. California Institute of Technology, 1992.

[93] G. S. Chirikjian and J. W. Burdick, "Design and experiments with a 30 dof robot," in *[1993] Proceedings IEEE International Conference on Robotics and Automation*, pp. 113–119, IEEE, 1993.

[94] N. Simaan, R. Taylor, and P. Flint, "A dexterous system for laryngeal surgery," in *IEEE International Conference on Robotics and Automation, 2004. Proceedings. ICRA'04. 2004*, vol. 1, pp. 351–357, IEEE, 2004.

[95] T. Kamegawa, T. Yarnasaki, H. Igarashi, and F. Matsuno, "Development of the snake-like rescue robot" kohga"," in *IEEE International Conference on Robotics and Automation, 2004. Proceedings. ICRA'04. 2004*, vol. 5, pp. 5081–5086, IEEE, 2004.

[96] A. Martín-Barrio, J. J. Roldán-Gómez, I. Rodríguez, J. Del Cerro, and A. Barrientos, "Design of a hyper-redundant robot and teleoperation using mixed reality for inspection tasks," *Sensors*, vol. 20, no. 8, p. 2181, 2020.

[97] C. Canali, A. Pistone, D. Ludovico, P. Guardiani, R. Gagliardi, L. De Mari Casareto Dal Verme, G. Sofia, and D. G. Caldwell, "Design of a novel long-reach cable-driven hyper-redundant snake-like manipulator for inspection and maintenance," *Applied Sciences*, vol. 12, no. 7, p. 3348, 2022.

[98] G. S. Chirikjian and J. W. Burdick, "A modal approach to hyper-redundant manipulator kinematics," *IEEE Transactions on Robotics and Automation*, vol. 10, no. 3, pp. 343–354, 1994.

[99] I. A. Gravagne and I. D. Walker, "Kinematic transformations for remotely-actuated planar continuum robots," in *Proceedings 2000 ICRA. Millennium Conference. IEEE International Conference on Robotics and Automation. Symposia Proceedings (Cat. No. 00CH37065)*, vol. 1, pp. 19–26, IEEE, 2000.

[100] V. S. Chembuly and H. K. Voruganti, "An efficient approach for inverse kinematics and redundancy resolution of spatial redundant robots for cluttered environment," *SN Applied Sciences*, vol. 2, no. 6, p. 1012, 2020.

[101] P. F. Muir and C. P. Neuman, "Kinematic modeling of wheeled mobile robots," *Journal of robotic systems*, vol. 4, no. 2, pp. 281–340, 1987.

[102] M. H. Raibert, "Legged robots," *Communications of the ACM*, vol. 29, no. 6, pp. 499–514, 1986.

[103] C. D. Bellicoso, M. Bjelonic, L. Wellhausen, K. Holtmann, F. Günther, M. Tranzatto, P. Fankhauser, and M. Hutter, "Advances in real-world applications for legged robots," *Journal of Field Robotics*, vol. 35, no. 8, pp. 1311–1326, 2018.

[104] A. Ollero, M. Tognon, A. Suarez, D. Lee, and A. Franchi, "Past, present, and future of aerial robotic manipulators," *IEEE Transactions on Robotics*, vol. 38, no. 1, pp. 626–645, 2021.

[105] M. Bernard, K. Kondak, I. Maza, and A. Ollero, "Autonomous transportation and deployment with aerial robots for search and rescue missions," *Journal of Field Robotics*, vol. 28, no. 6, pp. 914–931, 2011.

[106] L. E. Parker, "Alliance: An architecture for fault tolerant, cooperative control of heterogeneous mobile robots," in *Proceedings of IEEE/RSJ international conference on intelligent robots and systems (IROS'94)*, vol. 2, pp. 776–783, IEEE, 1994.

[107] B. Yamauchi, "Frontier-based exploration using multiple robots," in *Proceedings of the second international conference on Autonomous agents*, pp. 47–53, 1998.

[108] A. Yamashita, T. Arai, J. Ota, and H. Asama, "Motion planning of multiple mobile robots for cooperative manipulation and transportation," *IEEE Transactions on Robotics and Automation*, vol. 19, no. 2, pp. 223–237, 2003.

[109] J. Chen, M. Gauci, W. Li, A. Kolling, and R. Groß, "Occlusion-based cooperative transport with a swarm of miniature mobile robots," *IEEE Transactions on Robotics*, vol. 31, no. 2, pp. 307–321, 2015.

[110] J.-H. Lee and H. Hashimoto, "Controlling mobile robots in distributed intelligent sensor network," *IEEE Transactions on Industrial Electronics*, vol. 50, no. 5, pp. 890–902, 2003.

[111] J. Li, K. Li, and W. Zhu, "Improving sensing coverage of wireless sensor networks by employing mobile robots," in *2007 IEEE International Conference on Robotics and Biomimetics (ROBIO)*, pp. 899–903, IEEE, 2007.

[112] E. Michael and T. Simonson, "How much can physics do for protein design?," *Current Opinion in Structural Biology*, vol. 72, pp. 46–54, 2022.

[113] D. Trivedi, C. D. Rahn, W. M. Kier, and I. D. Walker, "Soft robotics: Biological inspiration, state of the art, and future research," *Applied bionics and biomechanics*, vol. 5, no. 3, pp. 99–117, 2008.

[114] T. George Thuruthel, Y. Ansari, E. Falotico, and C. Laschi, "Control strategies for soft robotic manipulators: A survey," *Soft robotics*, vol. 5, no. 2, pp. 149–163, 2018.

[115] J. Fryman and B. Matthias, "Safety of industrial robots: From conventional to collaborative applications," in *ROBOTIK 2012; 7th German Conference on Robotics*, pp. 1–5, VDE, 2012.

[116] Z. Feng, G. Hu, Y. Sun, and J. Soon, "An overview of collaborative robotic manipulation in multi-robot systems," *Annual Reviews in Control*, vol. 49, pp. 113–127, 2020.

[117] S. Errede, "Lecture notes on acoustical physics of music," *Department of Physics, University of Illinois at Urbana-Champagne, IL. https://bit.ly/3p8gh7z*, 2017.

[118] H. Mochiyama, E. Shimemura, and H. Kobayashi, "Shape control of manipulators with hyper degrees of freedom," *The International Journal of Robotics Research*, vol. 18, no. 6, pp. 584–600, 1999.

[119] B. A. Jones and I. D. Walker, "Kinematics for multisection continuum robots," *IEEE Transactions on Robotics*, vol. 22, no. 1, pp. 43–55, 2006.

[120] B. J. Zhang, K. Peterson, C. A. Sanchez, and N. T. Fitter, "Exploring consequential robot sound: Should we make robots quiet and kawaii-et?," in *2021 IEEE/RSJ International Conference on Intelligent Robots and Systems (IROS)*, pp. 3056–3062, IEEE, 2021.

[121] G. Lemasurier, G. Bejerano, V. Albanese, J. Parrillo, H. A. Yanco, N. Amerson, R. Hetrick, and E. Phillips, "Methods for expressing robot intent for human–robot collaboration in shared workspaces," *ACM Transactions on Human-Robot Interaction (THRI)*, vol. 10, no. 4, pp. 1–27, 2021.

[122] A. M. Kohl, E. Kelasidi, A. Mohammadi, M. Maggiore, and K. Y. Pettersen, "Planar maneuvering control of underwater snake robots using virtual holonomic constraints," *Bioinsp. Biomim.*, vol. 11, no. 6, p. 065005, 2016.

[123] T. Hermann, "Wave space sonification," in *Pro. 24th Int. Conf. Audit. Disp. (ICAD)*, (Michigan Tech. Univ., Houghton, MI), 2018.

[124] S. Kalonaris and I. Zannos, "High-order surrogacy for the audiovisual display of dance," in *Proc. 26th Int. Conf. Audit. Disp. (ICAD)*, (Virtual), 2021.

[125] R. Siegwart, I. R. Nourbakhsh, and D. Scaramuzza, *Introduction to Autonomous Mobile Robots*. The MIT Press, 2nd ed., 2011.

[126] P. Goel, A. Datta, and M. S. Mannan, "Industrial alarm systems: Challenges and opportunities," *J. Loss Prev. Process Ind.*, vol. 50, pp. 23–36, 2017.

[127] Omron Corporation, "LD-Series Datasheet." URL https://www.ia.omron.com/products/family/3664/specification.html (Accessed: 2022-04-06).

[128] P. Leber and K. Dalm, "Using MR to interact with a mobile robot based on ROS," in *Proc. 12th Conf. Learn. Factories (CLF)*, 2022.